


Vacuum stability and electroweak precision in the two-Higgs-doublet model with vectorlike quarks

Kivanc Y. Cingiloglu^{*} and Mariana Frank[†]

*Department of Physics, Concordia University,
7141 Sherbrooke St. West, Montreal, Quebec, Canada H4B 1R6*

 (Received 18 September 2023; accepted 12 January 2024; published 15 February 2024)

We present a comprehensive analysis of the vacuum stability of the two-Higgs-doublet model, for both type-I and type-II, augmented by vectorlike quarks in singlet, doublet, or triplet representations. We review the model briefly before introducing the extra fermionic states and their interactions, and impose restrictions on the parameters coming from both theoretical considerations and experimental bounds. We then study the renormalization group equation evolution of the parameters of the model in order to isolate the parameter regions that satisfy vacuum stability requirements. We then add the electroweak precision observables to ensure that the resulting parameter space is consistent with the data. We include complete expressions for the renormalization group equations and the \mathbb{S} and \mathbb{T} parameters used. Finally, we summarize the effects of various vectorlike quark representations on the parameter space. We indicate the regions constrained, highlighting the differences between representations in type-I and type-II, and pinpoint the effects of the interplay between the extended model and the additional fermions.

DOI: [10.1103/PhysRevD.109.036016](https://doi.org/10.1103/PhysRevD.109.036016)

I. INTRODUCTION

The discovery of the Higgs boson [1,2] marked a significant milestone in particle physics, validating the existence of the missing piece of the Standard Model (SM). Yet the data collected supporting the Higgs discovery seem to indicate that principles of stability, renormalizability, and naturalness, which motivated the introduction of the Higgs boson in the first place, appear in conflict with the properties of the Higgs field itself. The idea of naturalness seems to be in conflict with the surprising degree of fine-tuning of both parameters in the Higgs field potential [3,4]. Related to this is the issue of the stability of the electroweak vacuum that arises from the behavior of the Higgs potential under renormalization group equations. To address this issue, it became imperative to explore extensions of the SM that could resolve this instability while remaining consistent with experimental observations. These explorations involve extending the particle content by additional states and/or extending the symmetry group (which in turn, result in the presence of new particles).

Such additional particles can be fermions or bosons. While the former are limited, the latter appear to have a wider range of applicability. The issue with additional fermions is the following. In the SM, gauge invariance does not allow for the introduction of bare mass terms for quarks and leptons, since these terms are not gauge invariant. So quark and lepton masses only arise from Yukawa interactions, after spontaneous gauge symmetry breaking. Additional fermionic families (quark or lepton) are ruled out by the Higgs data, since both the digluon production cross section (and decay) and the diphoton decay channel agree with the SM predictions and thus are inconsistent with the existence of additional fermions in the loops. The reason is the following. For the gluon fusion, the lowest order process proceeds through a loop involving quarks. The loop function depends on the ratio of the quark mass over the Higgs mass, both squared. The loop function is negligible for light quarks, where this ratio is <1 , leaving only the top contribution to be significant. However, if there are additional generations of *chiral* fermions, their contributions will also add to that of the top quark and enhance the cross section, rendering it inconsistent with the experimental value [5,6]. Thus surprisingly, heavy chiral quark contributions do not decouple [7,8].

However, if the fermionic components have vectorlike structure, rather than SM-chiral-like, their left- and right-handed components have the same couplings, allowing for bare mass terms that are gauge invariant. The addition of these particles is one of the simplest extensions of the SM. Because of their vectorlike nature, they do not contribute to

^{*}kivanc.cingiloglu@concordia.ca

[†]mariana.frank@concordia.ca

Published by the American Physical Society under the terms of the Creative Commons Attribution 4.0 International license. Further distribution of this work must maintain attribution to the author(s) and the published article's title, journal citation, and DOI. Funded by SCOAP³.

gauge anomalies and are less restricted than their chiral counterparts by current experimental data. They may populate the desert between the SM and the scale of grand unification, without worsening the hierarchy problem. Vectorlike quarks (VLQs), allowed to mix that couple with the third generation quarks (top and bottom partners), appear in composite Higgs models with a partially composite top quark [9–12]. They are naturally present in theories with extra dimensions [13–18] and in little Higgs models [19–21]. Finally, VLQs can be introduced in nonminimal supersymmetric models to increase corrections to the Higgs mass without significantly affecting electroweak precision observables [22–24], and they appear also in grand unified theory (GUT)-inspired, supersymmetric models [25].

Additionally, VLQ may explain some of the mismatch between the SM predictions and observed data. For instance, the Cabibbo-Kobayashi-Maskawa (CKM) matrix, which encodes couplings for each of the three generation quarks is, by construction, unitarity. However, the recent dataset collected after 2018 [26] disfavors the CKM unitarity of the first row for three generations of quarks to 99.998% confidence limits (C.L.), a problem confirmed by the determination of V_{ud} from superallowed beta decays [27]. While improved lattice evaluations of decay constants and form factors for kaons and pions, and corrections to the nuclear beta decay, have shrunk the discrepancy to 3σ , referred to as the Cabibbo angle anomaly [28,29], introducing VLQs seems the most promising avenue, because they are able to yield right-handed charged quark currents, which can modify the CKM matrix results [30]. An additional VLQ family could also explain quark and lepton mass hierarchies [31].

In the context of the SM, VLQs contribute to the stability of the vacuum, due to their strong coupling. It is well-known that in the SM, the stability of the vacuum is threatened by the strong coupling of the top to the Higgs boson [32]. The simplest cure is to add a scalar singlet field, which mixes with the SM Higgs boson and compensates for the top quark contribution [33]. Vectorlike quarks, due to their distinct representation under the electroweak group, offer a promising avenue for mitigating the vacuum stability problem. The question remains, how would the vacuum stability be affected by the addition of VLQs to the particle content?

In a previous work [34], we analyzed the effects of all possible representations of vectorlike quarks and their implications for maintaining vacuum stability within the SM augmented by an additional scalar. We have shown that, even with the addition of VLQs, the presence of the additional scalar was still a necessity. We extend this analysis to the study of the effect of introducing vectorlike quarks into a simple extension of the SM, the two-Higgs-doublet model (2HDM). Thus, we effectively replace the singlet scalar by scalars in a doublet representation. Our

study involves analyzing all anomaly-free representations of vectorlike quarks and their implications for maintaining vacuum stability within this model. As several versions of the model exist, we shall concentrate here on type-I (where the fermions couple to only one Higgs doublet and the other is inert) and type-II (where up quarks and neutrinos couple to one Higgs doublet, while down quarks and charged leptons couple to the other). The latter is of particular interest as it is consistent with the interaction structure required in supersymmetry.

The two-Higgs-doublet models, seen as one of the simplest extensions of the SM, have received a great deal of attention in the literature; see, for example, [35–53] and references therein. There are several motivations for extending the SM to 2HDMs. The best known is, as alluded to before, supersymmetry. In supersymmetric theories, the scalars belonging to multiplets of different chiralities cannot couple together in the Lagrangian, and thus a single Higgs doublet cannot give mass to both up- and down-type quarks. In addition, cancellation of anomalies also requires the presence of an additional doublet. Another motivation for 2HDMs comes from axion models [54]. It was noted [55] that a possible CP -violating term in the QCD Lagrangian can be rotated away if the Lagrangian contains a global $U(1)$ symmetry, but this is possible only if there are two Higgs doublets. And yet another motivation for 2HDMs comes from the fact that the SM is unable to generate a sufficiently large baryon asymmetry of the Universe, while 2HDMs can, due to additional sources of CP violation [56].

In this paper, we investigate the effects of vectorlike quarks in the context of extending the SM to the 2HDM framework. By incorporating vectorlike quarks into 2HDM, we analyze whether we can overcome the negativity of quartic Higgs boson self-couplings by finding a viable parameter space consistent with various theoretical and experimental constraints in type-I and type-II 2HDM scenarios. Furthermore, we delve into the consequences of these extensions on precision electroweak observables. We focus on two separate components: first, the oblique parameters originating from purely the 2HDM, and second, the impact of vectorlike quark contributions on these observables. These analyses shed light on the potential alterations to electroweak measurements that arise from the inclusion of vectorlike quarks in multi-Higgs scenarios. Through numerical simulations, we demonstrate the significant role that vectorlike quarks play in stabilizing the electroweak vacuum while maintaining agreement with precision electroweak measurements. Our aim is to provide insights into the potential avenues for extending the SM to address some of its shortcomings and set the theoretical framework for future explorations and for experimental validations.

Our work is organized as follows. In Sec. II we review the 2HDM. In Sec. III we review vectorlike quarks, in

singlet, doublet, or triplet representations, setting the general Lagrangian responsible for their interaction, as well as reviewing experimental searches and theoretical considerations responsible for restricting their masses. Section IV is dedicated to our exploration of the parameter space of the 2HDM with VLQs, which satisfies vacuum stability bounds. Section V explores the constraints imposed by electroweak precision observables on the surviving parameter space, looking separately at the restrictions coming from the 2HDM alone, in Sec. VA, and from the VLQs, in Sec. VB. We summarize our findings and conclude in Sec. VI. Finally, in the Appendix we gather all renormalization group equations (RGE) for the VLQ representations used in this work.

II. THE TWO-HIGGS-DOUBLET MODEL

In what follows, we present a brief summary of the 2HDM. Extensive reviews of the 2HDMs of type-I and type-II are in, e.g., [35,36]. The most general scalar potential contains 14 parameters and can have CP -conserving, CP -violating, and charge-violating minima. We make several simplifying assumptions: that CP is conserved in the Higgs sector, allowing one to distinguish between scalars and pseudoscalars, that CP is not spontaneously broken, and that discrete symmetries eliminate from the potential all quartic terms odd in either of the doublets.

The 2HDM scalar potential for the two-doublet fields with hypercharge $Y = 1$, which is invariant under the gauge symmetry of the SM, $SU(3)_C \otimes SU(2)_L \otimes U(1)_Y$, and satisfies a discrete \mathcal{Z}_2 symmetry, is given by [35]

$$\begin{aligned} V(\Phi_1, \Phi_2) = & m_{11}^2 \Phi_1^\dagger \Phi_1 + m_{22}^2 \Phi_2^\dagger \Phi_2 - m_{12}(\Phi_1^\dagger \Phi_2 + \Phi_2^\dagger \Phi_1) \\ & + \frac{\lambda_1}{2} (\Phi_1^\dagger \Phi_1)^2 + \frac{\lambda_2}{2} (\Phi_2^\dagger \Phi_2)^2 \\ & + \lambda_3 (\Phi_1^\dagger \Phi_1)(\Phi_2^\dagger \Phi_2) + \lambda_4 (\Phi_1^\dagger \Phi_2)(\Phi_2^\dagger \Phi_1) \\ & + \frac{\lambda_5}{2} [(\Phi_1^\dagger \Phi_2)^2 + (\Phi_2^\dagger \Phi_1)^2], \end{aligned} \quad (1)$$

where the complex doublets are perturbed around their minimums v_i as

$$\Phi_i = \begin{pmatrix} w_i^+ \\ \frac{v_i + \rho_i + i\eta_i}{\sqrt{2}} \end{pmatrix} \quad (i = 1, 2) \quad (2)$$

with $\sqrt{v_1^2 + v_2^2} = v = 246$ GeV, and the m_{12}^2 term softly breaks the \mathcal{Z}_2 symmetry. The reason for introducing \mathcal{Z}_2 symmetry is to avoid tree-level flavor-changing neutral currents. Minimizing the 2HDM potential Eq. (1) breaks electroweak symmetry and allows the scalar potential to be fully described in terms of seven independent parameters. The scalar couplings at μ_0 can be expressed in terms of the physical masses of the two CP -even scalars, h and H , as

$$\begin{aligned} \lambda_1 &= \frac{M_H^2 \cos^2 \alpha + M_h^2 \sin^2 \alpha}{v^2 \cos^2 \beta}, \\ \lambda_2 &= \frac{M_h^2 \cos^2 \alpha + M_H^2 \sin^2 \alpha}{v^2 \sin^2 \beta}, \\ \lambda_3 &= \frac{\sin 2\alpha}{v^2 \sin 2\beta} (M_H^2 - M_h^2) + \frac{2M_{H^\pm}^2}{v^2}, \\ \lambda_4 &= \frac{M_A^2 - 2M_{H^\pm}^2}{v^2}, \\ \lambda_5 &= -\frac{M_A^2}{v^2}, \end{aligned} \quad (3)$$

along with $\tan \beta = v_2/v_1$ and α the mixing angle between the two CP -even scalars. In contrast to the SM vacuum that conserves CP symmetry but breaks $SU(2)_L \otimes U(1)_Y$ symmetry, there are four possible vacuum states in 2HDM. Charge-breaking (CB) vacuum occurs when the charged component of either of the scalars acquires a nonzero vacuum expectation value (VEV). $U(1)$ symmetry is spontaneously broken, and the photon gets a nonzero mass

$$\langle \Phi_1 \rangle_{\text{CB}} = \frac{1}{\sqrt{2}} \begin{pmatrix} 0 \\ c_1 \end{pmatrix}, \quad \langle \Phi_2 \rangle_{\text{CB}} = \frac{1}{\sqrt{2}} \begin{pmatrix} c_2 \\ c_3 \end{pmatrix}. \quad (4)$$

CP -breaking vacuum occurs when there is a relative phase difference between the VEVs of the neutral components of the scalar doublets

$$\langle \Phi_1 \rangle_{\text{CP}} = \frac{1}{\sqrt{2}} \begin{pmatrix} 0 \\ v_1 \end{pmatrix}, \quad \langle \Phi_2 \rangle_{\text{CP}} = \frac{1}{\sqrt{2}} \begin{pmatrix} 0 \\ v_1 e^{i\eta} \end{pmatrix}. \quad (5)$$

The inert vacuum state happens when either one of the scalar fields acquires a nonzero VEV,

$$\langle \Phi_1 \rangle_{\text{IN}} = \frac{1}{\sqrt{2}} \begin{pmatrix} 0 \\ v \end{pmatrix}, \quad \langle \Phi_2 \rangle_{\text{IN}} = \frac{1}{\sqrt{2}} \begin{pmatrix} 0 \\ 0 \end{pmatrix}, \quad (6)$$

while mixed (normal) vacuum occurs when both of the neutral components of the scalar doublets have nonzero and positive VEVs,

$$\langle \Phi_1 \rangle_{\text{N}} = \frac{1}{\sqrt{2}} \begin{pmatrix} 0 \\ v_1 \end{pmatrix}, \quad \langle \Phi_2 \rangle_{\text{N}} = \frac{1}{\sqrt{2}} \begin{pmatrix} 0 \\ v_2 \end{pmatrix}. \quad (7)$$

If all different vacua could have existed simultaneously in a 2HDM potential, then one can undoubtedly think that the probability of transition between these states is nonzero. It was shown in Ref. [57] that if the 2HDM potential has a CP -conserving vacuum, then the different vacua (CP and CB) become saddle points,¹ with energy larger than that of

¹This is not necessarily so for the CP -breaking case, though normal vacua remain deeper.

the CP -preserving vacuum, ensuring that normal vacua stay global. If two different pairs of normal vacua can coexist, for a choice of $\tan\beta$ value, more than one pair of $v_1, v_2(\hat{v}_1, \hat{v}_2)$, might survive away from the origin [58]. The relative depth of the potentials is given by²

$$\Delta V = \frac{1}{2} \left[\left(\frac{M_{H^\pm}^2}{v_1^2 + v_2^2} \right) - \left(\frac{M_{H^\pm}^2}{\hat{v}_1^2 + \hat{v}_2^2} \right) \right] (v_1 \hat{v}_2 - v_2 \hat{v}_1)^2. \quad (8)$$

However, a new pair of deeper minima (\hat{v}_1, \hat{v}_2) in a special form of the 2HDM potential conflicts with SM phenomenology (the Higgs boson data) for a large region of the parameter space while a small parameter space still survives, preserving the mass spectrum of the SM and yet developing a nonzero transition rate between different normal vacua pairs. Nevertheless, the coexistence of two pairs of neutral vacua $\sqrt{v_1^2 + v_2^2} < \sqrt{\hat{v}_1^2 + \hat{v}_2^2}$ results in a particle spectrum that might yield decays conflicting with the SM predictions, even without RG flow, given the age of the universe exceeds the tunneling time. A sufficient condition that the normal vacua $v^2 = v_1^2 + v_2^2$ remain a global minimum is [49]

$$m_{12}^2 \left(m_{11}^2 - \sqrt{\frac{\lambda_1}{\lambda_2}} m_{22}^2 \right) \left(\tan\beta - \left[\frac{\lambda_1}{\lambda_2} \right]^{1/4} \right) > 0. \quad (9)$$

Additionally, one-loop effects rise in the effective 2HDM potential, and hence the relative depth of potential under the presence of the coexistence of inert [59] and of CB vacua [60] cases involve further corrections. Consequently, the parameter space extracted from the relative depth of the potential is extended. In fact, such an effect is an alternative way for renormalized couplings to manifest themselves according to RGEs, since the complete form of the effective potential runs over all gauge boson, fermion, and scalar field contributions. In return, renormalized couplings and masses according to a cutoff scale modify the relative depth between two effective potentials under the coexistence of vacua. The procedure follows according to the general structure of β -functions under the SM symmetry group, whereas gauge and scalar couplings extend the parameter space in a similar way. The Yukawa couplings do not affect the inertlike minimum since the fermions remain massless. The noncoexistence of CB and normal vacua is assured by the relative depth between different vacua natures $V_{\text{CB}} - V_{\text{EW}} > 0$; hence, the normal vacuum remains global minimum at tree level. However, there exists a finite allowed region [60] from one-loop corrections to $V_{\text{EW}}^{\text{eff}}$ that might develop a larger effective potential than the one of $V_{\text{CB}}^{\text{eff}}$. Since the effective potential is RG scale independent, this phenomena is not related to the energy scale for which the loop corrections are performed. Thus, at one-loop level,

²A similar relation in terms of inert and inertlike minimum cases is given elsewhere [59].

different from at tree level, the effective scalar potential that measures transition rates between EW and CB vacua is extremely dependent on particle content given. Nonetheless, the study of the surviving rates is meaningful in the case where $V_{\text{EW}} - V_{\text{CB}} > 0$ and concludes remarkably that the tree-level relation for EW vacuum stability may not hold for a unique choice of parameters.

Furthermore, tree-level vacuum stability is ensured if the following necessary and sufficient conditions are satisfied for the potential parameters in softly broken \mathcal{Z}_2 symmetry [61]:

$$\begin{aligned} \lambda_1(\mu) > 0, \quad \lambda_2(\mu) > 0, \quad \lambda_3(\mu) + \sqrt{\lambda_1(\mu)\lambda_2(\mu)} > 0, \\ \lambda_3(\mu) + \lambda_4(\mu) - |\lambda_5(\mu)| > -\sqrt{\lambda_1(\mu)\lambda_2(\mu)}. \end{aligned} \quad (10)$$

While these conditions may not necessarily hold true at the one-loop level, within the range where perturbative methods apply, the minor adjustments in the one-loop corrections to the effective potential should not substantially alter the potential's asymptotic trends. Typically, this is managed by scrutinizing the RG evolution of scalar couplings in the potential and ensuring that the criteria outlined in Eq. (10) remain applicable across all scales. Throughout our work in Sec. IV, the conditions Eqs. (10) and (11) on all the quartic couplings are satisfied up to the Planck scale. In principle, assuming the most general 2HDM potential (e.g., \mathcal{Z}_2 is not preserved, and $\lambda_6, \lambda_7 \neq 0$), it was shown [39,62,63] that necessary and sufficient conditions for boundedness from below (BFB) can be numerically solved for limited cases. The inclusion of λ_6 and λ_7 extends the parameter space that satisfies BFB conditions. Without loss of generality, the BFB conditions for the most general 2HDM potential reduce to Eq. (10). To this end, by adopting the \mathcal{Z}_2 -conserving case only, our scanning of complete RGEs in Sec. IV obeys Eq. (10) at all energy scales up to $\mu = M_{\text{Pl}}$. Additional conditions on the parameters of the 2HDM potential at the tree level emerge when ensuring the theory maintains unitarity [64,65]:

$$\begin{aligned} |\lambda_3 - \lambda_4| &< 8\pi, \\ |\lambda_3 + 2\lambda_4 \pm 3\lambda_5| &< 8\pi, \\ \left| \frac{1}{2} \left(\lambda_1 + \lambda_2 \sqrt{(\lambda_1 - \lambda_2)^2 + 4\lambda_4^2} \right) \right| &< 8\pi, \\ \left| \frac{1}{2} \left(\lambda_1 + \lambda_2 \sqrt{(\lambda_1 - \lambda_2)^2 + 4\lambda_5^2} \right) \right| &< 8\pi. \end{aligned} \quad (11)$$

At the end of Sec. III B, the tree-level expressions,³ Eq. (11), will be further modified to one-loop corrections for perturbative unitarity conditions in order to be examined throughout the complete 2HDM + VLQ RGE scan. We consider the case where $M_h < M_H$ (with h the SM-like Higgs boson), the

³The analytic expressions for the most general 2HDM potential appear elsewhere [63].

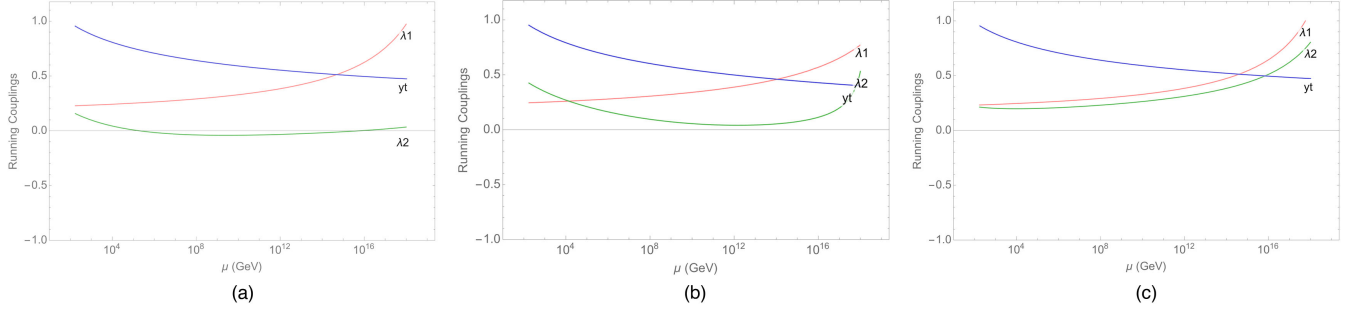


FIG. 1. The RGE running of the top Yukawa and scalar couplings λ_1 and λ_2 in the 2HDM fixed at $\tan\beta = 6$ for (a) $M_H = 450$ GeV, (b) $M_H = 600$ GeV, and (c) $M_H = 700$ GeV.

light Higgs masses scenario, and the normal vacuum in this study. Based on how \mathcal{Z}_2 symmetry is imposed on the 2HDM Lagrangian, four types of Yukawa interactions arise. Here we consider only two versions of the model:

- (i) Type-I: All fermions couple to the Φ_2 doublet, and the discrete symmetry is described as $\Phi_2 \rightarrow -\Phi_2$.
- (ii) Type-II: All charged leptons and down-type quarks couple to Φ_1 , and all up-type quarks couple to Φ_2 .

Although the conditions Eqs. (9) and (10) are necessary, they are not sufficient to guarantee absolute stability of the electroweak vacuum at next-to-leading order (NLO). In fact, the RGE running of quartic couplings $\lambda_{1,2}$ in type-I and type-II are severely affected by negative corrections of top and bottom Yukawa couplings,

$$\begin{aligned} \frac{d\lambda_2^I}{d\ln\mu^2} &= \frac{1}{16\pi^2} [12\lambda_2^2 + 4\lambda_3^2 + 4\lambda_3\lambda_4 + 2\lambda_4^2 + 2\lambda_5^2 \\ &\quad - 3\lambda_1(-4y_t^2 + g_1^2 + 3g_2^2) - 12y_t^4 - 12y_b^4 + \dots], \\ \frac{d\lambda_1^{II}}{d\ln\mu^2} &= \frac{1}{16\pi^2} [12\lambda_1^2 + 4\lambda_3^2 + 4\lambda_3\lambda_4 + 2\lambda_4^2 + 2\lambda_5^2 \\ &\quad - 3\lambda_1(g_1^2 + 3g_2^2) - 12y_b^4 + \dots], \\ \frac{d\lambda_2^{II}}{d\ln\mu^2} &= \frac{1}{16\pi^2} [12\lambda_2^2 + 4\lambda_3^2 + 4\lambda_3\lambda_4 + 2\lambda_4^2 + 2\lambda_5^2 \\ &\quad - 3\lambda_2(-4y_t^2 + g_1^2 + 3g_2^2) - 12y_t^4 + \dots], \end{aligned} \quad (12)$$

where gauge portal terms are not shown here due to their positive contributions. In Fig. 1, we present the running couplings of the quartic couplings λ_1 and λ_2 in 2HDM type-II by considering a toy model, without showing the RG evolution of $\lambda_{3,4,5}$. The first two conditions in Eq. (10) are not satisfied at the one-loop level by simply imposing the existence of a mixing between scalars. We adopt this toy model to show that, unlike the common misconception rising from the absence of an additional scalar in the SM, the model including an additional scalar also relies on the other free parameters of 2HDM.⁴ According to the initial value of

λ_2 in Eq. (3), $M_H = 450$ GeV is insufficient to preserve the positivity of λ_2 around $\mu \sim 10^5$ GeV. Increasing the mass to $M_H = 600$ GeV and $M_H = 700$ GeV lifted the initial value and ameliorated the positivity of quartic coupling up to M_{Pl} . Introducing additional freedom in the scalar sector proved to be the best scenario for a remedy for the vacuum stability as well as enlarging the allowed parameter space consistent with the SM phenomenology so far, because the SM can be recovered in the decoupling of the beyond the Standard Model (BSM) scalar extension (mixing angle $\alpha = 0$). We further use the radiative decay constant on the scalar initial conditions at the RGE level [67]

$$\delta_\lambda(\mu) = \frac{G_F M_Z^2}{8\sqrt{2}\pi^2} [\xi f_1(\xi, \mu) + f_0(\xi, \mu) + \xi^{-1} f_{-1}(\xi, \mu)], \quad (13)$$

with $\xi = M_H^2/M_Z^2$, $G_F = 1.16635 \times 10^{-5}$ GeV⁻², and

$$\begin{aligned} f_1(\xi, \mu) &= 6 \ln \frac{\mu^2}{M_H^2} + \frac{3}{2} \ln \xi - \frac{1}{2} Z \left(\frac{1}{\xi} \right) - Z \left(\frac{c_W^2}{\xi} \right) - \ln c_W^2 \\ &\quad + \frac{9}{2} \left(\frac{25}{9} - \sqrt{\frac{1}{3}\pi} \right), \\ f_0(\xi, \mu) &= 6 \ln \frac{\mu^2}{M_Z^2} \left[1 + 2c_W^2 - 2 \frac{m_t^2}{M_Z^2} \right] + \frac{3c_W^2 \xi}{\xi - c_W^2} \\ &\quad + 2Z \left(\frac{1}{\xi} \right) + 4c^2 Z \left(\frac{c_W^2}{\xi} \right) + \frac{3c_W^2 \ln c_W^2}{s_W^2} \\ &\quad + 12c_W^2 \ln c_W^2 - \frac{15}{2} (1 + 2c_W^2) \\ &\quad - 3 \frac{m_t^2}{M_Z^2} \left[2Z \left(\frac{m_t^2}{\xi M_Z^2} \right) + 4 \ln \frac{m_t^2}{M_Z^2} - 5 \right], \\ f_{-1}(\xi, \mu) &= 6 \ln \frac{\mu^2}{M_Z^2} \left[1 + 2c_W^4 - 24 \frac{m_t^2}{M_Z^2} \right] - 6Z \left(\frac{1}{\xi} \right) \\ &\quad - 12c_W^4 Z \left(\frac{c_W^2}{\xi} \right) - 12c_W^4 \ln c_W^2 + 8(1 + 2c_W^4) \\ &\quad + \left[Z \left(\frac{m_t^2}{\xi M_Z^2} \right) + \ln \frac{m_t^2}{M_Z^2} - 2 \right] \end{aligned} \quad (14)$$

⁴Similar analyses for the Higgs singlet model (HSM) and 2HDM have been performed in Refs. [33,66].

with

$$Z(z) = \begin{cases} 2A \tan^{-1}(1/A), & z > 1/4, \\ A \ln[(1+A)/(1-A)], & z < 1/4, \end{cases} \quad (15)$$

$$A = |1 - 4z|^{1/2}. \quad (16)$$

These corrections are taken into consideration from the $h \rightarrow \gamma\gamma$ amplitude. Since the signals from the photon decay of the Higgs also have corrections from the loop level diagrams, we only take the account of the SM gauge bosons and the top quark appearing in the one-loop level.

The deviation patterns in the Yukawa couplings due to mixing effects at the tree level remain consistent with the Standard Model predictions even when considering the inclusion of radiative corrections. Moreover, the scale factor corrections in the one-loop level due to extra scalars remain under 5% due to stability and perturbativity constraints in the 2HDM. This emerges from

$$\begin{aligned} \hat{\Gamma}_{hff}^{2\text{HDM}} &\sim \hat{\Gamma}_{hff}^{\text{SM}} + \frac{1}{16\pi^2} \frac{m_f M_\Phi^2}{v^3} (1 - M^2/M_\Phi^2)^2 \\ &\sim \hat{\Gamma}_{hff}^{\text{SM}} + \frac{1}{16\pi^2} \frac{m_f v \lambda_i^2}{M_\Phi^2}. \end{aligned} \quad (17)$$

Specifically for the top quark radiative correction, if the soft breaking scale of the Z_2 symmetry is around the masses of extra scalars H^\pm , H , and A , then the corrections remain under 1% for $\tan\beta > 3$. In fact, the peak value is around 6% for $\tan\beta = 1$, and this scale becomes even smaller and negligible for $\tan\beta > 3$ [68]. This is also shown to be correct for all the SM fermions studied therein. Hence, we can safely assume that for $\tan\beta$ and the mass range of extra scalars we choose for this work, the following electroweak radiative corrections to the initial condition on the top quark for increased accuracy hold [69]:

$$\Delta_t(\mu_0) = \Delta_W(\mu_0) + \Delta_{\text{QED}}(\mu_0) + \Delta_{\text{QCD}}(\mu_0), \quad (18)$$

with

$$\begin{aligned} \Delta_W(\mu_0) &= \frac{G_F m_t^2}{16\sqrt{2}\pi^2} \left(-9 \ln \frac{m_t^2}{\mu_0^2} - 4\pi \frac{M_H}{m_t} + 11 \right), \\ \Delta_{\text{QED}}(\mu_0) &= \frac{\alpha}{9\pi} \left(3 \ln \frac{m_t^2}{\mu_0^2} - 4 \right), \\ \Delta_{\text{QCD}}(\mu_0) &= \frac{\alpha_s}{9\pi} \left(3 \ln \frac{m_t^2}{\mu_0^2} - 4 \right). \end{aligned} \quad (19)$$

Therefore, the initial condition for the top Yukawa coupling becomes

$$y_t = \frac{\sqrt{2}m_t}{v} [1 + \Delta_t(\mu_0)]. \quad (20)$$

We now proceed with adding the contributions of VLQs into the model.

III. THE 2HDM WITH VECTORLIKE QUARKS

A. Theoretical considerations

Using the 2HDM potential in Sec. II, we investigate the effect of introducing vectorlike quarks on the stability of the electroweak vacuum. Unlike SM-like (chiral) fermions whose left-handed and right-handed components transform differently under $SU(3)_C \otimes SU(2)_L \otimes U(1)_Y$, vectorlike fermions have the same interactions regardless of chirality. However, when we consider incorporating them into the SM framework, it becomes necessary to introduce a new scalar boson into the Lagrangian. The additional scalar boson plays a crucial role in maintaining the stability of the 2HDM potential up to the Planck scale. The rationale behind this requirement stems from the fact that the inclusion of extra fermions leads to a decrease in the effective self-coupling of the Higgs boson. Consequently, this extension could potentially exacerbate the negative evolution of the Higgs quartic coupling when compared to the scenario within the SM without additional particles. The presence of the new scalar boson serves as a remedy to this situation.

The question remains, how would VLQs affect models with different scalar representations, such as 2HDMs? Throughout our work, we uphold the condition that the potential of the 2HDM must remain positive up to the Planck scale. Previous works analyzed several collider signatures that would be expected in type-II 2HDM with vectorlike quarks (singlets and doublets) [70–74]. The main motivation for our study is to establish the limitations that constrain the masses of vectorlike quarks and the mixing angles with the SM quarks. Establishing these constraints is essential in preserving the stability of the electroweak vacuum. While VLQ are also allowed to appear in the loop level of the radiative Higgs decay and their contributions, because of their vectorlike character, they do not affect the branching ratio. The oblique corrections to the mass of the W -boson rely on various VLQ representations as well, and thus making Eq. (13) model dependent. Because of this, only the corrections from the W -boson and the top quark are considered to slightly increase the relevant initial conditions on the quartic couplings without contradicting experimental data. Furthermore, if effects from $m_{\text{VLQ}} \sim \mathcal{O}$ TeV are taken into account in Eq. (17), effects due to VLQ break perturbativity of the top Yukawa coupling as setting its initial value too large. Moreover, as to be seen in Figs. 2–4, the initial value of the top Yukawa coupling according to radiative corrections we assume herein ensures the observed top quark mass throughout all representations of VLQ + 2HDM – I, II. Since all the initial conditions are set at $\mu_0 = m_t$, any VLQ effect contradicts with the experimental data. One might argue that the mixing relations between the SM quarks and VLQ

TABLE I. Representations of vectorlike quarks, with quantum numbers under $SU(2)_L \times U(1)_Y$.

Name	\mathcal{U}_1	\mathcal{D}_1	\mathcal{D}_2	\mathcal{D}_X	\mathcal{D}_Y	\mathcal{T}_X	\mathcal{T}_Y
Type	Singlet	Singlet	Doublet	Doublet	Doublet	Triplet	Triplet
	T	B	$\begin{pmatrix} T \\ B \end{pmatrix}$	$\begin{pmatrix} X \\ T \end{pmatrix}$	$\begin{pmatrix} B \\ Y \end{pmatrix}$	$\begin{pmatrix} X \\ T \\ B \end{pmatrix}$	$\begin{pmatrix} T \\ B \\ Y \end{pmatrix}$
$SU(2)_L$	1	1	2	2	2	3	3
Y	2/3	-1/3	1/6	7/6	-5/6	2/3	-1/3

could further correct the initial condition on the top Yukawa; however, Eqs. (34) and (35) are allowed to reduce $y_i(\mu_0)$ only if the mixing angle (denoted below by $\sin \theta'_{L,R}$) becomes larger than the constraints⁵ in Sec. III B.

The new VLQ states interact with the Higgs bosons through Yukawa interactions. The allowed anomaly-free multiplet states for the vectorlike quarks, together with their nomenclature, are listed in Table I [75–78]. The first two representations are U -like and D -like singlets [25,79,80], the next three are doublets (one SM-like, two non-SM like), and the last two are triplets. Note that the latter allow for quarks with exotic charges, $Q_X = 5/3$ and $Q_Y = -4/3$. The various representations are distinguished by their $SU(2)_L$ and hypercharge numbers.

The Yukawa and other relevant interaction terms between the vectorlike quarks and SM quarks are, in the bare (Φ_1, Φ_2) basis for type-I,

$$\begin{aligned}
\mathcal{L}_{\text{SM}}^I &= -y_u \bar{q}_L \Phi_2^c u_R - y_d \bar{q}_L \Phi_2 d_R, \\
\mathcal{L}_{\mathcal{U}_1, \mathcal{D}_1}^I &= -y_T \bar{q}_L \Phi_2^c U_{1R} - y_B \bar{q}_L \Phi_2 D_{1R} \\
&\quad - y_M (\bar{U}_{1L} \Phi_2 U_{1R} + \bar{D}_{1L} \Phi_2 D_{1R}) \\
&\quad - M_U \bar{U}_L U_R - M_D \bar{D}_L D_R, \\
\mathcal{L}_{\mathcal{D}_2}^I &= -y_T \bar{D}_{2L} \Phi_2^c u_R - y_B \bar{D}_{2L} \Phi_2^c d_R \\
&\quad - y_M (\bar{D}_{2L} \Phi_2^c D_{2R} + y_B \bar{D}_{2L} \Phi_2 D_{2R}) - M_D \bar{D}_{2L} D_{2R}, \\
\mathcal{L}_{\mathcal{D}_X, \mathcal{D}_Y}^I &= -y_T \bar{D}_{XL} \Phi_2^c u_R - y_B \bar{D}_{YL} \Phi_2^c d_R \\
&\quad - y_M (\bar{D}_{XL} \Phi_2 D_{XR} + y_B \bar{D}_{YL} \Phi_2^c D_{YR}) \\
&\quad - M_X \bar{D}_{XL} D_{XR} - M_Y \bar{D}_{YL} D_{YR}, \\
\mathcal{L}_{\mathcal{T}_X, \mathcal{T}_Y}^I &= -y_T \bar{q}_L \tau^a \Phi_2^c T_{XR}^a - y_B \bar{q}_L \tau^a \Phi_2 T_{YR}^a \\
&\quad - y_M (\bar{T}_{XL} \tau^a \Phi_2^c T_{XR}^a + y_B \bar{T}_{YL} \tau^a \Phi_2 T_{YR}^a) \\
&\quad - M_X \bar{T}_{XL} T_{XR} - M_Y \bar{T}_{YL} T_{YR}, \tag{21}
\end{aligned}$$

and for type-II

⁵Nonetheless, for the mixing scale between the SM quarks and VLQ set here, the radiative corrections for $y_i(\mu_0)$ can always be neglected without significantly affecting the parameter space generated by the complete RGE analysis.

$$\begin{aligned}
\mathcal{L}_{\text{SM}}^{II} &= -y_u \bar{q}_L \Phi_2^c u_R - y_d \bar{q}_L \Phi_1 d_R, \\
\mathcal{L}_{\mathcal{U}_1, \mathcal{D}_1}^{II} &= -y_T \bar{q}_L \Phi_2^c U_{1R} - y_B \bar{q}_L \Phi_1 D_{1R} \\
&\quad - y_M (\bar{U}_{1L} \Phi_2 U_{1R} + \bar{D}_{1L} \Phi_1 D_{1R}) \\
&\quad - M_U \bar{U}_L U_R - M_D \bar{D}_L D_R, \\
\mathcal{L}_{\mathcal{D}_2}^{II} &= -y_T \bar{D}_{2L} \Phi_2^c u_R - y_B \bar{D}_{2L} \Phi_1 d_R \\
&\quad - y_M (\bar{D}_{2L} \Phi_2^c D_{2R} + y_B \bar{D}_{2L} \Phi_1 D_{2R}) - M_D \bar{D}_{2L} D_{2R}, \\
\mathcal{L}_{\mathcal{D}_X, \mathcal{D}_Y}^{II} &= -y_T \bar{D}_{XL} \Phi_2^c u_R - y_B \bar{D}_{YL} \Phi_1^c d_R \\
&\quad - y_M (\bar{D}_{XL} \Phi_2 D_{XR} + y_B \bar{D}_{YL} \Phi_1^c D_{YR}) \\
&\quad - M_X \bar{D}_{XL} D_{XR} - M_Y \bar{D}_{YL} D_{YR}, \\
\mathcal{L}_{\mathcal{T}_X, \mathcal{T}_Y}^{II} &= -y_T \bar{q}_L \tau^a \Phi_2^c T_{XR}^a - y_B \bar{q}_L \tau^a \Phi_1 T_{YR}^a \\
&\quad - y_M (\bar{T}_{XL} \tau^a \Phi_2^c T_{XR}^a + y_B \bar{T}_{YL} \tau^a \Phi_1 T_{YR}^a) \\
&\quad - M_X \bar{T}_{XL} T_{XR} - M_Y \bar{T}_{YL} T_{YR}, \tag{22}
\end{aligned}$$

where $\Phi_i^c = i\sigma^2 \Phi_i^*$ ($i = 1, 2$), y_u , y_d , y_T , and y_B are the Yukawa couplings of the scalar fields $\Phi_{1,2}$ to vectorlike and to SM quarks, while y_M is the Yukawa coupling of the scalar fields to only vectorlike quarks.

The gauge eigenstate fermion fields resulting from the mixing can be written in general as

$$\mathbf{T}_{L,R} = \begin{pmatrix} t \\ T \end{pmatrix}_{L,R}, \quad \mathbf{B}_{L,R} = \begin{pmatrix} b \\ B \end{pmatrix}_{L,R}. \tag{23}$$

The mass eigenstate fields are denoted as (t_1, t_2) and (b_1, b_2) , and they are found through bi-unitary transformations,

$$\begin{aligned}
\mathbf{T}_{L,R} &= \begin{pmatrix} t_1 \\ t_2 \end{pmatrix}_{L,R} = V_{L,R}^t \begin{pmatrix} t \\ T \end{pmatrix}_{L,R}, \\
\mathbf{B}_{L,R} &= \begin{pmatrix} b_1 \\ b_2 \end{pmatrix}_{L,R} = V_{L,R}^b \begin{pmatrix} b \\ B \end{pmatrix}_{L,R}, \tag{24}
\end{aligned}$$

where

$$V_{L,R}^t = \begin{pmatrix} \cos \theta^t & -\sin \theta^t \\ \sin \theta^t & \cos \theta^t \end{pmatrix}_{L,R},$$

$$V_{L,R}^b = \begin{pmatrix} \cos \theta^b & -\sin \theta^b \\ \sin \theta^b & \cos \theta^b \end{pmatrix}_{L,R}. \quad (25)$$

In the following we abbreviate $\cos \theta_L^t \equiv c_L^t, \dots$. Through these rotations we obtain the diagonal mass matrices

$$M_{\text{diag}}^t = V_L^t M^t (V_R^t)^\dagger = \begin{pmatrix} m_{t_1} & 0 \\ 0 & m_{t_2} \end{pmatrix},$$

$$M_{\text{diag}}^b = V_L^b M^b (V_R^b)^\dagger = \begin{pmatrix} m_{b_1} & 0 \\ 0 & m_{b_2} \end{pmatrix}. \quad (26)$$

By using the gauge eigenstate fields, the mass matrices in the top and bottom sectors are given, after spontaneous symmetry breaking,

$$-\mathcal{L}_{Yuk}^t = (t_L \quad T_L) \begin{pmatrix} y_t \frac{v}{\sqrt{2}} & y_T \frac{v}{\sqrt{2}} \\ y_T \frac{v}{\sqrt{2}} & y_M \frac{v}{\sqrt{2}} + M_T \end{pmatrix} \begin{pmatrix} t_R \\ T_R \end{pmatrix},$$

$$-\mathcal{L}_{Yuk}^b = (b_L \quad B_L) \begin{pmatrix} y_b \frac{v}{\sqrt{2}} & y_B \frac{v}{\sqrt{2}} \\ y_B \frac{v}{\sqrt{2}} & y_M \frac{v}{\sqrt{2}} + M_B \end{pmatrix} \begin{pmatrix} b_R \\ B_R \end{pmatrix}. \quad (27)$$

The mass eigenvalues for top partners in type-I, II + VLQ models are

$$m_{t_{1,2}}^2 = \frac{1}{4} [(y_t^2 + y_T^2 + y_M^2) v^2] \left[1 \pm \sqrt{1 - \left(\frac{2y_t y_M}{(y_t^2 + y_T^2 + y_M^2)} \right)^2} \right] \quad (28)$$

with eigenvectors

$$\begin{pmatrix} t_1 \\ t_2 \end{pmatrix}_{L,R} = \begin{pmatrix} \cos \theta_{L,R}^t & \sin \theta_{L,R}^t \\ -\sin \theta_{L,R}^t & \cos \theta_{L,R}^t \end{pmatrix} \begin{pmatrix} t \\ T \end{pmatrix}_{L,R}. \quad (29)$$

Diagonalization of the mass matrices Eq. (26) is useful for expressing the mixing angles for top and bottom sectors in terms of the free parameters of the model,

$$\tan(2\theta_L^t) = \frac{2y_t y_M}{y_M^2 - y_t^2 - y_T^2},$$

$$\tan(2\theta_R^t) = \frac{2y_t y_T}{y_M^2 + y_t^2 - y_T^2}. \quad (30)$$

Charge assignments of the non-SM-like quarks do not allow the X and Y fields to mix with the other fermions. Therefore, these vectorlike quarks are also mass eigenstates. The bottom sector mixing angle can be obtained with the replacement $t \rightarrow b$ and $\theta^t \rightarrow \theta^b$. And solving Eq. (30) for the Yukawa couplings we end up with the relations between mass eigenvalues and mixing angles:

$$\frac{y_T}{y_t} = s_L^t c_L^t \frac{m_t^2 \frac{\tan \theta_L^t}{\tan \theta_R^t} - m_T^2 \frac{\tan \theta_R^t}{\tan \theta_L^t}}{m_T m_t}. \quad (31)$$

The connection between mass eigenstates and mixing angles of the SM quarks to VLQs in anomaly-free states is unique for each representation [75]:

$$\text{For doublets: } (XT): m_X^2 = m_T^2 (\cos \theta_R^t)^2 + m_t^2 (\sin \theta_R^t)^2,$$

$$(TB): m_T^2 (\cos \theta_R^t)^2 + m_t^2 (\sin \theta_R^t)^2 = m_B^2 (\cos \theta_R^b)^2 + m_b^2 (\sin \theta_R^b)^2,$$

$$(BY): m_Y^2 = m_B^2 (\cos \theta_R^b)^2 + m_b^2 (\sin \theta_R^b)^2,$$

$$\text{For triplets: } (XTB): m_X^2 = m_T^2 (\cos \theta_L^t)^2 + m_t^2 (\sin \theta_L^t)^2 = m_B^2 (\cos \theta_L^b)^2 + m_b^2 (\sin \theta_L^b)^2,$$

$$\text{where } \sin(2\theta_L^b) = \sqrt{2} \frac{m_T^2 - m_t^2}{(m_B^2 - m_b^2)} \sin(2\theta_L^t);$$

$$(TBY): m_Y^2 = m_B^2 (\cos \theta_L^b)^2 + m_b^2 (\sin \theta_L^b)^2 = m_T^2 (\cos \theta_L^t)^2 + m_t^2 (\sin \theta_L^t)^2,$$

$$\text{where } \sin(2\theta_L^b) = \frac{m_T^2 - m_t^2}{\sqrt{2}(m_B^2 - m_b^2)} \sin(2\theta_L^t); \quad (32)$$

and where

$$m_{T,B}(\tan \theta_R^{t,b}) = m_{t,b}(\tan \theta_L^{t,b}) \quad \text{for singlets, triplets,}$$

$$m_{T,B}(\tan \theta_L^{t,b}) = m_{t,b}(\tan \theta_R^{t,b}) \quad \text{for doublets.} \quad (33)$$

We defined here $m_T = M_U + y_T v \sin \beta / \sqrt{2}$, $m_B = M_D + y_B v \cos \beta / \sqrt{2}$, $m_t = y_t v \sin \beta / \sqrt{2}$, and $m_b = y_b v \cos \beta / \sqrt{2}$ for type-II models (for type-I, replace $v \cos \beta$ and $v \sin \beta$ by v), while $m_X = M_X$ and $m_Y = M_Y$. Initial conditions for all Yukawa couplings are modified with mixing relations.

For type-I + VLQ, all fermions acquire mass by interacting with the VEV of Φ_2 ,

$$\begin{aligned}
 y_i^I(\mu_0) &= \frac{\sqrt{2}m_i}{v} \frac{1}{\sqrt{\cos^2 \theta_L + x_i^2 \sin^2 \theta_L}}, \\
 y_T^I(\mu_0) &= \frac{\sqrt{2}m_T}{v} \frac{\sin \theta_L \cos \theta_L (1 - x_T^2)}{\sqrt{\cos^2 \theta_L + x_T^2 \sin^2 \theta_L}}, \\
 y_B^I(\mu_0) &= \frac{\sqrt{2}m_B}{v} \frac{\sin \theta_L \cos \theta_L (1 - x_B^2)}{\sqrt{\cos^2 \theta_L + x_B^2 \sin^2 \theta_L}}, \\
 y_M^I(\mu_0) &= \sum_{i=X,T,B,Y} \frac{C_R m_i}{v} \sqrt{\cos^2 \theta_L + x_i^2 \sin^2 \theta_L}, \quad (34)
 \end{aligned}$$

whereas in type-II + VLQ, $\tan \beta$, which is the ratio of VEVs, modifies the initial conditions to read

$$\begin{aligned}
 y_i^{II}(\mu_0) &= \frac{\sqrt{2}m_i}{v \sin \beta} \frac{1}{\sqrt{\cos^2 \theta_L + x_i^2 \sin^2 \theta_L}}, \\
 y_T^{II}(\mu_0) &= \frac{\sqrt{2}m_T}{v \sin \beta} \frac{\sin \theta_L \cos \theta_L (1 - x_T^2)}{\sqrt{\cos^2 \theta_L + x_T^2 \sin^2 \theta_L}}, \\
 y_B^{II}(\mu_0) &= \frac{\sqrt{2}m_B}{v \cos \beta} \frac{\sin \theta_L \cos \theta_L (1 - x_B^2)}{\sqrt{\cos^2 \theta_L + x_B^2 \sin^2 \theta_L}}, \\
 y_M^{II}(\mu_0) &= \sum_{i=X,T,B,Y} \frac{C_R m_i}{v} \sqrt{\cos^2 \theta_L + x_i^2 \sin^2 \theta_L}, \quad (35)
 \end{aligned}$$

where $C_R = (\sqrt{2}, \frac{1}{\sqrt{2}}, \frac{\sqrt{2}}{3})$ is the representation dependent weight factor with $x_b = m_b/m_B$ and as before $x_i = m_i/m_T$. Since X and Y fields do not mix with other fermions of the model, their low-energy Yukawa couplings are not altered by mixing relations. However, y_X and y_Y have indirect effects on the coupled RGEs, as seen from Eq. (7) for type-I and type-II analyzed in this work. Furthermore, the initial conditions on the VLQ Yukawa couplings in type-II have different β dependences in Eq. (35) based on which field is an up- or down-type member of the multiplets.

B. Restrictions on VLQ masses

Bounds on masses of VLQs were established by the direct searches at the LHC by ATLAS [81–85] and by CMS [86–91] Collaborations, obtained from specific mechanisms such as single production [92] and pair production [93,94] at $s = \sqrt{13}$ TeV. The constraints are sensitively dependent on the assumed decay channels of the light VLQs, which are allowed by kinematics to decay into a SM quark. If VLQs decay only to the third generation quarks,

then the following channels could be observed⁶: $T(B) \rightarrow W^+(W^-)t(b)$, $T(B) \rightarrow Zt(b)$, $T(B) \rightarrow Ht(b)$; hence, the bounds become relatively stronger due to the final states. The constraints $m_T > 1.27$ TeV and $m_B > 1.2$ TeV are obtained for singlets, whereas doublets require slightly higher mass limits $m_T > 1.46$ TeV and $m_B > 1.32$ TeV through pair production. Nonetheless, the lower limits on the VLQ masses in the range of [800, 1400] GeV and $\sin \theta < 0.18$ from Run 2 [95] are still compatible with the data [96]. It should be noted that these limits are decreased if the first and the second generation SM quarks are also included. However, since the Yukawa couplings play an essential role due to their direct relations to masses, these models are commonly disfavored. As our work concerns 2HDMs, we consider a lowest limit on m_T of 800 GeV, to allow for the consideration of the largest parameter space for the electroweak vacuum stability and electroweak observables (EWPOs).

Corrections to the mass of the W -boson are calculated using the oblique parameters. To this end, precision experiments carried out at the Tevatron [97] that signal any type of shift in ΔM_W are used to describe effects from new physics (NP). Since both the scalar and the fermion sectors contribute to EWPO, the combined corrections significantly rely on scalar extensions in addition to vectorlike fermions. Singlet (HSM) [98,99] and triplet (HTM) scalar models [100,101] have already been studied. However, for 2HDM + VLQ, we are only interested in constraints coming from the $\chi^2(S, T)$ [VLQ + 2HDM] analysis in order to generate a viable space for the electroweak vacuum stability requirements.

There are alternative ways for corrections to Higgs self-energies that would manifest themselves, especially when the new particles carry SM-like color and electroweak quantum numbers. In these scenarios, for every diagrammatic contribution to the self-energies, one could replace one of the Higgs bosons by its vacuum expectation value and attach two SM gauge bosons to the loop. From there, one can obtain a corresponding diagrammatic contribution to the Higgs decays to SM gauge bosons. A rough estimation of possible deviations from precision electroweak measurements, which pushed new physics to $\Lambda_{\text{NP}} \sim 1$ TeV, is based on the estimate of the size of Higgs oblique corrections roughly given by $\mathcal{O}(v^2/\Lambda^2) \sim 5\%$. If VLQs enter the loop diagrams, new fermions or charged bosons contribute to the loop-induced diphoton decay and/or gluon fusion channels of the Higgs bosons. The effects of VLQs on Higgs couplings have been explored in studies for singlet [99,102], doublet [103], and triplet models [104]. The T -singlet VLQ model established an upper bound $\sin \theta_L < 0.4$ from the combined $H \rightarrow gg$ and $H \rightarrow \gamma\gamma$ cross section and branching ratio, respectively, while

⁶For VLQs that carry non-SM-like hypercharges, the following CC and NC channels are also allowed and searched for accordingly: $X \rightarrow tW^+$, $Y \rightarrow bW^-$, $T(B) \rightarrow X(Y)W^-(W^+)$. See also [75].

in the doublet (TB) representation an upper limit $\sin\theta_L < 0.115$ was obtained only from a contribution to the gluon fusion cross section $\mu_{\gamma\gamma} \leq 1.03$, while the triplet (XTB) model contribution is $\mu_{\gamma\gamma} \leq 1.18$ around $m_{\text{VLQ}} \simeq 1$ TeV. Consequently, all these studies have shown VLQ corrections that match the earlier correction scale from NP models.

By far the most significant constraint here comes from B -physics, namely from $b \rightarrow s\gamma$, since $\tan\beta$ alone varies in a significantly large interval for the 2HDM models without VLQs. Studies in literature that extend 2HDM with singlet [105] and doublet [106] VLQs provide solid constraints to working around $\tan\beta \leq 12$, $M_{H^\pm} = [80, 1000]$ GeV for 2HDM-I and $M_{H^\pm} = [580, 1000]$ GeV for 2HDM-II along with $m_{\text{VLQ}} > 1$ TeV and small mixings, $\sin\theta_L < 0.2$, between VLQ and the SM quarks. We further explain the difference between mass regimes regarding the charged scalars of type-I and of type-II as RG evolutions are analyzed in the next section.

In what follows, we will scan the parameter space for $\tan\beta \in [6, 12]$. The reasons for such a restriction is as follows:

- (i) LHC data mostly constrain the $\tan\beta - \cos(\beta - \alpha)$ plane in 2HDM-II models. This is known from [107] within the exceptional region beyond the alignment limit (Fig. 2 in the reference). The LHC data alone in 2HDM do not exclude $\tan\beta < 6$. However, the addition of VLQ to 2HDM slightly extends the space [105]. Hence, taking both the exceptional and the ordinary regions into account, $\tan\beta > 5$ is favored for 2HDM in the alignment region and if VLQ mixing < 0.2 , although smaller values for $\tan\beta$ are still possible, too.
- (ii) The biggest motivation to assuming $\tan\beta > 5$ throughout our study is unique to us. This is because in the regime we choose for VLQ masses, if $\tan\beta$ becomes slightly smaller, meaning that v_2 becomes smaller with respect to v_1 , the initial conditions on uplike quark Yukawa couplings (VLQ or SM) become larger [Eq. (35)], and these break the perturbativity of Yukawa couplings as well as violate the stability conditions due to the excess weight of Yukawa couplings on the evolutions of all λ 's. As a consequence, if $\tan\beta \ll 6$, then VLQ masses need to be < 0.8 TeV to satisfy perturbative unitarity and stability conditions. This mass scale is ruled out by the experimental data.

Unitarity requires the S -matrix for scalar scattering to be unitary at high energy [65]. At tree level, this translates into imposing upper limits as $M_{\Phi^0} < \sqrt{\frac{4\pi}{\sqrt{2}G_F}} = 870$ GeV for scalar-scalar scattering and $M_{\Phi^0} < \sqrt{\frac{8\pi}{3\sqrt{2}G_F}} = 712$ GeV for gauge boson-scalar scattering in 2HDM. At NLO, a unitarity condition of the S -matrix yields terms proportional to $\mathcal{O}(\lambda_i \lambda_j / 16\pi^2)$; hence, one-loop corrections to the

tree-level unitarity conditions are modified by β -functions of scalar couplings. The combined perturbativity and unitarity conditions for the quartic couplings are bounded under RG evolutions [108]

$$|\lambda_i(\mu)| \lesssim 4, \quad (36)$$

and hence this will be required up to M_{Pl} in the next section. The perturbativity of the Yukawa couplings y_i is one of the weakest constraints at tree level, extending the upper bound of the mixing angle as $\sin\theta_L^t = [0.77, 0.31]$ for $m_T = [0.8, 2]$ TeV [75]. Last, for VLQ mixing, we choose the recent unitarity constraints [30] at the $\mathcal{O}(\text{TeV})$ scale.

IV. RGE ANALYSIS OF THE PARAMETER SPACE OF 2HDM WITH VLQS

The effect of fermions on the stability of the electroweak vacuum without extending the scalar sector beyond the SM Higgs field is to drive the Higgs self-coupling negative at larger scales, so the potential becomes unbounded from below, and there is no resulting stability. Theoretical considerations indicate that if the validity of the SM is extended to M_{Pl} , a second, deeper minimum is located near the Planck scale such that the electroweak vacuum is metastable [3,4]. The additional scalar bosons maintain positivity of the Higgs self-coupling while the renormalization flow tends to decrease it further at higher-energy scales [32]. Moreover, a common feature of both observed and exotic fermions is that Yukawa couplings are generally further lower scalar couplings since Yukawa couplings are negatively affected by NLO contributions. However, this is not always the case, and it depends on how the structure of gauge interactions have been affected by new fields. Through the possibility of various interaction portals, vectorlike fermions open new ways to remedy stabilizing the electroweak vacuum.

A straightforward approach would be to extend the gauge sector of the SM as the gauge β -functions have positive effects on quartic coupling RGEs [109]. However, additional gauge symmetries might also come short of being able to express the current SM interactions as they have relatively small contributions compared to other remedies. Nonetheless, these corrections, $\Delta\beta_1 = \frac{8}{3}n_F G_2 G_3 y_f^2$ and $\Delta\beta_{2,3} = \frac{8}{3}n_F d_{2,3} S_2(G_{2,3})$,⁷ are multiplicative with respect to new fermion families, and these contributions are already manifest at the RGE level, as we shall see in the Appendix. Yukawa and scalar portals have shown promising results, providing noncritical surfaces of electroweak vacuum stability [110]. As shown in Sec. III A, Yukawa portals lead to mixing between vectorlike quarks and the SM quarks. Because of mixing constraints, for an energy scale less than the mass of m_{VLQ} , decoupling occurs and VLQs contribute

⁷Here $S_2(G_i)$ are Dynkin indices for the groups G_2 and G_3 .

to RGE running as if they were massless. Furthermore, in the presence of VLQs, beyond-SM gauge couplings have larger values compared to the SM ones, thus reducing the corrections to Yukawa couplings running at energy scale $\mu \geq m_{\text{VLQ}}$. This could be shown, for instance, for the top quark, where the β -function

$$\beta_t \supset y_t [C_f y_f - C_1 g_1 - C_2 g_2 - C_3 g_3], \quad (37)$$

which in turn shows that $y_t(\mu) < y_t^{\text{SM}}(\mu)$. Moreover, gauge and Yukawa couplings have opposite sign contributions in scalar RGEs, Eq. (7), when fermions are allowed to interact with the scalars of the model. This characteristic can be seen from all scalar RGEs except the one that governs λ_1' , which is not allowed to interact with fermions through Yukawa couplings due to \mathcal{Z}_2 symmetry. Thus, from the RGE structure, the gauge and Yukawa couplings could lead to upward shifts in the Higgs quartic couplings though the condition $\lambda_{1,2} > \lambda_{1,2}^{\text{SM}}$ in the presence of VLQ. We note that, in this context, vectorlike quarks have been studied with only the SM Higgs field [111] and within the additional Higgs singlet model [34].

In Figs. 2–4 we present the RGE evolution for all vectorlike quark representations given in Eqs. (21) and (22), combined with 2HDM couplings, respectively, for type-I and type-II, in the case where the lightest CP -even scalar is taken to be the observed 125 GeV Higgs boson.

Among various bare 2HDM constraints, the limits on M_{H^\pm} and M_A are extremely sensitive to the VEV ratios $\tan\beta$ and to experimental data from B -physics [112], which affects how quarks are coupled in type-I and type-II models. Electroweak corrections to the W -boson, for a fixed value of $\tan\beta = 5$ in the type-I model, yield a degenerate mass spectrum for all scalars in the model, found to be $M = [100, 1000]$ GeV, if these EW corrections remain $\Delta_{\text{EW}}^W < 5\%$ as indicated from Higgs oblique corrections [113]. We have also compared our parameter space from the oblique parameters in 2HDM, Fig. 5 indicating that larger values of $\tan\beta$ reduce the upper bound of M_{H^\pm} and M_A , in good agreement with the results in Ref. [113]. The allowed parameter space from the oblique corrections yields a solid interval for the stability and perturbativity analyses throughout this work, as we choose some of the fixed parameters from the scalar sector to run the RG evolutions. However, bounds on M_{H^\pm} as a function of $\tan\beta$ from B -physics constraints are different in type-I and type-II models [114]. Lower bounds on M_{H^\pm} are inversely proportional to the $\tan\beta$ value in the type-I model, yielding a relatively lower minimum than the LEP result $M_{H^\pm} > 80$ GeV [115]. On the other hand, the lower bound on M_{H^\pm} in the type-II model behaves almost as $\tan\beta$ independent as $\tan\beta > 2$ and scales about the minimum $M_{H^\pm} = 580$ GeV. Apart from this distinguishing feature, both types are constrained to generate lower bounds on M_{H^\pm} as $\tan\beta$ increases. The type-II model in the heavy Higgs scenario is

affected by the lower bound on M_{H^\pm} , while the mass difference between 2HDM scalars is required to be small $M_{H^\pm} - M_A \lesssim 160$ GeV in order for the RG evolutions to survive about $\Lambda_{\text{cut}} \sim M_{\text{Pl}}$ [116]. As we run RG evolutions from 2HDM + VLQ up to $\mu = M_{\text{Pl}}$, type-I and type-II models can be better compared in the light Higgs scenario while setting fixed values to RGEs. The relative difference between masses $M_H - M_{H^\pm}$ and $M_{H^\pm} - M_A$ is important, though theoretical constraints do not strictly forbid large splittings between these parameters. However, bounds from EWPO [42] and from B -physics [41, 117] strongly correlate these mass differences if 2HDM + VLQ RGEs are to survive without having a Landau pole up to the Planck scale. We have investigated that large splitting between M_H, M_{H^\pm} , and M_A could not satisfy RG evolutions for 2HDM – II + VLQ, due to the nonperturbativity of scalar couplings and the vacuum instability in the sub-Planckian region. The parameter space of 2HDM that survives from RGEs running will be discussed in detail below.

We note that the overall effect of RGE on running couplings up to a cutoff scale Λ_{cut} is sensitively dependent on initial conditions given for a fixed set of parameters. Scalar couplings tend to generate a Landau pole and break perturbativity if they start from relatively large initial values due to their evolution (increase with energy scales). On the other hand, new in this work, when combined with $m_{\text{VLQ}} \gtrsim \mathcal{O}(\text{TeV})$, scalar RG evolutions also result in vacuum instability in case the initial values are too small and the mass limits of VLQ are too large. Although RGEs of the fermion sector are coupled due to the Yukawa couplings in the model, scalar RGEs are coupled due to any free parameters in 2HDM + VLQ. The parameter space of scalar masses that survive up to the Planck scale according to the initial conditions given in Eq. (3) and to bare 2HDM RGEs scanning, spans over a wide range for $\tan\beta = [1, 50]$ [117]. Nonetheless, the spectrum for $\tan\beta$ activated from 2HDM RGEs alone faces experimental constraints related to VLQ contributions to LHC Higgs data from diboson channels [105] and constraints from B -physics results [106]. The presence of VLQs at $\mathcal{O}(\text{TeV})$, carrying the SM-like quantum numbers, further constrain $\tan\beta = [1, 15]$ and $M_{H^\pm} > 600$ GeV in 2HDM – II + VLQ. Before delving into RGEs results, we also discuss the analytical nature of initial conditions depending on the mass difference $M_{H^\pm} - M_A$ and on $\tan\beta$. The quartic coupling $\lambda_1(\mu_0)$ rapidly grows for larger M_H and $\tan\beta$ values; therefore, it can generate a Landau pole faster than the rest of the couplings in the sub-Planckian scale, particularly in the type-I model without the presence of any Yukawa term to drive it lower. In contrast, $\lambda_2(\mu_0)$ and $\lambda_3(\mu_0)$ become heavily suppressed for larger $\tan\beta$ and smaller M_H values; hence, vacuum instability can occur due to the evolution of λ_2 , more dominantly so in the type-I model. The initial condition on λ_4 is by far the most sensitive to the constraints on the mass difference between

the pseudoscalar and the charged scalar. Being $\tan\beta$ independent, and due to a large separation between M_A and M_{H^\pm} , the quartic coupling λ_4 can easily reach a Landau pole in either direction⁸; hence, this initial condition alone develops an approximate limit for the separation $|M_{H^\pm} - M_A|$. As shown in [41], by inverting Eq. (3) and relating the separation between scalar masses to numerical values of $\lambda_4 + \lambda_5$ that survive up to M_{Pl} , the mass difference is bound to ~ 160 GeV. However, this scale is based on scanning over all values of $\tan\beta = [1, 50]$. Consequently, we have cross-checked that such a separation is allowed by RG analyses, considering smaller VEV ratios $\tan\beta = [6, 12]$ [117]. Taking into account that VLQs become unfrozen at $\Lambda \sim \mathcal{O}(\text{TeV})$, the strategy we follow to search the parameter space can be summarized as follows:

- (i) We scan RGE over a large number of parameters from 2HDM + VLQ by imposing theoretical and experimental bounds discussed above from both sectors.
- (ii) We extract the parameter space that survives from running RGEs requiring stability, perturbativity, and unitarity conditions up to the Planck scale.
- (iii) The initial conditions for all of the couplings that appear in the combined model are set at the energy scale $\mu_0 = m_t$.
- (iv) We calculate the corrections to the oblique parameters \mathbb{S} and \mathbb{T} from 2HDM and VLQs, and then check if the allowed parameter space for $\tan\beta$ range is consistent with the RG analyses.

The scanning ranges in the VLQ and 2HDM sectors are the following:

- (i) VLQ: $m_T = [0.8, 2] \text{ TeV}$, $m_B = [0.85, 2] \text{ TeV}$, $m_X = m_Y = [0.9, 2] \text{ TeV}$, $\sin\theta_{L,R} = [0.08, 0.15]$.
- (ii) 2HDM-I: $M_{H^\pm} = [80, 900] \text{ GeV}$, $M_A = [300, 1000] \text{ GeV}$, $M_H = [400, 1100] \text{ GeV}$, $t_\beta = [6, 12]$, $\sin\alpha = [0.06, 0.1]$.
- (iii) 2HDM-II: $M_{H^\pm} = [600, 900] \text{ GeV}$, $M_A = [300, 1000] \text{ GeV}$, $M_H = [400, 1100] \text{ GeV}$, $t_\beta = [6, 12]$, $\sin\alpha = [0.06, 0.1]$.

Note that the parameter space of VLQ + 2HDM that satisfies the vacuum stability constraint extends to $m_{\text{VLQ}} < \mathcal{O}(\text{TeV})$ and to larger mixing angle $\sin\theta_{L,R}^{t,b}$

(not shown). However, the recent experimental constraints [92,93,96,118] and constraints from EWPO, Fig. 7, discard large mixings and the light m_{VLQ} domain. The mixing angle $\alpha \neq 0$ (means the neutral scalars are not decoupled), because otherwise the perturbativity and the stability conditions are not satisfied at initial condition μ_0 as seen from Eq. (3) with respect to the range of M_H and $\tan\beta$ we scanned, especially for the minimum bound on M_{H^\pm} in type-II.

A. Singlet VLQ: \mathcal{U}_1 and \mathcal{D}_1

Type-I 2HDM + VLQ singlets yield the most stringent mass limits for VLQs required to satisfy the stability bounds, as expected from the form of the Yukawa terms that appear in both scalar and fermion RGEs. We present RG running of the couplings for singlet VLQ+2HDM-I,II in Fig. 2. The relative difference regarding the initial condition of top Yukawa coupling between \mathcal{U}_1 and \mathcal{D}_1 occurs due to the absence of top mixing in the \mathcal{D}_1 model. For mixing angles $\sin\theta_{L,R} > 0.15$, the mass scale region $m_T > \mathcal{O}(\text{TeV})$ leads to negative top Yukawa coupling in the sub-Planckian region. The RGEs of singlet VLQ in type-I are similar, and therefore the difference between the initial values of λ_2 stems from the mass difference between the top and the bottom VLQ sectors. Although all the initial conditions are set at the top quark mass, the overall shift of VLQ Yukawa couplings between type-I and type-II is always due to how strong extra fermions couple to scalars, depending on $\tan\beta$. As discussed previously, a small separation between mass values of scalars in type-II models together with a larger value of the minimum bound on M_{H^\pm} ameliorate the stability result compared to type-I models, and hence larger λ_2 values in type-II models are allowed by extending the bounds on scalar parameter space. In contrast to the proximity of λ_2 values to the instability region, λ_1 evolves safer away from the nonperturbativity region in type-II models, as expected from the splitting of Yukawa couplings in top and bottom sectors. Below we list the allowed mass ranges due to RG analyses of the combined model that survive from stability, perturbativity, and unitarity up to $\mu = M_{\text{Pl}}$:

$$\begin{aligned}
\mathcal{U}_1 + \text{type-I: } & m_T \in [800, 920] \text{ GeV}, M_{H^\pm} \in [80, 830] \text{ GeV}, M_H \in [700, 810] \text{ GeV}, M_A \in [510, 770] \text{ GeV}. \\
\mathcal{U}_1 + \text{type-II: } & m_T \in [820, 930] \text{ GeV}, M_{H^\pm} \in [600, 840] \text{ GeV}, M_H \in [720, 860] \text{ GeV}, M_A \in [715, 600] \text{ GeV}. \\
\mathcal{D}_1 + \text{type-I: } & m_B \in [850, 970] \text{ GeV}, M_{H^\pm} \in [80, 840] \text{ GeV}, M_H \in [725, 870] \text{ GeV}, M_A \in [500, 800] \text{ GeV}. \\
\mathcal{D}_1 + \text{type-II: } & m_B \in [870, 980] \text{ GeV}, M_{H^\pm} \in [600, 840] \text{ GeV}, M_H \in [740, 870] \text{ GeV}, M_A \in [770, 860] \text{ GeV}.
\end{aligned}$$

⁸We observed that for larger VLQs multiplets, λ_4 tends to diverge from a positive direction if $|M_{H^\pm} - M_A| \gg 150$ GeV, due to a relatively large number of Yukawa terms, though λ_4 always starts from a negative direction.

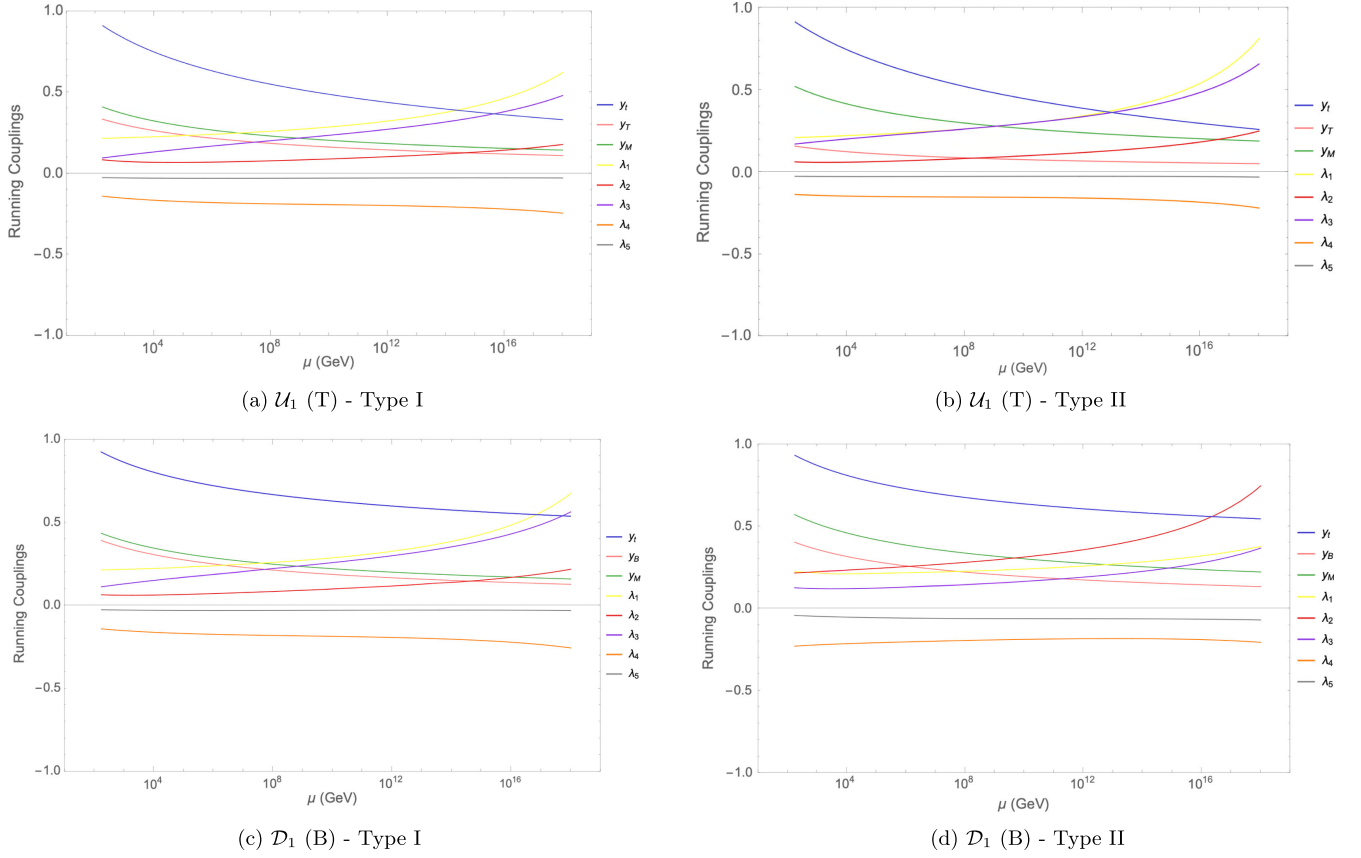


FIG. 2. The RGE running of the Yukawa and scalar couplings for models with vectorlike quarks. We plot results for type-I on the left column and for type-II on the right column. Subfigures (a) and (b): singlet vectorlike representation, \mathcal{U}_1 . Subfigures (c) and (d): singlet vectorlike representation, \mathcal{D}_1 . For singlet models, we have set $m_T = 0.8$ TeV, $m_B = 0.85$ TeV, $M_H = 800$ GeV, $M_{H^\pm} = 750$ GeV, $M_A = 650$ GeV $\mu_0 = m_t$, $\tan\beta = 10$, and mixing angles $\sin\alpha = 0.1$ and $\sin\theta_L = 0.08$.

A few comments regarding the behavior of the couplings for all VLQ representations are in order:

- (i) The upper mass bounds on the scalars of 2HDM can be extended further if $\tan\beta$ is increased according to the RG scanning. Otherwise, larger $\tan\beta$ leads to λ_i suppressions by flattening all scalar RG flows and might lead to instabilities by causing Yukawa divergences for $\tan\beta > 12$ beyond the range scanned. This characteristic can always be read from the denominator term through initial conditions in Eq. (3). The authors of Ref. [119] discuss the details of “squeezing” regions of stability for VLQ in various models.
- (ii) The high-energy enhancement of λ_2 in type-II models occurs due to the presence of the Yukawa terms y_M^2 and $y_T^2 y_M^2$ appearing in the $\lambda_{3,4,5}$ contribution to running coupling constants as y_M approaches M_{P1} , this being the largest correction among all VLQ Yukawa couplings.
- (iii) Because of the splitting of Yukawa terms between Φ_1 and Φ_2 , type-II + VLQ models are safer for vacuum stability as λ_2^I stays closer to zero as compared to λ_2^{II} , though this distinction alone is not enough for the stability requirements.

B. Doublet VLQ: \mathcal{D}_X , \mathcal{D}_2 , and \mathcal{D}_Y

As seen in Fig. 3, where we plot the variation of the scalar and Yukawa coupling constants as functions of the energy scale, the evolution of λ_1 in type-I+ \mathcal{D}_2 is safer compared to \mathcal{D}_X and \mathcal{D}_Y models. In fact, faster coupling increases for these models are seen from the upper bound of scalar masses, which exceeds the bounds extracted from \mathcal{D}_2 . Furthermore, the allowed space for the heavier CP -even scalar M_H in \mathcal{D}_Y is quite restricted compared to other type-I+doublet VLQ models; hence, λ_2 increases very fast, consistent with its initial condition as well. Because of the fact that B and Y VLQs are relatively heavier than T and X VLQs, the evolution of λ_1 stays closer to zero in the \mathcal{D}_Y + type-II model as this coupling is connected to the down-sector VLQ. Among all the doublet models, \mathcal{D}_X^{II} yields the most sensitive parameter space for the mass of heavier CP -even scalar M_H , resulting in a very narrow range for the combined RG scanning. Furthermore, as seen from the absence of bottom and top sector mixings in \mathcal{D}_X and \mathcal{D}_Y , respectively, and also the fact that these VLQ are pure eigenstates, the evolution of y_X and y_Y is enhanced compared to y_T and y_B in \mathcal{D}_2 . Therefore, the quartic Yukawa cross terms proportional to $y_M^2 y_{X,Y}^2$ lead to positive evolution for λ_4 , within the

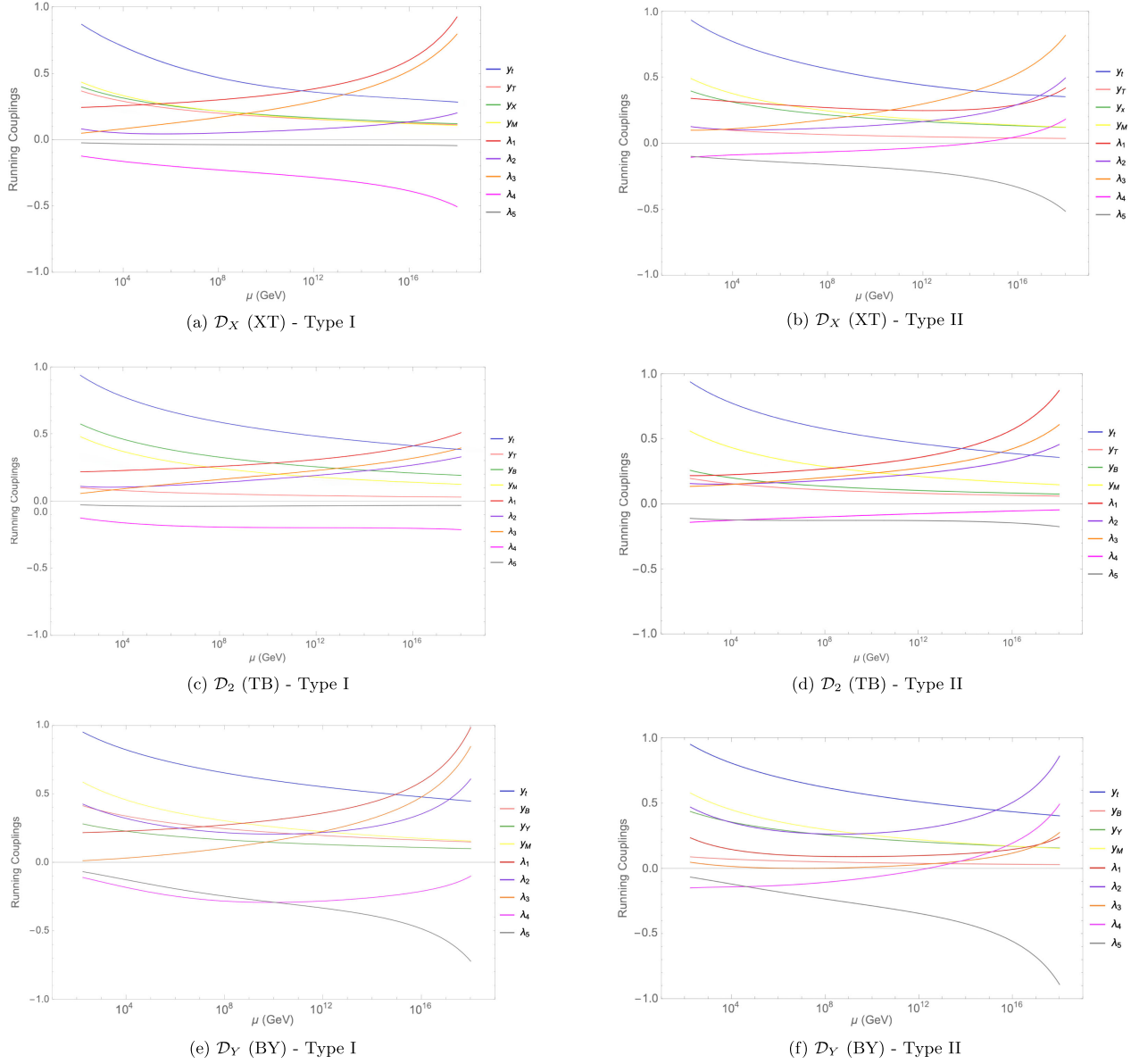


FIG. 3. The RGE running of the Yukawa and scalar couplings for models with vectorlike fermions. As before, we plot results for Type-I on the left column and for Type-II on the right column. Subfigures (a) and (b): doublet vectorlike representation, \mathcal{D}_X . Middle panel: doublet vectorlike representation, \mathcal{D}_2 . Subfigures (c) and (d): doublet vectorlike representation, \mathcal{D}_Y . For doublet models, we have set $m_T = 0.85$ TeV, $m_B = 1$ TeV, $m_X = 1$ TeV, $m_Y = 1$ TeV, $M_H = 800$ GeV, $M_{H^\pm} = 750$ GeV, $M_A = 650$ GeV, $\mu_0 = m_T$, $\tan\beta = 10$, and mixing angles $\sin\alpha = 0.1$ and $\sin\theta_L = 0.08$.

perturbative range for VLQ models with non-SM-like quantum numbers. Actually, this reciprocal RG connection between λ_4 and λ_5 determines how stringent the scalar parameter space is constrained. This will be further shown in

the analysis of the parameter space for triplet VLQ + 2HDM. The complete allowed mass ranges for doublet models that survive from stability, perturbativity, and unitarity up to $\mu = M_{\text{Pl}}$ are as follows:

\mathcal{D}_X + type-I:	$m_X \in [800, 1040]$ GeV,	$m_T \in [850, 970]$ GeV,	$M_{H^\pm} \in [80, 840]$ GeV,	$M_H \in [690, 870]$ GeV,
	$M_A \in [520, 860]$ GeV.			
\mathcal{D}_X + type-II:	$m_X \in [880, 1050]$ GeV,	$m_T \in [870, 1000]$ GeV,	$M_{H^\pm} \in [600, 865]$ GeV,	$M_H \in [820, 890]$ GeV,
	$M_A \in [760, 880]$ GeV.			
\mathcal{D}_2 + type-I:	$m_T \in [800, 930]$ GeV,	$m_B \in [860, 970]$ GeV,	$M_{H^\pm} \in [80, 810]$ GeV,	$M_H \in [670, 830]$ GeV,
	$M_A \in [490, 870]$ GeV.			

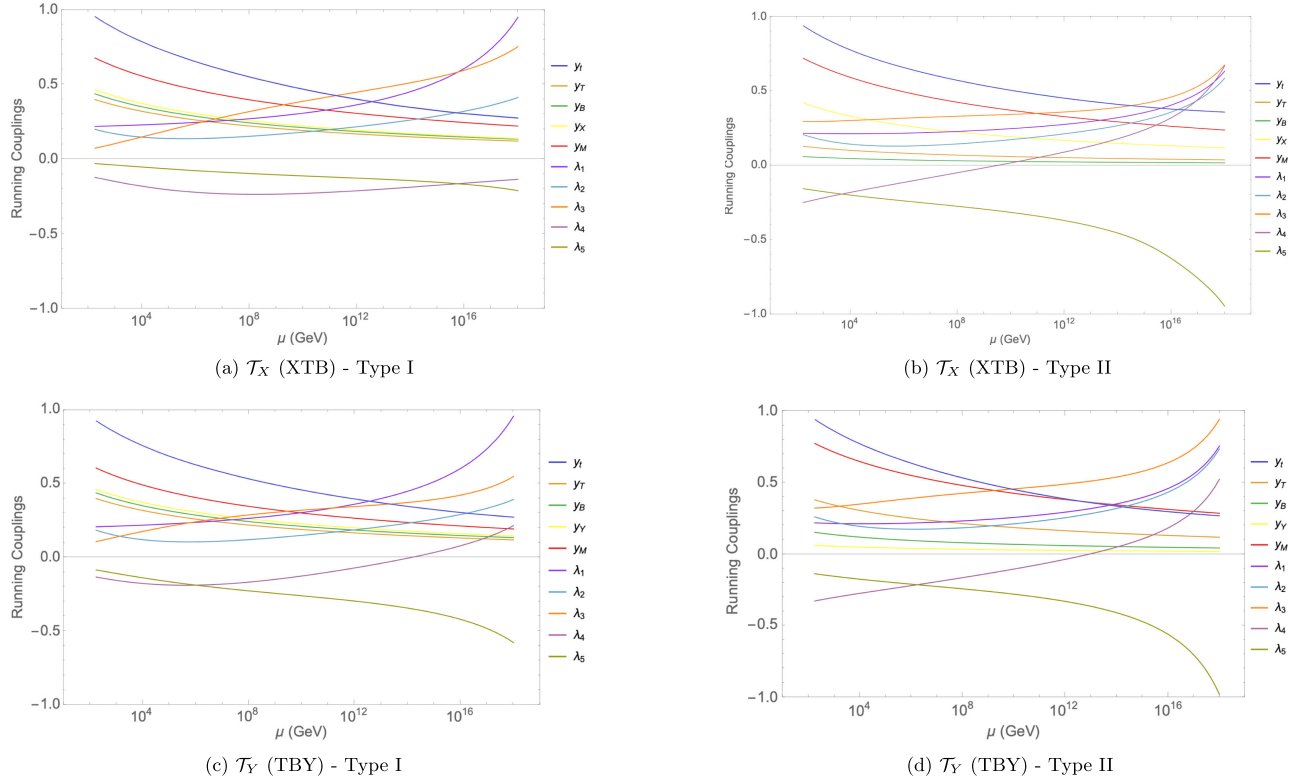


FIG. 4. The RGE running of the Yukawa and scalar couplings for models with vectorlike fermions. As before, we plot results for type-I on the left column and for type-II on the right column. Subfigures (a) and (b): triplet vectorlike representation, \mathcal{T}_X . Subfigures (c) and (d): triplet vectorlike representation, \mathcal{T}_Y . For triplet models, we have set $m_T = 0.9$ TeV, $m_B = 1$ TeV, $m_X = 1$ TeV, $m_Y = 1$ TeV, $M_H = 850$ GeV, $M_{H^\pm} = 800$ GeV, $M_A = 650$ GeV, $\mu_0 = m_t$, $\tan\beta = 10$, and mixing angles $\sin\alpha = 0.1$ and $\sin\theta_L = 0.08$.

$$\mathcal{D}_2 + \text{type-II: } m_T \in [840, 1010] \text{ GeV, } m_B \in [900, 1040] \text{ GeV, } M_{H^\pm} \in [600, 840] \text{ GeV, } M_H \in [810, 980] \text{ GeV, } M_A \in [640, 860] \text{ GeV.}$$

$$\mathcal{D}_Y + \text{type-I: } m_B \in [900, 970] \text{ GeV, } m_Y \in [900, 990] \text{ GeV, } M_{H^\pm} \in [80, 840] \text{ GeV, } M_H \in [750, 890] \text{ GeV, } M_A \in [610, 875] \text{ GeV.}$$

$$\mathcal{D}_Y + \text{type-II: } m_B \in [925, 1010] \text{ GeV, } m_Y \in [950, 1050] \text{ GeV, } M_{H^\pm} \in [600, 870] \text{ GeV, } M_H \in [750, 930] \text{ GeV, } M_A \in [670, 890] \text{ GeV.}$$

C. Triplet VLQ: \mathcal{T}_X and \mathcal{T}_Y

Finally, for triplets, plotted in Fig. 4, our RGE scanning indicates that the mass of the CP -even scalar exceeds 1 TeV, whereas M_{H^\pm} approaches an upper limit < 1 TeV, which is in good agreement with the mass limits extracted from the deviation of the oblique parameters according to CDF W -mass anomaly [120]. For triplet VLQs, a unique feature of the Yukawa couplings is that due to the dependence on y_M , their evolution becomes less suppressed as the energy scale grows. In fact, y_M , which is the Yukawa representation of Dirac mass terms for VLQs, surpasses the top Yukawa coupling at a scale around 10^{13} GeV. The parameter space for triplet VLQ + 2HDM extends the

upper bounds compared to other representations, because the opposite convolution of λ_4 and λ_5 always occurs for triplet VLQs due to the abundance of coupled terms. We also note that the stability condition on the electroweak vacuum is at its most critical state around 10^6 GeV regardless of the 2HDM type for triplet VLQs. This critical proximity to the instability case occurs at almost the same energy level regardless of all the parameters that satisfy the combined stability, perturbativity, and unitarity conditions.

The allowed parameter space for VLQ + 2HDM-I,II that survives from stability, perturbativity, and unitarity up to $\mu = M_{\text{Pl}}$ is as follows:

$$\mathcal{T}_X + \text{type-I: } m_X \in [900, 1070] \text{ GeV, } m_T \in [870, 990] \text{ GeV, } m_B \in [900, 1040] \text{ GeV, } M_{H^\pm} \in [80, 890] \text{ GeV, } M_H \in [780, 1030] \text{ GeV, } M_A \in [560, 930] \text{ GeV.}$$

$$\begin{aligned}
\mathcal{T}_X + \text{type-II:} & \quad m_X \in [950, 1100] \text{ GeV}, \quad m_T \in [890, 1000] \text{ GeV}, \quad m_B \in [925, 1040] \text{ GeV}, \quad M_{H^\pm} \in [600, 890] \text{ GeV}, \\
& \quad M_H \in [790, 910] \text{ GeV}, \quad M_A \in [700, 890] \text{ GeV}. \\
\mathcal{T}_Y + \text{type-I:} & \quad m_T \in [840, 950] \text{ GeV}, \quad m_B \in [890, 970] \text{ GeV}, \quad m_Y \in [880, 1020] \text{ GeV}, \quad M_{H^\pm} \in [80, 900] \text{ GeV}, \\
& \quad M_H \in [740, 1050] \text{ GeV}, \quad M_A \in [525, 940] \text{ GeV}. \\
\mathcal{T}_Y + \text{type-II:} & \quad m_T \in [860, 975] \text{ GeV}, \quad m_B \in [910, 1035] \text{ GeV}, \quad m_Y \in [950, 1100] \text{ GeV}, \quad M_{H^\pm} \in [600, 890] \text{ GeV}, \\
& \quad M_H \in [820, 1020] \text{ GeV}, \quad M_A \in [580, 910] \text{ GeV}.
\end{aligned}$$

For completeness, explicit expressions for all the relevant RGE for the Yukawa couplings, the couplings between the bosons and coupling constants, are included in the Appendix.

V. ELECTROWEAK PRECISION CONSTRAINTS

Signals from new physics are also constrained through electroweak precision observables, which are highly correlated to large logarithms of extra masses when the scale of a new model is significantly larger than the electroweak scale [121–123]. The modifications to electroweak gauge boson loops at loop level are calculated through the oblique parameters, \mathbb{S} , \mathbb{T} , and \mathbb{U} , defined as [124]

$$\begin{aligned}
\mathbb{S} &= 16\pi\mathfrak{R}[\bar{\Pi}_\gamma^{3Q}(M_Z^2) - \bar{\Pi}_Z^{33}(0)], \\
\mathbb{T} &= \frac{4\sqrt{2}G_F}{\alpha_e}\mathfrak{R}[\bar{\Pi}^{3Q}(0) - \bar{\Pi}^{11}(0)], \\
\mathbb{U} &= 16\pi\mathfrak{R}[\bar{\Pi}_Z^{33}(0) - \bar{\Pi}_W^{11}(0)]. \tag{38}
\end{aligned}$$

The \mathbb{S} and \mathbb{T} parameters in new physics models, such as VLQ scenarios and 2HDMs, are different from those in the SM due to extra scalars and fermions appearing in gauge boson self-energies at the loop level. Additionally, the mixing between the SM fields and the new particles modifies the Higgs and electroweak couplings as well. Consequently, electroweak precision observables are universal. The current experimental values [125] are obtained by fixing the differences between the new physics and the SM contributions by setting $\Delta\mathbb{U} = 0$, yielding $\Delta\mathbb{T} = 0.09 \pm 0.07$ and $\Delta\mathbb{S} = 0.05 \pm 0.08$ (and $\rho_{S,T} = 0.92 \pm 0.11$). For the work carried out here, we can split the oblique parameters calculation of \mathbb{S} , \mathbb{T} , and \mathbb{U} parameters via loop contributions into two independent contributions, one due to bosons and the other to fermions circulating in self-energy diagrams. We extracted

gauge boson self-energies using LoopTools and FormCalc [126], and implemented analytical expressions of Passarino-Veltman (PV) functions in FeynCalc [127] to obtain oblique parameters.

A. Contributions to the \mathbb{S} and \mathbb{T} parameters from 2HDM

Further expanding Eq. (38) explicitly in terms of the scalar loop contributions to the gauge boson two-point functions

$$\begin{aligned}
\mathbb{S}_{2\text{HDM}} &= 16\pi\mathfrak{R}\left[\frac{\Pi_{2\text{HDM}}^{Z\gamma}(M_Z^2)}{s_W c_W g_Z^2} + \frac{\Pi_{2\text{HDM}}^{\gamma\gamma}(M_Z^2)}{c_W^2 g_Z^2} \right. \\
&\quad \left. - \frac{\Pi_{2\text{HDM}}^{ZZ}(M_Z^2) - \Pi_{2\text{HDM}}^{ZZ}(0)}{g_Z^2} - \frac{2s_W \Pi_{2\text{HDM}}^{Z\gamma}(0)}{c_W g_Z^2} \right], \\
\mathbb{T}_{2\text{HDM}} &= \frac{4\sqrt{2}G_F}{\alpha_e}\mathfrak{R}\left[\frac{\Pi_{2\text{HDM}}^{ZZ}(0)}{g_Z^2} + \frac{2s_W \Pi_{2\text{HDM}}^{Z\gamma}(0)}{c_W g_Z^2} \right. \\
&\quad \left. - \frac{\Pi_{2\text{HDM}}^{WW}(0)}{c_W^2 g_Z^2} \right]. \tag{39}
\end{aligned}$$

The coupling factors are $g_Z = g/c_W$ and the photon two-point function in the 2HDM is

$$\begin{aligned}
\Pi_{2\text{HDM}}^{\gamma\gamma}(p^2) &= e^2 B_5(p^2, M_{H^\pm}^2, M_{H^\pm}^2) \\
&\quad - e^2 p^2 \left[5B_0(p^2, M_W^2, M_W^2) \right. \\
&\quad \left. + 12B_3(p^2, M_W^2, M_W^2) + \frac{2}{3} \right], \tag{40}
\end{aligned}$$

The photon-Z mixing is given by

$$\begin{aligned}
\Pi_{2\text{HDM}}^{Z\gamma}(p^2) &= \frac{eg_Z}{2} B_5(p^2, M_{H^\pm}^2, M_{H^\pm}^2) - eg_Z p^2 \left(\frac{11}{2} B_0(p^2, M_W^2, M_W^2) + 10B_3(p^2, M_W^2, M_W^2) + \frac{2}{3} \right) \\
&\quad - \frac{s_W}{c_W} \left[e^2 B_5(p^2, M_{H^\pm}^2, M_{H^\pm}^2) - e^2 p^2 \left[5B_0(p^2, M_W^2, M_W^2) + 12B_3(p^2, M_W^2, M_W^2) + \frac{2}{3} \right] \right]. \tag{41}
\end{aligned}$$

The Z-boson two-point function in the 2HDM is

$$\begin{aligned}
\Pi_{2\text{HDM}}^{ZZ}(p^2) = & g_Z^2 \left[\frac{s_{\beta-\alpha}^2}{4} B_5(p^2, M_H^2, M_A^2) + \frac{c_{\beta-\alpha}^2}{4} B_5(p^2, M_h^2, M_A^2) + \frac{1}{4} B_5(p^2, M_{H^\pm}^2, M_{H^\pm}^2) - \frac{2p^2}{3} \right. \\
& + s_{\beta-\alpha}^2 \left[M_Z^2 B_0(p^2, M_h^2, M_Z^2) + \frac{1}{4} B_5(p^2, M_h^2, M_Z^2) \right] + c_{\beta-\alpha}^2 \left[M_Z^2 B_0(p^2, M_H^2, M_Z^2) \right. \\
& + \left. \frac{1}{4} B_5(p^2, M_H^2, M_Z^2) \right] + 2M_W^2 B_0(p^2, M_W^2, M_W^2) - \frac{23p^2}{4} B_0(p^2, M_W^2, M_W^2) - 9p^2 B_3(p^2, M_W^2, M_W^2) \left. \right] \\
& - \frac{s_W^2}{c_W^2} \left(e^2 B_5(p^2, M_{H^\pm}^2, M_{H^\pm}^2) - e^2 p^2 \left[5B_0(p^2, M_W^2, M_W^2) + 12B_3(p^2, M_W^2, M_W^2) + \frac{2}{3} \right] \right) \\
& - \frac{2s_W}{c_W} \left[\frac{eg_Z}{2} B_5(p^2, M_{H^\pm}^2, M_{H^\pm}^2) - eg_Z p^2 \left(\frac{11}{2} B_0(p^2, M_W^2, M_W^2) + 10B_3(p^2, M_W^2, M_W^2) + \frac{2}{3} \right) \right. \\
& \left. - \frac{s_W}{c_W} \left(e^2 B_5(p^2, M_{H^\pm}^2, M_{H^\pm}^2) - e^2 p^2 \left[5B_0(p^2, M_W^2, M_W^2) + 12B_3(p^2, M_W^2, M_W^2) + \frac{2}{3} \right] \right) \right]. \tag{42}
\end{aligned}$$

The W -boson two-point function in the 2HDM follows as

$$\begin{aligned}
\Pi_{2\text{HDM}}^{WW}(p^2) = & g^2 \left[\frac{1}{4} B_5(p^2, M_A^2, M_{H^\pm}^2) + \frac{s_{\beta-\alpha}^2}{4} B_5(p^2, M_H^2, M_{H^\pm}^2) + \frac{c_{\beta-\alpha}^2}{4} B_5(p^2, M_h^2, M_{H^\pm}^2) - \frac{2p^2}{3} \right. \\
& + s_{\beta-\alpha}^2 \left[M_W^2 B_0(p^2, M_h^2, M_W^2) + \frac{1}{4} B_5(p^2, M_h^2, M_W^2) \right] - 8p^2 c_W^2 B_0(p^2, M_Z^2, M_W^2) \\
& + c_{\beta-\alpha}^2 \left[M_W^2 B_0(p^2, M_H^2, M_W^2) + \frac{1}{4} B_5(p^2, M_H^2, M_W^2) \right] + \left(\frac{1}{4} + 2c_W^2 \right) B_5(p^2, M_Z^2, M_W^2) \\
& + M_W^2 (1 - 4s_W^2) B_0(p^2, M_Z^2, M_W^2) + M_Z^2 B_0(p^2, M_Z^2, M_W^2) + 2s_W^2 B_5(p^2, 0, M_W^2) \\
& \left. + 2M_W^2 B_0(p^2, 0, M_W^2) - 4p^2 B_0(p^2, 0, M_W^2) \right]. \tag{43}
\end{aligned}$$

The Passarino-Veltman functions and relevant identities are given in Appendix A 5. Subtracting the SM contributions from the \mathbb{S} and \mathbb{T} parameters of the 2HDM yields the new physics contributions to oblique parameters:

$$\begin{aligned}
\Delta\mathbb{T}_{2\text{HDM}} = & \frac{1}{4\pi M_Z^2 c_W^2 s_W^2} [B_{00}(0, M_A^2, M_{H^\pm}^2) + B_{00}(0, M_Z^2, M_W^2) - B_{00}(0, M_W^2, M_h^2) - B_{00}(0, M_W^2, M_Z^2) \\
& + (4s_W^4 - 1) B_{00}(0, M_{H^\pm}^2, M_{H^\pm}^2) - 2M_{H^\pm}^2 s_W^4 [1 + B_0(0, M_{H^\pm}^2, M_{H^\pm}^2)] + s_{\beta-\alpha}^2 [B_{00}(0, M_H^2, M_{H^\pm}^2) \\
& + B_{00}(0, M_h^2, M_W^2) - B_{00}(0, M_H^2, M_A^2)] + c_{\beta-\alpha}^2 [M_W^2 B_0(0, M_h^2, M_W^2) + B_{00}(0, M_h^2, M_Z^2) \\
& - M_Z^2 B_0(0, M_h^2, M_Z^2) + B_{00}(0, M_h^2, M_{H^\pm}^2) - B_{00}(0, M_h^2, M_A^2) + B_{00}(0, M_H^2, M_W^2) \\
& - M_W^2 B_0(0, M_H^2, M_W^2) + M_Z^2 B_0(0, M_H^2, M_Z^2) - B_{00}(0, M_H^2, M_Z^2)], \tag{44}
\end{aligned}$$

$$\begin{aligned}
\Delta\mathbb{S}_{2\text{HDM}} = & \frac{1}{\pi M_Z^2} [2s_W^2 c_W^2 A_0(M_{H^\pm}^2) - B_{00}(M_Z^2, M_{H^\pm}^2, M_{H^\pm}^2) + (c_W^2 - s_W^2)^2 B_{00}(0, M_{H^\pm}^2, M_{H^\pm}^2) \\
& + s_{\beta-\alpha}^2 [B_{00}(M_Z^2, M_H^2, M_A^2) - B_{00}(0, M_H^2, M_A^2)] + c_{\beta-\alpha}^2 [B_{00}(M_Z^2, M_h^2, M_A^2) \\
& + B_{00}(0, M_h^2, M_Z^2) + B_{00}(M_Z^2, M_h^2, M_Z^2) - B_{00}(M_Z^2, M_H^2, M_Z^2) - B_{00}(0, M_H^2, M_A^2) \\
& - B_{00}(0, M_H^2, M_Z^2) + M_Z^2 B_0(M_Z^2, M_h^2, M_Z^2) + M_Z^2 B_0(0, M_H^2, M_Z^2) \\
& - M_Z^2 B_0(0, M_h^2, M_Z^2) - M_Z^2 B_0(M_Z^2, M_H^2, M_Z^2)]. \tag{45}
\end{aligned}$$

In Fig. 5 (left panel), the correlation between M_A and M_{H^\pm} due to EWPO does not constrain the masses in a stringent way, though when $M_A > 550$ GeV, the correlation becomes significantly important. The red region has

already been discarded by direct searches at LEP [115]. Considering the imposing theoretical bounds only, the findings from EWPO are consistent with the unitary bounds in the $M_A - M_{H^\pm}$ plane [65]. Note that $\tan\beta$

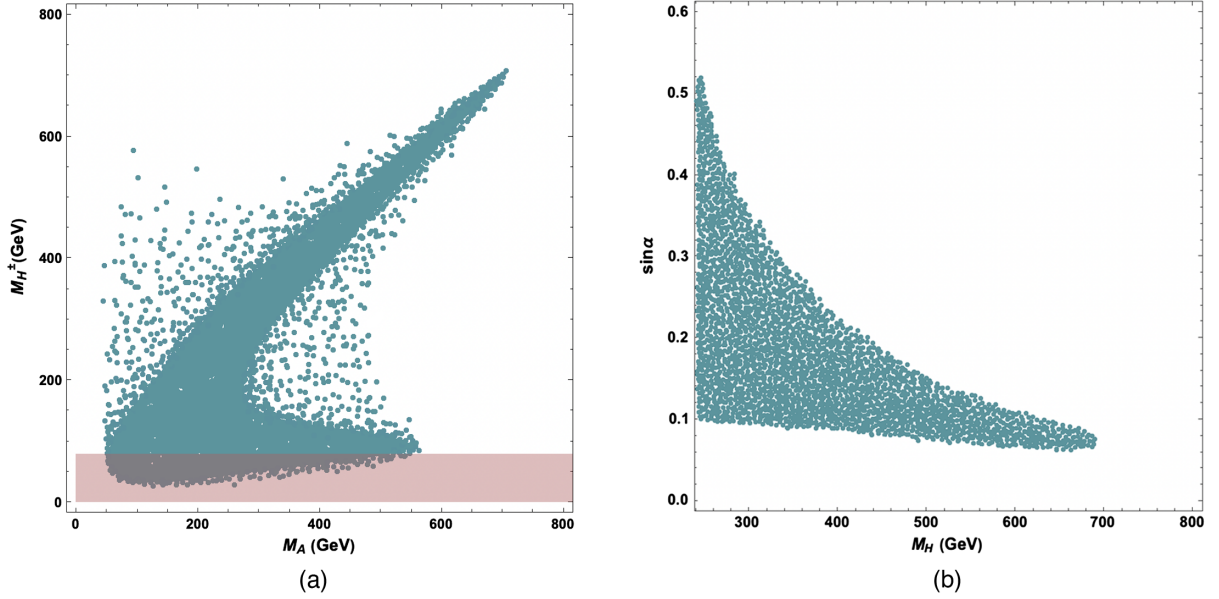


FIG. 5. The allowed mass regions from EWPO for the pseudoscalar boson mass M_A and charged Higgs mass M_{H^\pm} subfigure (a). The allowed parameter space from EWPO for scalar mass M_H and scalar mixing angle with the SM Higgs $\sin \alpha$ subfigure (b) in 2HDM. The $\sin \alpha = 0$ limit of CP -even scalars mixing is allowed by EWPO but excluded due to the vacuum stability constraint. We have set $\tan \beta = 6$.

dependence of the oblique parameters alone is more relaxed, allowing a wide mass spectrum. This is due to the fact that the mixing between CP -even scalars can be shifted away from the $\sin \alpha = 0$ (decoupling) limit; hence, the variation in $\tan \beta$ compensates for the Higgs data requirement of the near-alignment limit, $\cos(\beta - \alpha) \approx 0$. Consequently, imposing the alignment limit on the mass spectrum of scalars is by choice (to fit the Higgs data) rather than a requirement of the theory when RG running $\mu < 1$ TeV. This consequence is highlighted particularly for type-I with various $\tan \beta$ values [116]. On the other hand, as seen from Fig. 5 (right panel), the limit is stronger in the $M_H - \sin \alpha$ plane for a fixed value of $\tan \beta$ in both types of 2HDMs. It is seen that for $\tan \beta = 6$, EWPO constrain the masses in a way that the decoupling limit of CP -even scalars occurs in a natural way at a scale $\sim \mathcal{O}$ (TeV). Although the $\sin \alpha = 0$ (decoupling) limit is not forbidden by EWPO, we combined it with the minimum stability requirement on $\sin \alpha$ near the decoupling limit. Moreover, the constraints on M_H obtained from EWPO and from the vacuum stability match with the constraint for signal rates of $H \rightarrow WW^* \rightarrow e\nu\mu\nu$ [128,129]. Furthermore, we excluded the $\sin \alpha = 0$ region because a nonzero mixing between CP -even scalars ($\sin \alpha \neq 0$) is required to preserve the vacuum stability up to the Planck scale. As keeping $\cos(\beta - \alpha)$ closer to zero is motivated by the alignment limit from the Higgs data [42], we impose this along with the requirement that the couplings evolved with the RGEs remain away from the vacuum instability. Hence, using the mass spectrum allowed from EWPO constraints fits with the stability analysis. It is important

that the theoretical constraints align with each other as the limits rising from vacuum stability become stronger at the scale $[10^3, 10^{10}]$ GeV [119], thus restricting $M_{H^\pm} > 580$ GeV with smaller mass differences between extra scalars, as the cutoff scale increases in type-II. However, the mass limits in type-I are weaker. Favored also by collider bounds [41], there exists a parameter space for which the mass separation between scalars remains small for 2HDM, while validated up to the Planck scale. Our results from the oblique parameters do not conflict with the parameter space obtained from RGE in Sec. IV; however, the effects of VLQs on RGE slightly shift the upper limits compared to the findings of EWPO.

In Fig. 6, we have considered the energy scale $\mu = [800-1000]$ GeV in self-energy diagrams, and scan

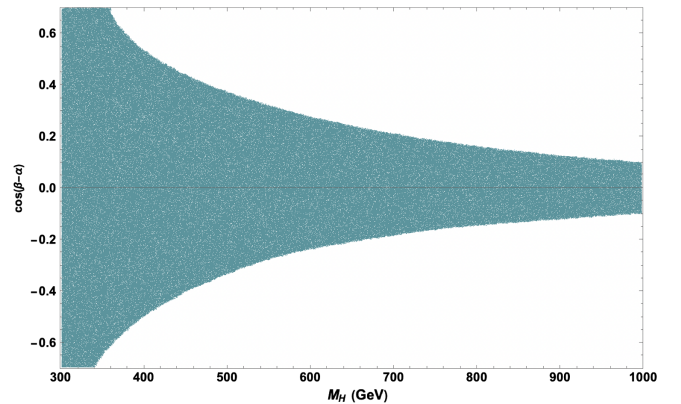


FIG. 6. The allowed mass regions extracted from EWPO for M_H versus $\cos(\beta - \alpha)$ mixing between CP -even scalars in 2HDM.

over values up to 1 TeV with respect to the oblique parameters. The upper limit of M_H is chosen to be in a good agreement with the limits from vacuum stability on scalars + VLQs at $\tan\beta = [6, 12]$. The current experimental data constraining h to having SM-like Higgs behavior restrict values of $\cos(\beta - \alpha)$ much closer to the decoupling limit. Consequently, the electroweak vacuum stability requirements and EWPO impose a naturally occurring near decoupling limit when $M_A, M_H > 600$ GeV. We should also note that type-I and type-II dependent effects are highly manifestable through Higgs channels, for which the signal strengths $\kappa_{hbb}, \kappa_{hcc}$ also favor regions slightly beyond the decoupling limit, particularly for $\tan\beta \sim [2, 12]$ [42]. The contribution to $\mathbb{T}_{2\text{HDM}}$ is twofold, depending on the mass parameter space of scalars and on $\sin(\beta - \alpha)$, whereas a negative contribution to $\mathbb{T}_{2\text{HDM}}$ can always be generated by varying M_{H^\pm} . For the general scale of $\sin(\beta - \alpha)$, M_h and M_H splitting has to be small for pushing $\mathbb{T}_{2\text{HDM}}$ to be large and negative values. Hence, negative corrections to \mathbb{T} in 2HDM can render overall positive corrections rising from various fermion representations and further enhancing limitations on additional scalars and mixing among Higgs bosons.

B. VLQ contributions to the \mathbb{S} and \mathbb{T} parameters

The contributions of VLQs to \mathbb{S} and \mathbb{T} parameters are different for each representation (singlets, doublets, or triplets) in the current framework. Since the electroweak Lagrangian is constructed with gauge eigenstate fields, any mixing of fermions with extra anomaly-free fields alters the structure of the bare electroweak Lagrangian, as seen from Eq. (46). As we have already seen in Sec. III A, the mixing regime is model dependent. Reference [130] highlighted the emergence of disagreement of the oblique parameters for triplets in [131], where the external momenta of gauge

bosons are omitted in self-energy diagrams Π_{VV} . This leads to a discrepancy in the \mathbb{S} parameter, which becomes positive in triplet representations in the large logarithm of $m_T \sim \mathcal{O}$ (TeV), as in Ref. [132]. Following the corrections carried in Ref. [130], we obtained better approximations to $\Delta\mathbb{S}_{\mathcal{T}_X, \mathcal{T}_Y}$ and $\Delta\mathbb{T}_{\mathcal{T}_X, \mathcal{T}_Y}$. Consequently, in our calculations $\Delta\mathbb{S} < 0$ and $\Delta\mathbb{T} > 0$, and we found agreement with the results in [133]. As we mentioned in Sec. VA, the self-energies of gauge bosons are extracted so that UV divergences are properly canceled. Here we present the contributions of VLQs to the oblique parameters in terms of PV functions, and more complete expressions are available in the Appendix.

The couplings to W -boson and Z -boson have been modified by the VLQs through their mixing with SM quarks

$$\begin{aligned}\mathcal{L}_W &= \frac{g}{\sqrt{2}} \bar{Q}_i \gamma^\mu (C_{Q_i Q_j}^L P_L + C_{Q_i Q_j}^R P_R) Q_j W_\mu^+ + \text{H.c.}, \\ \mathcal{L}_Z &= \frac{g}{2c_W} \bar{Q}_i \gamma^\mu (N_{Q_i Q_j}^L P_L + N_{Q_i Q_j}^R P_R - 2\delta_{ij} Q_i s_W^2) Q_j Z^\mu,\end{aligned}\quad (46)$$

where $Q_{i,j}$ are any type of quarks in our convention of the electroweak Lagrangian. The condition $|\mathbb{Q}_i - \mathbb{Q}_j| = 1$ holds for all forms of $W - Q_i - Q_j$ interactions.

Further compression of the modified electroweak couplings take the following forms:

$$\begin{aligned}\mathcal{L}_W &\supset \gamma^\mu (\Omega_{W Q_i Q_j}^L \mathbb{L} + \Omega_{W Q_i Q_j}^R \mathbb{R}) W_\mu^+, \\ \mathcal{L}_Z &\supset \gamma^\mu (\Omega_{Z Q_i Q_j}^L \mathbb{L} + \Omega_{Z Q_i Q_j}^R \mathbb{R}) Z_\mu.\end{aligned}\quad (47)$$

For the cases $i = j$ of $Z - Q_i - Q_j$ interactions, the last term of Eq. (46) is absorbed in $\Omega_{Z Q_i Q_j}^{L,R}$ throughout all VLQ representations:

$$\begin{aligned}\mathbb{T}_{\text{VLQ}} &= \frac{1}{\alpha_e} \Re \left[\frac{2s_W}{c_W M_Z^2} \sum_i \mathcal{F}_{Z\gamma}(\Omega_{Z Q_i Q_i}^L, \Omega_{Z Q_i Q_i}^R, \mathbb{Q}_i, m_i^2, p^2 = 0) + \frac{-2}{M_Z^2} \sum_{i \neq j} \delta(\mathbb{Q}_i - \mathbb{Q}_j) \mathcal{F}_{ZZ}(\Omega_{Z Q_i Q_j}^L, \Omega_{Z Q_i Q_j}^R, m_i^2, m_j^2, p^2 = 0) \right. \\ &\quad \left. + \frac{1}{M_Z^2} \sum_i \mathcal{F}_{ZZ}(\Omega_{Z Q_i Q_i}^L, \Omega_{Z Q_i Q_i}^R, m_i^2, m_i^2, p^2 = 0) + \frac{1}{M_W^2} \sum_{i \neq j} \delta(\mathbb{Q}_i - \mathbb{Q}_j) \mathcal{F}_{WW}(\Omega_{W Q_i Q_j}^L, \Omega_{W Q_i Q_j}^R, m_i^2, m_j^2, p^2 = 0) \right],\end{aligned}\quad (48)$$

$$\begin{aligned}\mathbb{S}_{\text{VLQ}} &= \frac{4s_W^2 c_W^2}{\alpha_e} \Re \left[\left(\frac{c_W^2 - s_W^2}{s_W c_W M_Z^2} \right) \left(\sum_i \mathcal{F}_{Z\gamma}(\Omega_{Z Q_i Q_i}^L, \Omega_{Z Q_i Q_i}^R, \mathbb{Q}_i, m_i^2, M_Z^2) + \sum_i \mathcal{F}_{Z\gamma}(\Omega_{Z Q_i Q_i}^L, \Omega_{Z Q_i Q_i}^R, \mathbb{Q}_i, m_i^2, 0) \right) \right. \\ &\quad - \frac{1}{M_Z^2} \sum_i \mathcal{F}_{\gamma\gamma}(\mathbb{Q}_i, \mathbb{Q}_i, m_i^2, m_i^2, M_Z^2) + \frac{2}{M_Z^2} \sum_{i \neq j} \delta(\mathbb{Q}_i - \mathbb{Q}_j) \mathcal{F}_{ZZ}(\Omega_{Z Q_i Q_j}^L, \Omega_{Z Q_i Q_j}^R, m_i^2, m_j^2, M_Z^2) \\ &\quad - \frac{2}{M_Z^2} \sum_{i \neq j} \delta(\mathbb{Q}_i - \mathbb{Q}_j) \mathcal{F}_{ZZ}(\Omega_{Z Q_i Q_j}^L, \Omega_{Z Q_i Q_j}^R, m_i^2, m_j^2, 0) + \frac{1}{M_Z^2} \sum_i \mathcal{F}_{ZZ}(\Omega_{Z Q_i Q_i}^L, \Omega_{Z Q_i Q_i}^R, m_i^2, m_i^2, M_Z^2) \\ &\quad \left. - \frac{1}{M_Z^2} \sum_i \mathcal{F}_{ZZ}(\Omega_{Z Q_i Q_i}^L, \Omega_{Z Q_i Q_i}^R, m_i^2, m_i^2, 0) \right],\end{aligned}\quad (49)$$

where the fermion functions $\mathcal{F}_{VV,Z\gamma}$ contributing to the gauge boson two-point functions are calculated as

$$\begin{aligned}\mathcal{F}_{Z\gamma}(\Omega_1, \Omega_2, \mathbb{Q}, m^2, p^2) &= \frac{N_c}{8\pi^2} [\mathbb{Q}(\Omega_1 + \Omega_2)(2B_{00}(p^2, m^2, m^2) - p^2 B_1(p^2, m^2, m^2) - A_0(m^2))], \\ \mathcal{F}_{VV}(\Omega_1, \Omega_2, m_1^2, m_2^2, p^2) &= \frac{N_c}{8\pi^2} [((\Omega_1^2 + \Omega_2^2)m_1^2 - 2\Omega_1\Omega_2 m_1 m_2)B_0(p^2, m_1^2, m_2^2) \\ &\quad + (\Omega_1^2 + \Omega_2^2)(p^2 B_1(p^2, m_1^2, m_2^2) - 2B_{00}(p^2, m_1^2, m_2^2) + A_0(m_2^2))].\end{aligned}\quad (50)$$

Complete expressions of the oblique parameters for doublets and triplets are lengthy. Thus, we give the full contributions to \mathbb{S} and \mathbb{T} parameters from singlet VLQ representations \mathcal{U}_1 and \mathcal{D}_1 , while approximated expressions for all multiplets are given in Appendix A 3. The deviations $\Delta\mathbb{T}$ and $\Delta\mathbb{S}$ of the oblique parameters from their SM values are

$$\Delta\mathbb{T}_{\mathcal{U}_1} = \frac{N_c m_t^4 (s_L^t)^2}{16\pi s_W^2 M_Z^2 (m_T^2 - m_t^2)} \left[\frac{m_T^2 - m_t^2}{m_t^2} (s_L^t)^2 \left(\frac{m_T^2 + m_t^2}{m_t^2} \right) - 4 \frac{m_T^2}{m_t^2} (c_L^t)^2 \ln(x_T) + 2 - 2x_T^2 \right], \quad (51)$$

$$\begin{aligned}\Delta\mathbb{S}_{\mathcal{U}_1} &= \frac{N_c}{12\pi M_Z^2} [(s_L^t)^2 A_0(m_t^2)(6m_T^2(c_L^t)^2 - 6m_t^2(c_L^t)^2 - M_Z^2(9(s_L^t)^2 - 10)) - 32A_0(m_T^2)M_Z^2 s_W^2 c_W^2 \\ &\quad - 18m_t^2 (s_L^t)^2 (c_L^t)^2 B_0(0, m_t^2, m_T^2) + 6(s_L^t)^2 (c_L^t)^2 B_0(M_Z^2, m_t^2, m_T^2)(M_Z^2(m_t^2 + m_T^2) - 2M_Z^4 + (m_T^2 - m_t^2)^2) \\ &\quad + (s_L^t)^2 A_0(m_T^2)(M_Z^2(9(s_L^t)^2 - 10) - 6m_T^2(c_L^t)^2 + 6m_t^2(c_L^t)^2) + m_T^2((s_L^t)^2 + 32s_W^2 c_W^2) - (s_L^t)^2 m_t^2 \\ &\quad - 3m_t^2 (s_L^t)^2 B_0(0, m_t^2, m_t^2)(3(s_L^t)^2 - 10) + m_T^2 B_0(0, m_T^2, m_T^2)(32s_W^2 c_W^2 - 12(s_L^t)^2) \\ &\quad + 2(s_L^t)^2 B_0(M_Z^2, m_t^2, m_T^2)(m_T^2((s_L^t)^2 + 8) - M_Z^2(3(s_L^t)^2 - 4)) \\ &\quad + 2(s_L^t)^2 B_0(M_Z^2, m_t^2, m_t^2)(m_t^2(3(s_L^t)^2 - 16) - M_Z^2(3(s_L^t)^2 - 4))],\end{aligned}\quad (52)$$

$$\begin{aligned}\Delta\mathbb{T}_{\mathcal{D}_1} &= \frac{N_c}{8\pi c_W^2 s_W^2 M_Z^2} \left[\left((s_L^b)^2 (c_L^b)^2 \left[B_{00}(0, m_b^2, m_B^2) - \frac{A_0(m_B^2)}{2} \right] - \frac{m_b^2 (s_L^b)^2 (c_L^b)^2}{2} B_0(0, m_b^2, m_B^2) \right) \right. \\ &\quad + \left(\frac{1}{16} \left(1 - \frac{4s_W^2}{3} \right)^2 + \frac{4s_W^4}{9} \right) [A_0(m_t^2) - 2B_{00}(0, m_t^2, m_t^2)] \\ &\quad + \left(\frac{m_t^2}{4} \left(1 - \frac{4s_W^2}{3} \right)^2 + \frac{m_t^2}{9} (4s_W^4 - 18) + \frac{2m_t^2 s_W^2}{3} \left(1 - \frac{4s_W^2}{3} \right) \right) B_0(0, m_t^2, m_t^2) \\ &\quad + \left(\left(\frac{1}{4} \left(\frac{2s_W^2}{3} - (c_L^b)^2 \right)^2 + \frac{s_W^4}{9} \right) [A_0(m_b^2) - 2B_{00}(0, m_b^2, m_b^2)] \right) \\ &\quad + \left(\frac{m_b^2}{4} \left(\frac{2s_W^2}{3} - (c_L^b)^2 \right)^2 + \frac{m_b^2 s_W^4}{9} - \frac{m_b^2 s_W^2}{3} \left(\frac{2s_W^2}{3} - (c_L^b)^2 \right) \right) B_0(0, m_b^2, m_b^2) \\ &\quad + \left(\left(\frac{1}{4} \left(\frac{2s_W^2}{3} - (s_L^b)^2 \right)^2 + \frac{s_W^4}{9} \right) [A_0(m_B^2) - 2B_{00}(0, m_B^2, m_B^2)] \right) \\ &\quad + \left(\frac{m_B^2}{4} \left(\frac{2s_W^2}{3} - (s_L^b)^2 \right)^2 + \frac{m_B^2 s_W^4}{9} - \frac{m_B^2 s_W^2}{3} \left(\frac{2s_W^2}{3} - (s_L^b)^2 \right) \right) B_0(0, m_B^2, m_B^2) \\ &\quad + \frac{2}{3} \left(\frac{8s_W^4}{3} - s_W^2 \right) [A_0(m_t^2) - 2B_{00}(0, m_t^2, m_t^2)] + \frac{s_W^2}{3} \left(\frac{4s_W^2}{3} - (c_L^b)^2 \right) [A_0(m_b^2) - 2B_{00}(0, m_b^2, m_b^2)] \\ &\quad + \frac{s_W^2}{3} \left(\frac{4s_W^2}{3} - (s_L^b)^2 \right) [A_0(m_B^2) - 2B_{00}(0, m_B^2, m_B^2)] + \frac{(c_L^b)^2}{2} [A_0(m_b^2) - 2B_{00}(0, m_t^2, m_b^2)] \\ &\quad \left. + \frac{m_t^2 (c_L^b)^2}{2} B_0(0, m_t^2, m_b^2) + \frac{(s_L^b)^2}{2} [A_0(m_B^2) - 2B_{00}(0, m_t^2, m_b^2)] + \frac{m_t^2 (s_L^b)^2}{2} B_0(0, m_t^2, m_B^2) \right],\end{aligned}\quad (53)$$

$$\begin{aligned}
\Delta\mathcal{S}_{\mathcal{D}_1} = & \frac{N_c}{12\pi M_Z^2} \left[\frac{2}{3} \ln \left(\frac{m_t^2}{m_b^2} \right) - 2 + (s_L^b)^2 (c_L^b)^2 (6B_{00}(m_Z^2, m_b^2, m_b^2) - 6B_{00}(0, m_b^2, m_b^2) + 3m_Z^2 B_1(M_Z^2, m_b^2, m_b^2)) \right. \\
& + m_b^2 (s_L^b)^2 (c_L^b)^2 (B_0(M_Z^2, m_b^2, m_b^2) - B_0(0, m_b^2, m_b^2)) \\
& - \frac{1}{c_W^2 s_W^2} \left(\frac{16}{3} [A_0(m_t^2) - 2B_{00}(M_Z^2, m_t^2, m_t^2) + M_Z^2 B_1(M_Z^2, m_t^2, m_t^2)] \right) \\
& - \frac{1}{c_W^2 s_W^2} \left(\frac{4}{3} [A_0(m_b^2) - 2B_{00}(M_Z^2, m_b^2, m_b^2) + M_Z^2 B_1(M_Z^2, m_b^2, m_b^2)] \right) \\
& - \frac{1}{c_W^2 s_W^2} \left(\frac{4}{3} [A_0(m_B^2) - 2B_{00}(M_Z^2, m_B^2, m_B^2) + M_Z^2 B_1(M_Z^2, m_B^2, m_B^2)] \right) \\
& + \left(\frac{3}{2} \left(1 - \frac{4s_W^2}{3} \right)^2 + \frac{8s_W^4}{3} \right) [M_Z^2 B_1(M_Z^2, m_t^2, m_t^2) + 2B_{00}(0, m_t^2, m_t^2) - 2B_{00}(M_Z^2, m_t^2, m_t^2)] \\
& + \left(\frac{3m_t^2}{2} \left(1 - \frac{4s_W^2}{3} \right)^2 + \frac{8m_t^2 s_W^4}{3} + 4m_t^2 s_W^2 \left(1 - \frac{4s_W^2}{3} \right) \right) [B_0(M_Z^2, m_t^2, m_t^2) - B_0(0, m_t^2, m_t^2)] \\
& + \left(\frac{3}{2} \left(\frac{2s_W^2}{3} - (c_L^b)^2 \right)^2 + \frac{2s_W^4}{3} \right) [M_Z^2 B_1(M_Z^2, m_b^2, m_b^2) + 2B_{00}(0, m_b^2, m_b^2) - 2B_{00}(M_Z^2, m_b^2, m_b^2)] \\
& + \left(\frac{3m_b^2}{2} \left(\frac{2s_W^2}{3} - (c_L^b)^2 \right)^2 + \frac{2m_b^2 s_W^4}{3} - 2m_b^2 s_W^2 \left(\frac{2s_W^2}{3} - (c_L^b)^2 \right) \right) [B_0(M_Z^2, m_b^2, m_b^2) - B_0(0, m_b^2, m_b^2)] \\
& + \left(\frac{3}{2} \left(\frac{2s_W^2}{3} - (s_L^b)^2 \right)^2 + \frac{2s_W^4}{3} \right) [M_Z^2 B_1(M_Z^2, m_B^2, m_B^2) + 2B_{00}(0, m_B^2, m_B^2) - 2B_{00}(M_Z^2, m_B^2, m_B^2)] \\
& + \left(\frac{3m_B^2}{2} \left(\frac{2s_W^2}{3} - (s_L^b)^2 \right)^2 + \frac{2m_B^2 s_W^4}{3} - 2m_B^2 s_W^2 \left(\frac{2s_W^2}{3} - (s_L^b)^2 \right) \right) [B_0(M_Z^2, m_B^2, m_B^2) - B_0(0, m_B^2, m_B^2)] \\
& + (c_W^2 - s_W^2) \left[\left(\frac{16s_W^2}{3} - 2 \right) [M_Z^2 B_1(M_Z^2, m_t^2, m_t^2) - 2B_{00}(M_Z^2, m_t^2, m_t^2) - 2B_{00}(0, m_t^2, m_t^2)] \right. \\
& + \left. \left(\frac{4s_W^2}{3} - (c_L^b)^2 \right) [M_Z^2 B_1(M_Z^2, m_b^2, m_b^2) - 2B_{00}(M_Z^2, m_b^2, m_b^2) - 2B_{00}(0, m_b^2, m_b^2)] \right] \\
& + \left. \left(\frac{4s_W^2}{3} - (s_L^b)^2 \right) [M_Z^2 B_1(M_Z^2, m_B^2, m_B^2) - 2B_{00}(M_Z^2, m_B^2, m_B^2) - 2B_{00}(0, m_B^2, m_B^2)] \right]. \tag{54}
\end{aligned}$$

Contributions to \mathcal{S} and \mathcal{T} parameters from doublet and triplet VLQ representations follow from Eqs. (48) and (49) by a straightforward calculation with the relevant electroweak couplings as in Appendix A 4.

In Fig. 7, we plot the parameter space restricting the mixing between $t - T$ and $b - B$ versus the corresponding VLQ masses satisfying EWPO, in accordance with the expressions given before. The largest deviations arise from the \mathcal{T} parameter due to the large logarithm of $(m_T/m_t)^2$, yielding a wide range for the mass-mixing spectrum compared to the \mathcal{S} parameter for all multiplets. In analogy with the case of $\sin \alpha = 0$ behavior in the scalar sector, decoupling between the VLQs and the SM quarks becomes more prominent as $m_{\text{VLQ}} \rightarrow \mathcal{O}(\text{TeV})$ scale. The behavior of the decoupling zone due to larger values of m_{VLQ} can be seen from Eq. (51), $\frac{\Delta}{m_{\text{VLQ}}} \sim s_L^t$. This consequence can always be viewed as a rule-of-thumb to explain why EWPO constraints are already satisfied in the decoupling

limit. However, regardless of m_{VLQ} , there are no model parameter contributions to \mathcal{S} and \mathcal{T} parameters in the zero mixing ($\sin \alpha = 0$) domain.

The mixing angle in the singlet \mathcal{D}_1 model, Fig. 7(b), is much more relaxed compared to that in the \mathcal{U}_1 model due to the fact that up- and down-type mixings are exclusively dependent on mass splitting between VLQ and the SM quark as seen from Eq. (30). In fact, this holds true for all models if the parameter space allows for $b - B$ mixing. The allowed space for $t - T$ mixing in the \mathcal{U}_1 model matches input values we used to assure the stability in type-I and type-II models, whereas scenario \mathcal{D}_1 lifts the upper bound of $b - B$ mixing to a scale that cannot stabilize the electroweak vacuum around $m_B \geq 1 \text{ TeV}$. Hence, the stability requirements are more severe than the oblique parameter requirements for singlets. The values of $\Delta\mathcal{T}_{\text{VLQ}}$ in \mathcal{U}_1 are always positive and accordingly have more potential to compensate for the negative effect of

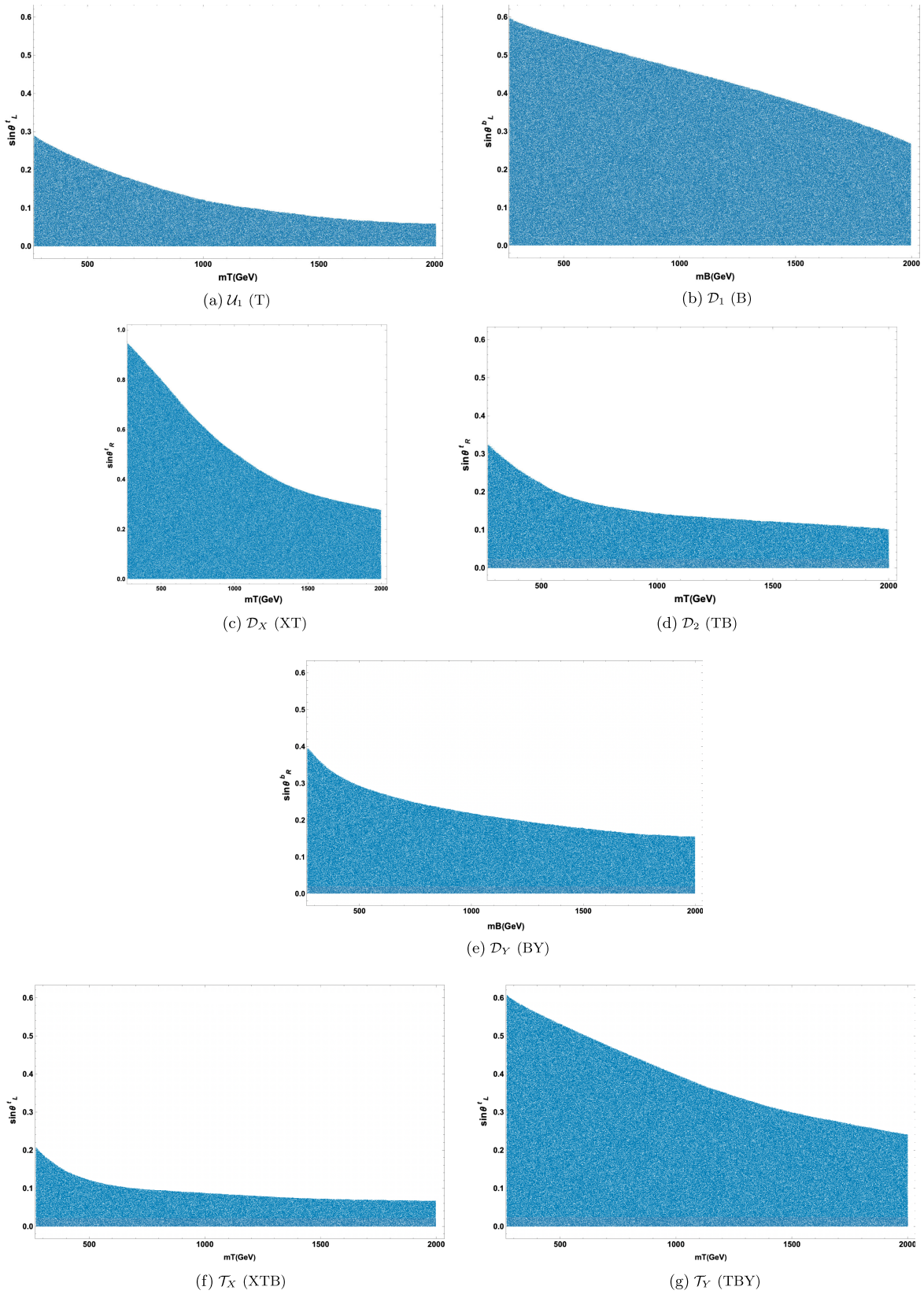


FIG. 7. The allowed parameter space from EWPO: T fermion mass and mixing angle with the top quark for the singlet \mathcal{U}_1 model (a), doublet \mathcal{D}_X (c), doublet \mathcal{D}_2 (d), triplet \mathcal{T}_X (f), and triplet \mathcal{T}_Y (g) models. The B fermion mass and mixing angle with the bottom quark for the singlet \mathcal{D}_1 model (b) and doublet \mathcal{D}_Y model (e). Loop functions are calculated at energy scale $\mu = m_t$.

$\Delta\mathbb{T}_{2\text{HDM}}$, whereas \mathcal{D}_1 features negative corrections to $\Delta\mathbb{T}_{\text{VLQ}}$. Thus, in terms of the oblique corrections between both sectors, \mathcal{U}_1 is capable of imposing more bounds on M_A, M_{H^\pm} , and $\cos(\beta - \alpha)$.

For doublets, the parameter space is larger than and similar to \mathcal{D}_1 except for \mathcal{D}_2 where $\Delta\mathbb{S}$ contributes negative values. We should emphasize that, for cases where \mathbb{S}_{VLQ} contributes negatively to cancel the positive effect of the \mathbb{T} parameter, the allowed parameter spaces are effectively enlarged as seen in Figs. 7(c) and 7(e) for \mathcal{D}_X and \mathcal{D}_Y models. In contrast, $\Delta\mathbb{S}$ is positive in \mathcal{D}_2 for $m_T \geq 645$ GeV. We also observe the behavior from Eq. (49), where the \mathcal{D}_2 model does not contribute to [flavor-changing-neutral-currents (FCNC) case] ZtT and ZbB channels; hence, \mathbb{S} is relatively larger than those in other doublets. Among all doublet models only \mathcal{D}_X has a negative $\Delta\mathbb{T}_{\text{VLQ}}$ contribution. On the other hand, $\Delta\mathbb{T}_{\text{VLQ}}$ stays close to zero in the \mathcal{D}_Y model, making it more limited for rendering $\Delta\mathbb{T}_{2\text{HDM}}$ negative, compared to the \mathcal{D}_2 model, where the correction $\Delta\mathbb{T}_{\text{VLQ}} \geq 0.08$ yields $m_T > 1$ TeV.

Furthermore, at the TeV scale, the EWPO parameter space of the \mathcal{D}_2 model is in good agreement with the vacuum stability requirements for $t - T$ mixing, while constraints in \mathcal{D}_X and $b - B$ mixing in \mathcal{D}_Y allow angles beyond the maximum allowed in the stability analysis.

The parameter space of the triplet \mathcal{T}_X model is quite restricted, and $t - T$ and $b - B$ mixing allowed by the oblique parameters do not cross beyond the vacuum stability requirements. However, for the model \mathcal{T}_Y , constraints are more relaxed, though $\sin\theta'_L > 0.2$ only exacerbate the constraints on vacuum stability. The relaxation of the mixing in the \mathcal{T}_Y scenario compared to that in \mathcal{T}_X can be described in terms of mixing relations Eq. (32). Since up- and down-type mixing angles are not independent for triplets, $s'_L \simeq \frac{s^b}{\sqrt{2}}$ ⁹ which enhances the Zbb coupling over the one in \mathcal{T}_Y , and thus leads to more severe corrections in \mathbb{S} [133]. $\Delta\mathbb{T}_{\text{VLQ}}$ is always positive in \mathcal{T}_Y , while \mathcal{T}_X has positive corrections to the \mathbb{T} parameter for $m_T > 400$ GeV. As a consequence, the \mathcal{T}_Y model is more relaxed as it compensates for the negative corrections in 2HDM, and it expands the parameter space through combined analysis of the oblique parameters.

VI. CONCLUSIONS

We analyzed the stability of the electroweak vacuum resulting from the interplay between vectorlike quarks and the extended bosonic sector of the two-Higgs-doublet model by adopting various representations to scrutinize the potential effects of vectorlike quarks on the Higgs sector. In particular, our work zooms in the effects of renormalization group flow that governs the energy scale

and flavor dependent behavior of interactions in the theory. Our investigation remains agnostic to specific parameter choices, while restricting the mixing of vectorlike quarks to solely with the third generation SM quarks. The core of the analysis revolves around the delicate balance of the Higgs potential stability. It has long been assumed that the SM lies in a metastable state or there is an alternative mechanics behind the absolute stability of the vacuum. In fact, there is an effective approach to extend the Higgs sector of the SM with additional scalar bosons, as allowed by certain symmetries of the model. To this end, an auxiliary scalar doublet is introduced here to ameliorate the SM vacuum predicament. Using RGEs in 2HDM, we showed the additional degree of freedom in the scalar sector enlarges the parameter space that might preserve the absolute stability of vacuum up to the Planck scale.

We then added all anomaly-free representations of vectorlike quarks (two singlet, three doublet, and two triplet representations). We showed that the inclusion of vectorlike quarks, although analogous in their couplings to SM quarks, has complicated consequences. Although fermions contribute negatively to the couplings at the RGE level, vectorlike quarks effectively modify β -functions through the gauge and Yukawa portals. Even though the gauge portal effects are weaker than those of the Yukawa couplings, the corrections are multiplicative with respect to the number of fermions in the family included. A natural and straightforward attempt could be to add more vectorlike quarks, considering their effect on gauge coupling modifications. However, there is a relationship between the number of vectorlike quarks and their masses that imposes an upper bound on each, for which the vacuum can be stabilized. If m_{VLQ} is too large and n_F is too small, then RG evolutions fall into the negative perturbativity region before lifting it up. On the other hand, if n_F is too large and m_{VLQ} too small, RG evolutions are too strong and abruptly diverge; thus, predictability is lost due to a Landau pole around $\mu < M_{\text{Pl}}$. Considering the strong gauge portal alone, this imposes the upper bounds: $m_{\text{VLQ}} \leq 10^6$ TeV and $n_F = [2, 18]$. Additionally, the hypercharge portal vanishes either by increasing m_{VLQ} , thus leaving insufficient RG evolution for the parameter space restrictions to be operative, or by increasing n_F causing a sub-Planckian theory breakdown. Increasing the hypercharge limits n_F to small values and to a narrower interval. Thus, allowed hypercharge values are obtained for the smallest number of flavors n_F , and there is a fine-tuned mutual relation between mass, flavor, and hypercharge of vectorlike quarks that is capable to generate absolute stability of the vacuum.

We imposed perturbative unitarity and stability constraints for $\lambda_i(\mu)$ and $y_i(\mu)$ in both type-I + VLQ and type-II + VLQ up to the Planck scale. All VLQ representations require $\tan\beta \in [6, 12]$ for the mass regime assumed from both sectors, with small fermionic mixing $\sin\theta_L < 0.2$. Although larger $\tan\beta$ values might satisfy

⁹This relation is valid for the triplet model \mathcal{T}_X .

the stability requirements, we observed that they lead to a heavy suppression of the quartic couplings in small perturbation regions due to the coupled nature. Initial conditions on $\lambda_{1,2}$ in type-II + VLQ are stronger due to the split of the Yukawa terms coupling to different scalar doublets. Generally, type-II + VLQs models require larger scalar masses compared to type-I model counterparts. Accordingly, for a given set of fixed parameters in both types, the vacuum stability conditions are safer in VLQ + type-II. Compared to T vectorlike quarks, constraints on the B -like fermion masses and mixing angles are much more relaxed. This is simply a consequence of the fact that the mixing between vectorlike quarks and the SM quarks is described in terms of the inverse of mass splitting between two quarks. Because of the excessive number of negative quartic Yukawa terms appearing at the RGE level, the constraints arising in bare 2HDM have to be enlarged from the considerations above. To this end, we checked both theoretically and experimentally allowed regions of 2HDM and VLQ models by preserving the validity of 2HDM up to the Planck scale.

We also scanned over EWPO and found the space for $t - T$ and $b - B$ mixings versus the mass of vectorlike quarks that includes stability regions, especially in the near decoupling limit. Furthermore, since the scalar and fermion parts of the oblique parameters are calculated separately and then combined, we found that the upper bound on the heavier CP -even scalar extends while preserving the vacuum stability conditions, especially when combined with triplet VLQs. For this reason, we assumed mass values of the heavier neutral scalar beyond the limits of 2HDM oblique parameters. However, the extension of the upper limit of M_H as $\cos(\beta - \alpha)$ approaches the alignment limit also confirms the stability requirement on scalar masses near the TeV scale.

Although mixing between CP -even states $\cos(\beta - \alpha) \neq 0$ is allowed by the oblique parameters, the stability requires at least near-alignment limit as $\cos(\beta - \alpha)$ remains close to zero. In fact, we observed that RGE running of λ_1 and λ_2 deteriorate, and the condition for the potential to be bounded from below cannot be satisfied as $\cos(\beta - \alpha)$ strays away from the alignment limit. Accordingly, the lower limit on the CP -even mixing angle from the stability and EWPO requirements also match the experimental Higgs bounds.

For the VLQ part of the oblique parameters, the allowed parameter space for $t - T$ and $b - B$ mixing is largest for cases where $\Delta\mathcal{S}$ contributes negatively and we have shown

that, for all vectorlike multiplets, the EWPO constraints lead to the alignment limit occurring naturally as $m_{\text{VLQ}} > 1$ TeV. In turn, constraints at a higher TeV range from the oblique parameters become more consistent with the stability requirements. Thus, the constraints to oblique parameters from vectorlike quarks, combined with $\Delta\mathcal{S}$ and $\Delta\mathcal{S}$ from the 2HDM, are VLQ representation dependent as well as different for type-I and type-II 2HDM and can be used to distinguish among different scenarios. In a specific representation and model-type, these corrections may indicate an allowed deviation from the required cancellations, and this would impose further restrictions on the extra scalar and its mixing with the SM Higgs boson.

ACKNOWLEDGMENTS

This work is funded in part by NSERC under Grant No. SAP105354.

APPENDIX

In the appendix sections below, for completeness, we give the renormalization group equations with respect to type-I and type-II models studied in the text, as well as expressions for the contributions of VLQs to the \mathcal{S} and \mathcal{T} parameters, together with the Passarino-Veltman integrals used. We also list the electroweak couplings of the VLQs of different representations.

1. RGEs for 2HDM + VLQ: Type-I

a. Singlet $\mathcal{U}_1(T)$, $Y = 2/3$

The relevant RGEs for the Yukawa couplings are

$$\begin{aligned} \frac{dy_t^2}{d \ln \mu^2} &= \frac{y_t^2}{16\pi^2} \left(\frac{9y_t^2}{2} + \frac{9y_T^2}{2} - \frac{17g_1^2}{12} - \frac{9g_2^2}{4} - 8g_3^2 \right), \\ \frac{dy_T^2}{d \ln \mu^2} &= \frac{y_T^2}{16\pi^2} \left(\frac{9y_t^2}{2} + \frac{9y_T^2}{2} + \frac{3y_M^2}{2} - \frac{17g_1^2}{12} - \frac{9g_2^2}{4} - 8g_3^2 \right), \\ \frac{dy_M^2}{d \ln \mu^2} &= \frac{y_M^2}{16\pi^2} \left(y_T^2 + \frac{9y_M^2}{2} - \frac{41g_1^2}{20} - 8g_3^2 \right). \end{aligned} \quad (\text{A1})$$

The Higgs sector RGEs, describing the interactions between the two bosons, are

$$\begin{aligned} \frac{d\lambda_1}{d \ln \mu^2} &= \frac{1}{16\pi^2} \left[-4\lambda_1 \left(\frac{3g_1^2}{4} + \frac{9g_2^2}{4} \right) + 12\lambda_1^2 + 4\lambda_3^2 + 4\lambda_3\lambda_4 + 2\lambda_4^2 + 2\lambda_5^2 + \frac{3g_1^4}{4} + \frac{9g_2^4}{4} + \frac{3g_1^2g_2^2}{2} \right], \\ \frac{d\lambda_2}{d \ln \mu^2} &= \frac{1}{16\pi^2} \left[4\lambda_2 \left(6y_t^2 + 6y_T^2 - \frac{3g_1^2}{4} - \frac{9g_2^2}{4} \right) + 12\lambda_2^2 + 4\lambda_3^2 + 4\lambda_3\lambda_4 + 2\lambda_4^2 + 2\lambda_5^2 \right. \\ &\quad \left. + \frac{3g_1^4}{16} + \frac{9g_2^4}{4} + \frac{3g_1^2g_2^2}{2} - 12y_t^4 - 24y_T^4 - 24y_t^2y_T^2 \right], \end{aligned}$$

$$\begin{aligned}
\frac{d\lambda_3}{d\ln\mu^2} &= \frac{1}{16\pi^2} \left[2\lambda_3 \left(6y_t^2 + 6y_T^2 + 12y_M^2 - \frac{3g_1^2}{2} - \frac{9g_2^2}{2} \right) + 4\lambda_3^2 + 2\lambda_4^2 + 2\lambda_5^2 + (\lambda_1 + \lambda_2)(6\lambda_3 + 2\lambda_4) \right. \\
&\quad \left. + \frac{3g_1^4}{4} + \frac{9g_2^4}{4} - \frac{3g_1^2g_2^2}{2} \right], \\
\frac{d\lambda_4}{d\ln\mu^2} &= \frac{1}{16\pi^2} \left[2\lambda_4 \left(6y_t^2 + 6y_T^2 + 12y_M^2 - \frac{3g_1^2}{2} - \frac{9g_2^2}{2} \right) + 3g_1^2g_2^2 + 4\lambda_4^2 + 8\lambda_5^2 + 8\lambda_3\lambda_4 + 2\lambda_4(\lambda_1 + \lambda_2) \right], \\
\frac{d\lambda_5}{d\ln\mu^2} &= \frac{1}{16\pi^2} \left[2\lambda_5 \left(6y_t^2 + 6y_T^2 + 12y_M^2 - \frac{3g_1^2}{2} - \frac{9g_2^2}{2} \right) + 2\lambda_5(\lambda_1 + \lambda_2 + 4\lambda_3 + 6\lambda_4) \right]. \tag{A2}
\end{aligned}$$

b. Singlet $\mathcal{D}_1(B)$, $Y = -1/3$

The relevant RGEs for the Yukawa couplings are

$$\begin{aligned}
\frac{dy_t^2}{d\ln\mu^2} &= \frac{y_t^2}{16\pi^2} \left(\frac{9y_t^2}{2} + \frac{3y_B^2}{2} - \frac{17g_1^2}{12} - \frac{9g_2^2}{4} - 8g_3^2 \right), \\
\frac{dy_B^2}{d\ln\mu^2} &= \frac{y_B^2}{16\pi^2} \left(\frac{3y_t^2}{2} + \frac{9y_B^2}{2} + \frac{3y_M^2}{2} - \frac{5g_1^2}{12} - \frac{9g_2^2}{4} - 8g_3^2 \right), \\
\frac{dy_M^2}{d\ln\mu^2} &= \frac{y_M^2}{16\pi^2} \left(\frac{9y_M^2}{2} + y_B^2 - \frac{17g_1^2}{20} - 8g_3^2 \right). \tag{A3}
\end{aligned}$$

The Higgs sector RGEs, describing the interactions between the two bosons, are

$$\begin{aligned}
\frac{d\lambda_1}{d\ln\mu^2} &= \frac{1}{16\pi^2} \left[-4\lambda_1 \left(\frac{3g_1^2}{4} + \frac{9g_2^2}{4} \right) + 12\lambda_1^2 + 4\lambda_3^2 + 4\lambda_3\lambda_4 + 2\lambda_4^2 + 2\lambda_5^2 + \frac{3g_1^4}{4} + \frac{9g_2^4}{4} + \frac{3g_1^2g_2^2}{2} \right], \\
\frac{d\lambda_2}{d\ln\mu^2} &= \frac{1}{16\pi^2} \left[4\lambda_2 \left(6y_t^2 + 6y_B^2 - \frac{3g_1^2}{4} - \frac{9g_2^2}{4} \right) + 12\lambda_2^2 + 4\lambda_3^2 + 4\lambda_3\lambda_4 + 2\lambda_4^2 + 2\lambda_5^2 \right. \\
&\quad \left. + \frac{3g_1^4}{16} + \frac{9g_2^4}{4} + \frac{3g_1^2g_2^2}{2} - 12y_t^4 - 24y_B^4 \right], \\
\frac{d\lambda_3}{d\ln\mu^2} &= \frac{1}{16\pi^2} \left[2\lambda_3 \left(6y_t^2 + 6y_B^2 + 12y_M^2 - \frac{3g_1^2}{2} - \frac{9g_2^2}{2} \right) + 4\lambda_3^2 + 2\lambda_4^2 + 2\lambda_5^2 + (\lambda_1 + \lambda_2)(6\lambda_3 + 2\lambda_4) \right. \\
&\quad \left. + \frac{3g_1^4}{4} + \frac{9g_2^4}{4} - \frac{3g_1^2g_2^2}{2} \right], \\
\frac{d\lambda_4}{d\ln\mu^2} &= \frac{1}{16\pi^2} \left[2\lambda_4 \left(6y_t^2 + 6y_B^2 + 12y_M^2 - \frac{3g_1^2}{2} - \frac{9g_2^2}{2} \right) + 3g_1^2g_2^2 + 4\lambda_4^2 + 8\lambda_5^2 + 8\lambda_3\lambda_4 + 2\lambda_4(\lambda_1 + \lambda_2) \right], \\
\frac{d\lambda_5}{d\ln\mu^2} &= \frac{1}{16\pi^2} \left[2\lambda_5 \left(6y_t^2 + 6y_B^2 + 12y_M^2 - \frac{3g_1^2}{2} - \frac{9g_2^2}{2} \right) + 2\lambda_5(\lambda_1 + \lambda_2 + 4\lambda_3 + 6\lambda_4) \right]. \tag{A4}
\end{aligned}$$

Finally, the coupling constants gain additional terms due to the new fermion, for both models \mathcal{U}_1 and \mathcal{D}_1 with singlet fermions as follows:

$$\frac{dg_1^2}{d\ln\mu^2} = \frac{g_1^4}{16\pi^2} \left(7 + \frac{4}{15} \right), \quad \frac{dg_2^2}{d\ln\mu^2} = \frac{g_2^4}{16\pi^2} (-3), \quad \frac{dg_3^2}{d\ln\mu^2} = \frac{g_3^4}{16\pi^2} \left(-7 + \frac{2}{3} \right). \tag{A5}$$

c. Doublet $\mathcal{D}_2 (T,B)$, $Y=1/6$

The relevant RGEs for the Yukawa couplings are

$$\begin{aligned}
\frac{dy_i^2}{d \ln \mu^2} &= \frac{y_i^2}{16\pi^2} \left(\frac{9y_i^2}{2} + \frac{9y_T^2}{2} + \frac{3y_B^2}{2} + 3y_M^2 - \frac{17g_1^2}{12} - \frac{9g_2^2}{4} - 8g_3^2 \right), \\
\frac{dy_T^2}{d \ln \mu^2} &= \frac{y_T^2}{16\pi^2} \left(\frac{9y_i^2}{2} + \frac{9y_T^2}{2} + \frac{3y_B^2}{2} + 3y_M^2 - \frac{17g_1^2}{12} - \frac{9g_2^2}{4} - 8g_3^2 \right), \\
\frac{dy_B^2}{d \ln \mu^2} &= \frac{y_B^2}{16\pi^2} \left(\frac{9y_i^2}{2} + \frac{3y_T^2}{2} + \frac{9y_B^2}{2} + 3y_M^2 - \frac{5g_1^2}{12} - \frac{9g_2^2}{4} - 8g_3^2 \right), \\
\frac{dy_M^2}{d \ln \mu^2} &= \frac{y_M^2}{16\pi^2} \left(y_T^2 + y_B^2 + \frac{11y_M^2}{2} - \frac{19g_1^2}{40} - \frac{9g_2^2}{2} - 8g_3^2 \right).
\end{aligned} \tag{A6}$$

The Higgs sector RGEs, describing the interactions between the two bosons, are

$$\begin{aligned}
\frac{d\lambda_1}{d \ln \mu^2} &= \frac{1}{16\pi^2} \left[-4\lambda_1 \left(\frac{3g_1^2}{4} + \frac{9g_2^2}{4} \right) + 12\lambda_1^2 + 4\lambda_3^2 + 4\lambda_3\lambda_4 + 2\lambda_4^2 + 2\lambda_5^2 + \frac{3g_1^4}{4} + \frac{9g_2^4}{4} + \frac{3g_1^2g_2^2}{2} \right], \\
\frac{d\lambda_2}{d \ln \mu^2} &= \frac{1}{16\pi^2} \left[4\lambda_2 \left(3y_i^2 + 6y_T^2 + 6y_B^2 - \frac{3g_1^2}{4} - \frac{9g_2^2}{4} \right) + 12\lambda_2^2 + 4\lambda_3^2 + 4\lambda_3\lambda_4 + 2\lambda_4^2 + 2\lambda_5^2 \right. \\
&\quad \left. + \frac{3g_1^4}{4} + \frac{9g_2^4}{4} + \frac{3g_1^2g_2^2}{2} - 12y_i^4 - 24y_T^4 - 24y_B^4 - 24y_i^2y_T^2 - 24y_T^2y_B^2 \right], \\
\frac{d\lambda_3}{d \ln \mu^2} &= \frac{1}{16\pi^2} \left[2\lambda_3 \left(3y_i^2 + 6y_T^2 + 6y_B^2 + 12y_M^2 - \frac{3g_1^2}{2} - \frac{9g_2^2}{2} \right) + 4\lambda_3^2 + 2\lambda_4^2 + 2\lambda_5^2 + (\lambda_1 + \lambda_2)(6\lambda_3 + 2\lambda_4) \right. \\
&\quad \left. + \frac{3g_1^4}{4} + \frac{9g_2^4}{4} - \frac{3g_1^2g_2^2}{2} \right], \\
\frac{d\lambda_4}{d \ln \mu^2} &= \frac{1}{16\pi^2} \left[2\lambda_4 \left(3y_i^2 + 6y_T^2 + 6y_B^2 + 12y_M^2 - \frac{3g_1^2}{2} - \frac{9g_2^2}{2} \right) + 3g_1^2g_2^2 + 4\lambda_4^2 + 8\lambda_5^2 + 8\lambda_3\lambda_4 + 2\lambda_4(\lambda_1 + \lambda_2) \right], \\
\frac{d\lambda_5}{d \ln \mu^2} &= \frac{1}{16\pi^2} \left[2\lambda_5 \left(3y_i^2 + 6y_T^2 + 6y_B^2 + 12y_M^2 - \frac{3g_1^2}{2} - \frac{9g_2^2}{2} \right) + 2\lambda_5(\lambda_1 + \lambda_2 + 4\lambda_3 + 6\lambda_4) \right].
\end{aligned} \tag{A7}$$

d. Doublet $\mathcal{D}_X (X,T)$, $Y=7/6$

The relevant RGEs for the Yukawa couplings are

$$\begin{aligned}
\frac{dy_i^2}{d \ln \mu^2} &= \frac{y_i^2}{16\pi^2} \left(\frac{9y_i^2}{2} + \frac{3y_T^2}{2} + \frac{9y_X^2}{2} + 3y_M^2 - \frac{17g_1^2}{12} - \frac{9g_2^2}{4} - 8g_3^2 \right), \\
\frac{dy_T^2}{d \ln \mu^2} &= \frac{y_T^2}{16\pi^2} \left(\frac{9y_i^2}{2} + \frac{3y_X^2}{2} + \frac{9y_T^2}{2} + 3y_M^2 - \frac{5g_1^2}{12} - \frac{9g_2^2}{4} - 8g_3^2 \right), \\
\frac{dy_X^2}{d \ln \mu^2} &= \frac{y_X^2}{16\pi^2} \left(\frac{9y_i^2}{2} + \frac{9y_X^2}{2} + \frac{3y_T^2}{2} + 3y_M^2 - \frac{17g_1^2}{12} - \frac{9g_2^2}{4} - 8g_3^2 \right), \\
\frac{dy_M^2}{d \ln \mu^2} &= \frac{y_M^2}{16\pi^2} \left(y_T^2 + y_X^2 + \frac{11y_M^2}{2} - \frac{67g_1^2}{40} - \frac{9g_2^2}{2} - 8g_3^2 \right).
\end{aligned} \tag{A8}$$

The Higgs sector RGEs, describing the interactions between the two bosons, are

$$\begin{aligned}
\frac{d\lambda_1}{d\ln\mu^2} &= \frac{1}{16\pi^2} \left[-4\lambda_1 \left(\frac{3g_1^2}{4} + \frac{9g_2^2}{4} \right) + 12\lambda_1^2 + 4\lambda_3^2 + 4\lambda_3\lambda_4 + 2\lambda_4^2 + 2\lambda_5^2 + \frac{3g_1^4}{4} + \frac{9g_2^4}{4} + \frac{3g_1^2g_2^2}{2} \right], \\
\frac{d\lambda_2}{d\ln\mu^2} &= \frac{1}{16\pi^2} \left[4\lambda_2 \left(3y_i^2 + 6y_T^2 + 6y_X^2 - \frac{3g_1^2}{4} - \frac{9g_2^2}{4} \right) + 12\lambda_2^2 + 4\lambda_3^2 + 4\lambda_3\lambda_4 + 2\lambda_4^2 + 2\lambda_5^2 \right. \\
&\quad \left. + \frac{3g_1^4}{4} + \frac{9g_2^4}{4} + \frac{3g_1^2g_2^2}{2} - 12y_i^4 - 24y_X^4 - 24y_T^4 - 24y_i^2y_T^2 - 24y_X^2y_T^2 \right], \\
\frac{d\lambda_3}{d\ln\mu^2} &= \frac{1}{16\pi^2} \left[2\lambda_3 \left(3y_i^2 + 6y_T^2 + 6y_X^2 + 12y_M^2 - \frac{3g_1^2}{2} - \frac{9g_2^2}{10} \right) + 4\lambda_3^2 + 2\lambda_4^2 + 2\lambda_5^2 + (\lambda_1 + \lambda_2)(6\lambda_3 + 2\lambda_4) \right. \\
&\quad \left. + \frac{3g_1^4}{4} + \frac{9g_2^4}{4} - \frac{3g_1^2g_2^2}{2} \right], \\
\frac{d\lambda_4}{d\ln\mu^2} &= \frac{1}{16\pi^2} \left[2\lambda_4 \left(3y_i^2 + 6y_T^2 + 6y_X^2 + 12y_M^2 - \frac{3g_1^2}{2} - \frac{9g_2^2}{10} \right) + 3g_1^2g_2^2 + 4\lambda_4^2 + 8\lambda_5^2 + 8\lambda_3\lambda_4 + 2\lambda_4(\lambda_1 + \lambda_2) \right], \\
\frac{d\lambda_5}{d\ln\mu^2} &= \frac{1}{16\pi^2} \left[2\lambda_5 \left(3y_i^2 + 6y_T^2 + 6y_X^2 + 12y_M^2 - \frac{3g_1^2}{2} - \frac{9g_2^2}{10} \right) + 2\lambda_5(\lambda_1 + \lambda_2 + 4\lambda_3 + 6\lambda_4) \right]. \tag{A9}
\end{aligned}$$

e. Additional non-SM-like quark doublet \mathcal{D}_Y (B, Y), $Y = -5/6$

The relevant RGEs for the Yukawa couplings are

$$\begin{aligned}
\frac{dy_i^2}{d\ln\mu^2} &= \frac{y_i^2}{16\pi^2} \left(\frac{9y_i^2}{2} + \frac{9y_B^2}{2} + \frac{3y_Y^2}{2} + 3y_M^2 - \frac{17g_1^2}{12} - \frac{9g_2^2}{4} - 8g_3^2 \right), \\
\frac{dy_B^2}{d\ln\mu^2} &= \frac{y_B^2}{16\pi^2} \left(\frac{9y_i^2}{2} + \frac{9y_B^2}{2} + \frac{3y_Y^2}{2} + 3y_M^2 - \frac{17g_1^2}{12} - \frac{9g_2^2}{4} - 8g_3^2 \right), \\
\frac{dy_Y^2}{d\ln\mu^2} &= \frac{y_Y^2}{16\pi^2} \left(\frac{3y_i^2}{2} + \frac{9y_Y^2}{2} + \frac{3y_B^2}{2} + 3y_M^2 - \frac{5g_1^2}{12} - \frac{9g_2^2}{4} - 8g_3^2 \right), \\
\frac{dy_M^2}{d\ln\mu^2} &= \frac{y_M^2}{16\pi^2} \left(y_Y^2 + y_B^2 + \frac{11y_M^2}{2} - \frac{43g_1^2}{40} - \frac{9g_2^2}{2} - 8g_3^2 \right). \tag{A10}
\end{aligned}$$

The Higgs sector RGEs, describing the interactions between the two bosons, are

$$\begin{aligned}
\frac{d\lambda_1}{d\ln\mu^2} &= \frac{1}{16\pi^2} \left[-4\lambda_1 \left(\frac{3g_1^2}{4} + \frac{9g_2^2}{4} \right) + 12\lambda_1^2 + 4\lambda_3^2 + 4\lambda_3\lambda_4 + 2\lambda_4^2 + 2\lambda_5^2 + \frac{3g_1^4}{4} + \frac{9g_2^4}{4} + \frac{3g_1^2g_2^2}{2} \right], \\
\frac{d\lambda_2}{d\ln\mu^2} &= \frac{1}{16\pi^2} \left[4\lambda_2 \left(3y_i^2 + 6y_B^2 + 6y_Y^2 - \frac{3g_1^2}{4} - \frac{9g_2^2}{4} \right) + 12\lambda_2^2 + 4\lambda_3^2 + 4\lambda_3\lambda_4 + 2\lambda_4^2 + 2\lambda_5^2 \right. \\
&\quad \left. + \frac{3g_1^4}{4} + \frac{9g_2^4}{4} + \frac{3g_1^2g_2^2}{2} - 12y_i^4 - 24y_B^4 - 24y_Y^4 - 24y_B^2y_Y^2 \right], \\
\frac{d\lambda_3}{d\ln\mu^2} &= \frac{1}{16\pi^2} \left[2\lambda_3 \left(3y_i^2 + 6y_B^2 + 6y_Y^2 + 12y_M^2 - \frac{3g_1^2}{2} - \frac{9g_2^2}{2} \right) + 4\lambda_3^2 + 2\lambda_4^2 + 2\lambda_5^2 + (\lambda_1 + \lambda_2)(6\lambda_3 + 2\lambda_4) \right. \\
&\quad \left. + \frac{3g_1^4}{4} + \frac{9g_2^4}{4} - \frac{3g_1^2g_2^2}{2} \right], \\
\frac{d\lambda_4}{d\ln\mu^2} &= \frac{1}{16\pi^2} \left[2\lambda_4 \left(3y_i^2 + 6y_Y^2 + 6y_B^2 + 12y_M^2 - \frac{3g_1^2}{2} - \frac{9g_2^2}{2} \right) + 3g_1^2g_2^2 + 4\lambda_4^2 + 8\lambda_5^2 + 8\lambda_3\lambda_4 + 2\lambda_4(\lambda_1 + \lambda_2) \right], \\
\frac{d\lambda_5}{d\ln\mu^2} &= \frac{1}{16\pi^2} \left[2\lambda_5 \left(3y_i^2 + 6y_Y^2 + 6y_B^2 + 12y_M^2 - \frac{3g_1^2}{2} - \frac{9g_2^2}{10} \right) + 2\lambda_5(\lambda_1 + \lambda_2 + 4\lambda_3 + 6\lambda_4) \right]. \tag{A11}
\end{aligned}$$

The coupling constants gain additional terms due to the new fermion in all doublet models as follows:

$$\frac{dg_1^2}{d \ln \mu^2} = \frac{g_1^4}{16\pi^2} \left(7 + \frac{6}{5}\right), \quad \frac{dg_2^2}{d \ln \mu^2} = \frac{g_2^4}{16\pi^2} (-3 + 2), \quad \frac{dg_3^2}{d \ln \mu^2} = \frac{g_3^4}{16\pi^2} \left(-7 + \frac{4}{3}\right). \quad (\text{A12})$$

f. Triplet $\mathcal{T}_X (X, T, B), Y = 2/3$

The relevant RGEs for the Yukawa couplings are

$$\begin{aligned} \frac{dy_i^2}{d \ln \mu^2} &= \frac{y_i^2}{16\pi^2} \left(\frac{9y_i^2}{2} + \frac{9y_X^2}{2} + \frac{9y_T^2}{2} + \frac{3y_B^2}{2} + \frac{3y_M^2}{2} - \frac{17g_1^2}{12} - \frac{9g_2^2}{4} - 8g_3^2 \right), \\ \frac{dy_T^2}{d \ln \mu^2} &= \frac{y_T^2}{16\pi^2} \left(\frac{9y_i^2}{2} + \frac{9y_X^2}{2} + \frac{9y_T^2}{2} + \frac{3y_B^2}{2} + \frac{3y_M^2}{2} - \frac{17g_1^2}{12} - \frac{9g_2^2}{4} - 8g_3^2 \right), \\ \frac{dy_X^2}{d \ln \mu^2} &= \frac{y_T^2}{16\pi^2} \left(\frac{9y_i^2}{2} + \frac{9y_X^2}{2} + \frac{9y_T^2}{2} + \frac{3y_B^2}{2} + \frac{3y_M^2}{2} - \frac{41g_1^2}{20} - \frac{9g_2^2}{4} - 8g_3^2 \right), \\ \frac{dy_B^2}{d \ln \mu^2} &= \frac{y_B^2}{16\pi^2} \left(\frac{3y_i^2}{2} + \frac{3y_X^2}{2} + \frac{9y_T^2}{2} + \frac{9y_B^2}{2} + \frac{3y_M^2}{2} - \frac{5g_1^2}{12} - \frac{9g_2^2}{4} - 8g_3^2 \right), \\ \frac{dy_M^2}{d \ln \mu^2} &= \frac{y_M^2}{16\pi^2} \left(y_X^2 + y_T^2 + y_B^2 + \frac{15y_M^2}{2} - \frac{41g_1^2}{20} - \frac{9g_2^2}{4} - 8g_3^2 \right). \end{aligned} \quad (\text{A13})$$

The Higgs sector RGEs, describing the interactions between the two bosons, are

$$\begin{aligned} \frac{d\lambda_1}{d \ln \mu^2} &= \frac{1}{16\pi^2} \left[-4\lambda_1 \left(\frac{3g_1^2}{4} + \frac{9g_2^2}{4} \right) + 12\lambda_1^2 + 4\lambda_3^2 + 4\lambda_3\lambda_4 + 2\lambda_4^2 + 2\lambda_5^2 + \frac{3g_1^4}{4} + \frac{9g_2^4}{4} + \frac{3g_1^2g_2^2}{2} \right], \\ \frac{d\lambda_2}{d \ln \mu^2} &= \frac{1}{16\pi^2} \left[4\lambda_2 \left(3y_i^2 + 6y_X^2 + 6y_T^2 + 6y_B^2 - \frac{3g_1^2}{2} - \frac{9g_2^2}{2} \right) + 12\lambda_2^2 + 4\lambda_3^2 + 4\lambda_3\lambda_4 + 2\lambda_4^2 + 2\lambda_5^2 \right. \\ &\quad \left. + \frac{3g_1^4}{2} + \frac{9g_2^4}{2} + 3g_1^2g_2^2 - 12y_i^4 - 24y_X^4 - 24y_T^4 - 24y_B^4 - 24y_i^2y_T^2 - 24y_T^2y_B^2 - 24y_X^2y_T^2 \right], \\ \frac{d\lambda_3}{d \ln \mu^2} &= \frac{1}{16\pi^2} \left[2\lambda_3(3y_i^2 + 6y_T^2 + 6y_X^2 + 6y_B^2 + 12y_M^2 - 3g_1^2 - 9g_2^2) + 4\lambda_3^2 + 2\lambda_4^2 + 2\lambda_5^2 + (\lambda_1 + \lambda_2)(6\lambda_3 + 2\lambda_4) \right. \\ &\quad \left. + \frac{3g_1^4}{2} + \frac{9g_2^4}{2} - 3g_1^2g_2^2 \right], \\ \frac{d\lambda_4}{d \ln \mu^2} &= \frac{1}{16\pi^2} [2\lambda_4(3y_i^2 + 6y_X^2 + 6y_T^2 + 6y_B^2 + 12y_M^2 - 3g_1^2 - 9g_2^2) + 6g_1^2g_2^2 + 4\lambda_4^2 + 8\lambda_5^2 + 8\lambda_3\lambda_4 + 2\lambda_4(\lambda_1 + \lambda_2)], \\ \frac{d\lambda_5}{d \ln \mu^2} &= \frac{1}{16\pi^2} [2\lambda_5(3y_i^2 + 6y_T^2 + 6y_X^2 + 6y_B^2 + 12y_M^2 - 3g_1^2 - 9g_2^2) + 2\lambda_5(\lambda_1 + \lambda_2 + 4\lambda_3 + 6\lambda_4)]. \end{aligned} \quad (\text{A14})$$

g. Triplet $\mathcal{T}_Y (T, B, Y), Y = -1/3$

The relevant RGEs for the Yukawa couplings are

$$\begin{aligned} \frac{dy_i^2}{d \ln \mu^2} &= \frac{y_i^2}{16\pi^2} \left(\frac{9y_i^2}{2} + \frac{9y_T^2}{2} + \frac{3y_B^2}{2} + \frac{3y_Y^2}{2} + 3y_M^2 - \frac{17g_1^2}{12} - \frac{9g_2^2}{4} - 8g_3^2 \right), \\ \frac{dy_T^2}{d \ln \mu^2} &= \frac{y_T^2}{16\pi^2} \left(\frac{9y_i^2}{2} + \frac{9y_T^2}{2} + \frac{3y_B^2}{2} + \frac{3y_Y^2}{2} + 3y_M^2 - \frac{17g_1^2}{12} - \frac{9g_2^2}{4} - 8g_3^2 \right), \\ \frac{dy_B^2}{d \ln \mu^2} &= \frac{y_B^2}{16\pi^2} \left(\frac{3y_i^2}{2} + \frac{3y_T^2}{2} + \frac{9y_B^2}{2} + \frac{9y_Y^2}{2} + \frac{3y_M^2}{2} - \frac{5g_1^2}{12} - \frac{9g_2^2}{4} - 8g_3^2 \right), \\ \frac{dy_Y^2}{d \ln \mu^2} &= \frac{y_Y^2}{16\pi^2} \left(\frac{9y_Y^2}{2} + \frac{9y_B^2}{2} + \frac{3y_i^2}{2} + \frac{3y_T^2}{2} + 3y_M^2 - \frac{17g_1^2}{20} - \frac{9g_2^2}{4} - 8g_3^2 \right), \\ \frac{dy_M^2}{d \ln \mu^2} &= \frac{y_M^2}{16\pi^2} \left(y_T^2 + y_B^2 + y_Y^2 + \frac{15y_M^2}{2} - \frac{17g_1^2}{20} - \frac{9g_2^2}{4} - 8g_3^2 \right). \end{aligned} \quad (\text{A15})$$

The Higgs sector RGEs, describing the interactions between the two bosons, are

$$\begin{aligned}
\frac{d\lambda_1}{d\ln\mu^2} &= \frac{1}{16\pi^2} \left[-4\lambda_1 \left(\frac{3g_1^2}{4} + \frac{9g_2^2}{4} \right) + 12\lambda_1^2 + 4\lambda_3^2 + 4\lambda_3\lambda_4 + 2\lambda_4^2 + 2\lambda_5^2 + \frac{3g_1^4}{4} + \frac{9g_2^4}{4} + \frac{3g_1^2g_2^2}{2} \right], \\
\frac{d\lambda_2}{d\ln\mu^2} &= \frac{1}{16\pi^2} \left[4\lambda_2 \left(3y_i^2 + 6y_T^2 + 6y_B^2 + 6y_Y^2 - \frac{3g_1^2}{2} - \frac{9g_2^2}{2} \right) + 12\lambda_2^2 + 4\lambda_3^2 + 4\lambda_3\lambda_4 + 2\lambda_4^2 + 2\lambda_5^2 \right. \\
&\quad \left. + \frac{3g_1^4}{2} + \frac{9g_2^4}{2} + 3g_1^2g_2^2 - 12y_i^4 - 24y_T^4 - 24y_B^4 - 24y_Y^4 - 24y_i^2y_T^2 - 24y_T^2y_B^2 - 24y_B^2y_Y^2 \right], \\
\frac{d\lambda_3}{d\ln\mu^2} &= \frac{1}{16\pi^2} \left[2\lambda_3(3y_i^2 + 6y_T^2 + 6y_B^2 + 6y_Y^2 + 12y_M^2 - 3g_1^2 - 9g_2^2) + 4\lambda_3^2 + 2\lambda_4^2 + 2\lambda_5^2 + (\lambda_1 + \lambda_2)(6\lambda_3 + 2\lambda_4) \right. \\
&\quad \left. + \frac{3g_1^4}{2} + \frac{9g_2^4}{4} - 3g_1^2g_2^2 \right], \\
\frac{d\lambda_4}{d\ln\mu^2} &= \frac{1}{16\pi^2} [2\lambda_4(3y_i^2 + 6y_T^2 + 6y_B^2 + 6y_Y^2 + 12y_M^2 - 3g_1^2 - 9g_2^2) + 6g_1^2g_2^2 + 4\lambda_4^2 + 8\lambda_5^2 + 8\lambda_3\lambda_4 + 2\lambda_4(\lambda_1 + \lambda_2)], \\
\frac{d\lambda_5}{d\ln\mu^2} &= \frac{1}{16\pi^2} [2\lambda_5(3y_i^2 + 6y_T^2 + 6y_B^2 + 6y_Y^2 + 12y_M^2 - 3g_1^2 - 9g_2^2) + 2\lambda_5(\lambda_1 + \lambda_2 + 4\lambda_3 + 6\lambda_4)]. \tag{A16}
\end{aligned}$$

The coupling constants gain additional terms due to the new fermions in both triplet models as follows:

$$\frac{dg_1^2}{d\ln\mu^2} = \frac{g_1^4}{16\pi^2} \left(7 + \frac{4}{5} \right), \quad \frac{dg_2^2}{d\ln\mu^2} = \frac{g_2^4}{16\pi^2} (-3 + 4), \quad \frac{dg_3^2}{d\ln\mu^2} = \frac{g_3^4}{16\pi^2} (-7 + 2). \tag{A17}$$

2. RGEs for 2HDM + VLQ: Type-II

a. Singlet $\mathcal{U}_1(T)$, $Y=2/3$

The relevant RGEs for the Yukawa couplings are

$$\begin{aligned}
\frac{dy_i^2}{d\ln\mu^2} &= \frac{y_i^2}{16\pi^2} \left(\frac{9y_i^2}{2} + \frac{9y_T^2}{2} - \frac{17g_1^2}{12} - \frac{9g_2^2}{4} - 8g_3^2 \right), \\
\frac{dy_T^2}{d\ln\mu^2} &= \frac{y_T^2}{16\pi^2} \left(\frac{9y_i^2}{2} + \frac{9y_T^2}{2} + \frac{3y_M^2}{2} - \frac{17g_1^2}{12} - \frac{9g_2^2}{4} - 8g_3^2 \right), \\
\frac{dy_M^2}{d\ln\mu^2} &= \frac{y_M^2}{16\pi^2} \left(y_T^2 + \frac{9y_M^2}{2} - \frac{41g_1^2}{20} - 8g_3^2 \right). \tag{A18}
\end{aligned}$$

The Higgs sector RGEs, describing the interactions between the two bosons, are

$$\begin{aligned}
\frac{d\lambda_1}{d\ln\mu^2} &= \frac{1}{16\pi^2} \left[-4\lambda_1 \left(\frac{3g_1^2}{4} + \frac{9g_2^2}{4} \right) + 12\lambda_1^2 + 4\lambda_3^2 + 4\lambda_3\lambda_4 + 2\lambda_4^2 + 2\lambda_5^2 + \frac{3g_1^4}{16} + \frac{9g_2^4}{4} + \frac{3g_1^2g_2^2}{2} \right], \\
\frac{d\lambda_2}{d\ln\mu^2} &= \frac{1}{16\pi^2} \left[4\lambda_2 \left(3y_i^2 + 6y_T^2 - \frac{3g_1^2}{4} - \frac{9g_2^2}{4} \right) + 12\lambda_2^2 + 4\lambda_3^2 + 4\lambda_3\lambda_4 + 2\lambda_4^2 + 2\lambda_5^2 \right. \\
&\quad \left. + \frac{3g_1^4}{16} + \frac{9g_2^4}{4} + \frac{3g_1^2g_2^2}{2} - 12y_i^4 - 24y_T^4 - 24y_M^4 - 24y_i^2y_T^2 \right], \\
\frac{d\lambda_3}{d\ln\mu^2} &= \frac{1}{16\pi^2} \left[2\lambda_3 \left(3y_i^2 + 6y_T^2 + 6y_M^2 - \frac{3g_1^2}{2} - \frac{9g_2^2}{2} \right) + 4\lambda_3^2 + 2\lambda_4^2 + 2\lambda_5^2 + (\lambda_1 + \lambda_2)(6\lambda_3 + 2\lambda_4) + \frac{3g_1^4}{4} + \frac{9g_2^4}{4} - \frac{3g_1^2g_2^2}{2} - 24y_T^2y_M^2 \right], \\
\frac{d\lambda_4}{d\ln\mu^2} &= \frac{1}{16\pi^2} \left[2\lambda_4 \left(3y_i^2 + 6y_T^2 + 6y_M^2 - \frac{3g_1^2}{2} - \frac{9g_2^2}{2} \right) + 3g_1^2g_2^2 + 4\lambda_4^2 + 8\lambda_5^2 + 8\lambda_3\lambda_4 + 2\lambda_4(\lambda_1 + \lambda_2) + 24y_T^2y_M^2 \right], \\
\frac{d\lambda_5}{d\ln\mu^2} &= \frac{1}{16\pi^2} \left[2\lambda_5 \left(3y_i^2 + 6y_T^2 + 6y_M^2 - \frac{3g_1^2}{2} - \frac{9g_2^2}{2} \right) + 2\lambda_5(\lambda_1 + \lambda_2 + 4\lambda_3 + 6\lambda_4) \right]. \tag{A19}
\end{aligned}$$

b. Singlet $\mathcal{D}_1(B)$, $Y = -1/3$

The relevant RGEs for the Yukawa couplings are

$$\begin{aligned}\frac{dy_i^2}{d \ln \mu^2} &= \frac{y_i^2}{16\pi^2} \left(\frac{9y_i^2}{2} + \frac{y_B^2}{2} - \frac{17g_1^2}{12} - \frac{9g_2^2}{4} - 8g_3^2 \right), \\ \frac{dy_B^2}{d \ln \mu^2} &= \frac{y_B^2}{16\pi^2} \left(\frac{y_i^2}{2} + \frac{9y_B^2}{2} + \frac{3y_M^2}{2} - \frac{5g_1^2}{12} - \frac{9g_2^2}{4} - 8g_3^2 \right), \\ \frac{dy_M^2}{d \ln \mu^2} &= \frac{y_M^2}{16\pi^2} \left(\frac{9y_M^2}{2} + y_B^2 - \frac{17g_1^2}{20} - 8g_3^2 \right).\end{aligned}\tag{A20}$$

The Higgs sector RGEs, describing the interactions between the two bosons, are

$$\begin{aligned}\frac{d\lambda_1}{d \ln \mu^2} &= \frac{1}{16\pi^2} \left[-4\lambda_1 \left(\frac{3g_1^2}{4} + \frac{9g_2^2}{4} - 6y_B^2 \right) + 12\lambda_1^2 + 4\lambda_3^2 + 4\lambda_3\lambda_4 + 2\lambda_4^2 + 2\lambda_5^2 + \frac{3g_1^4}{16} + \frac{9g_2^4}{4} + \frac{3g_1^2g_2^2}{2} - 24y_B^4 - 24y_M^4 \right], \\ \frac{d\lambda_2}{d \ln \mu^2} &= \frac{1}{16\pi^2} \left[4\lambda_2 \left(3y_i^2 - \frac{3g_1^2}{4} - \frac{9g_2^2}{4} \right) + 12\lambda_2^2 + 4\lambda_3^2 + 4\lambda_3\lambda_4 + 2\lambda_4^2 + 2\lambda_5^2 + \frac{3g_1^4}{16} + \frac{9g_2^4}{4} + \frac{3g_1^2g_2^2}{2} - 12y_i^4 \right], \\ \frac{d\lambda_3}{d \ln \mu^2} &= \frac{1}{16\pi^2} \left[2\lambda_3 \left(3y_i^2 + 6y_B^2 + 6y_M^2 - \frac{3g_1^2}{2} - \frac{9g_2^2}{2} \right) + 4\lambda_3^2 + 2\lambda_4^2 + 2\lambda_5^2 + (\lambda_1 + \lambda_2)(6\lambda_3 + 2\lambda_4) \right. \\ &\quad \left. + \frac{3g_1^4}{4} + \frac{9g_2^4}{4} - \frac{3g_1^2g_2^2}{2} - 24y_B^2y_M^2 \right], \\ \frac{d\lambda_4}{d \ln \mu^2} &= \frac{1}{16\pi^2} \left[2\lambda_4 \left(3y_i^2 + 6y_B^2 + 6y_M^2 - \frac{3g_1^2}{2} - \frac{9g_2^2}{2} \right) + 3g_1^2g_2^2 + 4\lambda_4^2 + 8\lambda_5^2 + 8\lambda_3\lambda_4 + 2\lambda_4(\lambda_1 + \lambda_2) + 24y_B^2y_M^2 \right], \\ \frac{d\lambda_5}{d \ln \mu^2} &= \frac{1}{16\pi^2} \left[2\lambda_5 \left(3y_i^2 + 6y_B^2 + 6y_M^2 - \frac{3g_1^2}{2} - \frac{9g_2^2}{2} \right) + 2\lambda_5(\lambda_1 + \lambda_2 + 4\lambda_3 + 6\lambda_4) \right].\end{aligned}\tag{A21}$$

Finally, the coupling constants gain additional terms due to the new fermion, for both models \mathcal{U}_1 and \mathcal{D}_1 with singlet fermions, as follows:

$$\frac{dg_1^2}{d \ln \mu^2} = \frac{g_1^4}{16\pi^2} \left(7 + \frac{4}{15} \right), \quad \frac{dg_2^2}{d \ln \mu^2} = \frac{g_2^4}{16\pi^2} (-3), \quad \frac{dg_3^2}{d \ln \mu^2} = \frac{g_3^4}{16\pi^2} \left(-7 + \frac{2}{3} \right).\tag{A22}$$

c. Doublet $\mathcal{D}_2(T,B)$, $Y=1/6$

The relevant RGEs for the Yukawa couplings are

$$\begin{aligned}\frac{dy_i^2}{d \ln \mu^2} &= \frac{y_i^2}{16\pi^2} \left(\frac{9y_i^2}{2} + \frac{9y_T^2}{2} + \frac{y_B^2}{2} + 3y_M^2 - \frac{17g_1^2}{12} - \frac{9g_2^2}{4} - 8g_3^2 \right), \\ \frac{dy_T^2}{d \ln \mu^2} &= \frac{y_T^2}{16\pi^2} \left(\frac{9y_i^2}{2} + \frac{9y_T^2}{2} + \frac{y_B^2}{2} + 3y_M^2 - \frac{17g_1^2}{12} - \frac{9g_2^2}{4} - 8g_3^2 \right), \\ \frac{dy_B^2}{d \ln \mu^2} &= \frac{y_B^2}{16\pi^2} \left(\frac{3y_i^2}{2} + \frac{y_T^2}{2} + \frac{9y_B^2}{2} + 3y_M^2 - \frac{5g_1^2}{12} - \frac{9g_2^2}{4} - 8g_3^2 \right), \\ \frac{dy_M^2}{d \ln \mu^2} &= \frac{y_M^2}{16\pi^2} \left(y_T^2 + y_B^2 + \frac{11y_M^2}{2} - \frac{19g_1^2}{40} - \frac{9g_2^2}{2} - 8g_3^2 \right).\end{aligned}\tag{A23}$$

The Higgs sector RGEs, describing the interactions between the two bosons, are

$$\begin{aligned}
\frac{d\lambda_1}{d\ln\mu^2} &= \frac{1}{16\pi^2} \left[4\lambda_1 \left(6y_B^2 - \frac{3g_1^2}{4} - \frac{9g_2^2}{4} \right) + 12\lambda_1^2 + 4\lambda_3^2 + 4\lambda_3\lambda_4 + 2\lambda_4^2 + 2\lambda_5^2 + \frac{3g_1^4}{4} + \frac{9g_2^4}{4} + \frac{3g_1^2g_2^2}{2} - 24y_B^4 - 24y_B^2y_M^2 \right], \\
\frac{d\lambda_2}{d\ln\mu^2} &= \frac{1}{16\pi^2} \left[4\lambda_2 \left(3y_i^2 + 6y_T^2 - \frac{3g_1^2}{4} - \frac{9g_2^2}{4} \right) + 12\lambda_2^2 + 4\lambda_3^2 + 4\lambda_3\lambda_4 + 2\lambda_4^2 + 2\lambda_5^2 \right. \\
&\quad \left. + \frac{3g_1^4}{4} + \frac{9g_2^4}{4} + \frac{3g_1^2g_2^2}{2} - 12y_i^4 - 24y_T^4 - 24y_i^2y_T^2 - 24y_T^2y_M^2 \right], \\
\frac{d\lambda_3}{d\ln\mu^2} &= \frac{1}{16\pi^2} \left[2\lambda_3 \left(3y_i^2 + 6y_T^2 + 6y_B^2 + 6y_M^2 - \frac{3g_1^2}{2} - \frac{9g_2^2}{2} \right) + 4\lambda_3^2 + 2\lambda_4^2 + 2\lambda_5^2 + (\lambda_1 + \lambda_2)(6\lambda_3 + 2\lambda_4) \right. \\
&\quad \left. + \frac{3g_1^4}{4} + \frac{9g_2^4}{4} - \frac{3g_1^2g_2^2}{2} - 24y_i^2y_M^2 - 24y_B^2y_M^2 \right], \\
\frac{d\lambda_4}{d\ln\mu^2} &= \frac{1}{16\pi^2} \left[2\lambda_4 \left(3y_i^2 + 6y_T^2 + 6y_B^2 + 6y_M^2 - \frac{3g_1^2}{2} - \frac{9g_2^2}{2} \right) + 3g_1^2g_2^2 + 4\lambda_4^2 + 8\lambda_5^2 + 8\lambda_3\lambda_4 + 2\lambda_4(\lambda_1 + \lambda_2) + 24y_T^2y_M^2 + 24y_B^2y_M^2 \right], \\
\frac{d\lambda_5}{d\ln\mu^2} &= \frac{1}{16\pi^2} \left[2\lambda_5 \left(3y_i^2 + 6y_T^2 + 6y_B^2 + 12y_M^2 - \frac{3g_1^2}{2} - \frac{9g_2^2}{2} \right) + 2\lambda_5(\lambda_1 + \lambda_2 + 4\lambda_3 + 6\lambda_4) \right]. \tag{A24}
\end{aligned}$$

d. Doublet $\mathcal{D}_X (X, T)$, $Y=7/6$

The relevant RGEs for the Yukawa couplings are

$$\begin{aligned}
\frac{dy_i^2}{d\ln\mu^2} &= \frac{y_i^2}{16\pi^2} \left(\frac{9y_i^2}{2} + \frac{y_T^2}{2} + \frac{9y_X^2}{2} + 3y_M^2 - \frac{17g_1^2}{12} - \frac{9g_2^2}{4} - 8g_3^2 \right), \\
\frac{dy_T^2}{d\ln\mu^2} &= \frac{y_T^2}{16\pi^2} \left(\frac{3y_i^2}{2} + \frac{y_X^2}{2} + \frac{9y_T^2}{2} + 3y_M^2 - \frac{5g_1^2}{12} - \frac{9g_2^2}{4} - 8g_3^2 \right), \\
\frac{dy_X^2}{d\ln\mu^2} &= \frac{y_X^2}{16\pi^2} \left(\frac{9y_i^2}{2} + \frac{9y_X^2}{2} + \frac{y_T^2}{2} + 3y_M^2 - \frac{17g_1^2}{12} - \frac{9g_2^2}{4} - 8g_3^2 \right), \\
\frac{dy_M^2}{d\ln\mu^2} &= \frac{y_M^2}{16\pi^2} \left(y_T^2 + y_X^2 + \frac{11y_M^2}{2} - \frac{67g_1^2}{40} - \frac{9g_2^2}{2} - 8g_3^2 \right). \tag{A25}
\end{aligned}$$

The Higgs sector RGEs, describing the interactions between the two bosons, are

$$\begin{aligned}
\frac{d\lambda_1}{d\ln\mu^2} &= \frac{1}{16\pi^2} \left[4\lambda_1 \left(6y_T^2 - \frac{3g_1^2}{4} - \frac{9g_2^2}{2} \right) + 12\lambda_1^2 + 4\lambda_3^2 + 4\lambda_3\lambda_4 + 2\lambda_4^2 + 2\lambda_5^2 + \frac{3g_1^4}{4} + \frac{9g_2^4}{4} + \frac{3g_1^2g_2^2}{2} - 24y_T^4 - 24y_T^2y_M^2 \right], \\
\frac{d\lambda_2}{d\ln\mu^2} &= \frac{1}{16\pi^2} \left[4\lambda_2 \left(3y_i^2 + 6y_X^2 - \frac{3g_1^2}{4} - \frac{9g_2^2}{4} \right) + 12\lambda_2^2 + 4\lambda_3^2 + 4\lambda_3\lambda_4 + 2\lambda_4^2 + 2\lambda_5^2 + \frac{3g_1^4}{4} + \frac{9g_2^4}{4} + \frac{3g_1^2g_2^2}{2} - 12y_i^4 - 24y_X^4 - 24y_X^2y_M^2 \right], \\
\frac{d\lambda_3}{d\ln\mu^2} &= \frac{1}{16\pi^2} \left[2\lambda_3 \left(3y_i^2 + 6y_T^2 + 6y_X^2 + 6y_M^2 - \frac{3g_1^2}{2} - \frac{9g_2^2}{10} \right) + 4\lambda_3^2 + 2\lambda_4^2 + 2\lambda_5^2 + (\lambda_1 + \lambda_2)(6\lambda_3 + 2\lambda_4) \right. \\
&\quad \left. + \frac{3g_1^4}{4} + \frac{9g_2^4}{4} - \frac{3g_1^2g_2^2}{2} - 24y_X^2y_M^2 - 24y_T^2y_M^2 \right], \\
\frac{d\lambda_4}{d\ln\mu^2} &= \frac{1}{16\pi^2} \left[2\lambda_4 \left(3y_i^2 + 6y_T^2 + 6y_X^2 + 6y_M^2 - \frac{3g_1^2}{2} - \frac{9g_2^2}{10} \right) + 3g_1^2g_2^2 + 4\lambda_4^2 + 8\lambda_5^2 + 8\lambda_3\lambda_4 + 2\lambda_4(\lambda_1 + \lambda_2) + 24y_X^2y_M^2 + 24y_T^2y_M^2 \right], \\
\frac{d\lambda_5}{d\ln\mu^2} &= \frac{1}{16\pi^2} \left[2\lambda_5 \left(3y_i^2 + 6y_T^2 + 6y_X^2 + 6y_M^2 - \frac{3g_1^2}{2} - \frac{9g_2^2}{10} \right) + 2\lambda_5(\lambda_1 + \lambda_2 + 4\lambda_3 + 6\lambda_4) \right]. \tag{A26}
\end{aligned}$$

e. Additional non-SM-like quark doublet \mathcal{D}_Y (B, Y), $Y = -5/6$

The relevant RGEs for the Yukawa couplings are

$$\begin{aligned}
\frac{dy_i^2}{d\ln\mu^2} &= \frac{y_i^2}{16\pi^2} \left(\frac{9y_i^2}{2} + \frac{3y_B^2}{2} + \frac{y_Y^2}{2} + 3y_M^2 - \frac{17g_1^2}{12} - \frac{9g_2^2}{4} - 8g_3^2 \right), \\
\frac{dy_B^2}{d\ln\mu^2} &= \frac{y_B^2}{16\pi^2} \left(\frac{3y_i^2}{2} + \frac{9y_B^2}{2} + \frac{y_Y^2}{2} + 3y_M^2 - \frac{17g_1^2}{12} - \frac{9g_2^2}{4} - 8g_3^2 \right), \\
\frac{dy_Y^2}{d\ln\mu^2} &= \frac{y_Y^2}{16\pi^2} \left(\frac{3y_i^2}{2} + \frac{9y_Y^2}{2} + \frac{y_B^2}{2} + 3y_M^2 - \frac{5g_1^2}{12} - \frac{9g_2^2}{4} - 8g_3^2 \right), \\
\frac{dy_M^2}{d\ln\mu^2} &= \frac{y_M^2}{16\pi^2} \left(y_Y^2 + y_B^2 + \frac{11y_M^2}{2} - \frac{43g_1^2}{40} - \frac{9g_2^2}{2} - 8g_3^2 \right).
\end{aligned} \tag{A27}$$

The Higgs sector RGEs, describing the interactions between the two bosons, are

$$\begin{aligned}
\frac{d\lambda_1}{d\ln\mu^2} &= \frac{1}{16\pi^2} \left[4\lambda_1 \left(6y_Y^2 - \frac{3g_1^2}{4} - \frac{9g_2^2}{4} \right) + 12\lambda_1^2 + 4\lambda_3^2 + 4\lambda_3\lambda_4 + 2\lambda_4^2 + 2\lambda_5^2 + \frac{3g_1^4}{4} + \frac{9g_2^4}{4} + \frac{3g_1^2g_2^2}{2} - 24y_Y^4 - 24y_Y^2y_M^2 \right], \\
\frac{d\lambda_2}{d\ln\mu^2} &= \frac{1}{16\pi^2} \left[4\lambda_2 \left(3y_i^2 + 6y_B^2 - \frac{3g_1^2}{4} - \frac{9g_2^2}{4} \right) + 12\lambda_2^2 + 4\lambda_3^2 + 4\lambda_3\lambda_4 + 2\lambda_4^2 + 2\lambda_5^2 + \frac{3g_1^4}{4} + \frac{9g_2^4}{4} + \frac{3g_1^2g_2^2}{2} - 12y_i^4 - 24y_B^4 - 24y_B^2y_M^2 \right], \\
\frac{d\lambda_3}{d\ln\mu^2} &= \frac{1}{16\pi^2} \left[2\lambda_3 \left(3y_i^2 + 6y_B^2 + 6y_Y^2 + 6y_M^2 - \frac{3g_1^2}{2} - \frac{9g_2^2}{2} \right) + 4\lambda_3^2 + 2\lambda_4^2 + 2\lambda_5^2 + (\lambda_1 + \lambda_2)(6\lambda_3 + 2\lambda_4) \right. \\
&\quad \left. + \frac{3g_1^4}{4} + \frac{9g_2^4}{4} - \frac{3g_1^2g_2^2}{2} - 24y_B^2y_M^2 - 24y_Y^2y_M^2 \right], \\
\frac{d\lambda_4}{d\ln\mu^2} &= \frac{1}{16\pi^2} \left[2\lambda_4 \left(3y_i^2 + 6y_Y^2 + 6y_B^2 + 6y_M^2 - \frac{3g_1^2}{2} - \frac{9g_2^2}{2} \right) + 3g_1^2g_2^2 + 4\lambda_4^2 + 8\lambda_5^2 + 8\lambda_3\lambda_4 + 2\lambda_4(\lambda_1 + \lambda_2) + 24y_B^2y_M^2 + 24y_Y^2y_M^2 \right], \\
\frac{d\lambda_5}{d\ln\mu^2} &= \frac{1}{16\pi^2} \left[2\lambda_5 \left(3y_i^2 + 6y_Y^2 + 6y_B^2 + 6y_M^2 - \frac{3g_1^2}{2} - \frac{9g_2^2}{2} \right) + 2\lambda_5(\lambda_1 + \lambda_2 + 4\lambda_3 + 6\lambda_4) \right].
\end{aligned} \tag{A28}$$

The coupling constants gain additional terms due to the new fermion in all doublet models as follows:

$$\frac{dg_1^2}{d\ln\mu^2} = \frac{g_1^4}{16\pi^2} \left(7 + \frac{6}{5} \right), \quad \frac{dg_2^2}{d\ln\mu^2} = \frac{g_2^4}{16\pi^2} (-3 + 2), \quad \frac{dg_3^2}{d\ln\mu^2} = \frac{g_3^4}{16\pi^2} \left(-7 + \frac{4}{3} \right). \tag{A29}$$

f. Triplet \mathcal{T}_X (X, T, B), $Y = 2/3$

The relevant RGEs for the Yukawa couplings are

$$\begin{aligned}
\frac{dy_i^2}{d\ln\mu^2} &= \frac{y_i^2}{16\pi^2} \left(\frac{9y_i^2}{2} + \frac{9y_X^2}{2} + \frac{9y_T^2}{2} + \frac{y_B^2}{2} + \frac{3y_M^2}{2} - \frac{17g_1^2}{12} - \frac{9g_2^2}{4} - 8g_3^2 \right), \\
\frac{dy_T^2}{d\ln\mu^2} &= \frac{y_T^2}{16\pi^2} \left(\frac{9y_i^2}{2} + \frac{9y_X^2}{2} + \frac{9y_T^2}{2} + \frac{y_B^2}{2} + \frac{3y_M^2}{2} - \frac{17g_1^2}{12} - \frac{9g_2^2}{4} - 8g_3^2 \right), \\
\frac{dy_X^2}{d\ln\mu^2} &= \frac{y_T^2}{16\pi^2} \left(\frac{9y_i^2}{2} + \frac{9y_X^2}{2} + \frac{9y_T^2}{2} + \frac{y_B^2}{2} + \frac{3y_M^2}{2} - \frac{41g_1^2}{20} - \frac{9g_2^2}{4} - 8g_3^2 \right), \\
\frac{dy_B^2}{d\ln\mu^2} &= \frac{y_B^2}{16\pi^2} \left(\frac{3y_i^2}{2} + \frac{y_X^2}{2} + \frac{3y_T^2}{2} + \frac{9y_B^2}{2} + \frac{3y_M^2}{2} - \frac{5g_1^2}{12} - \frac{9g_2^2}{4} - 8g_3^2 \right), \\
\frac{dy_M^2}{d\ln\mu^2} &= \frac{y_M^2}{16\pi^2} \left(y_X^2 + y_T^2 + y_B^2 + \frac{15y_M^2}{2} - \frac{41g_1^2}{20} - \frac{9g_2^2}{4} - 8g_3^2 \right).
\end{aligned} \tag{A30}$$

The Higgs sector RGEs, describing the interactions between the two bosons, are

$$\begin{aligned}
\frac{d\lambda_1}{d\ln\mu^2} &= \frac{1}{16\pi^2} \left[4\lambda_1 \left(6y_B^2 + 6y_T^2 - \frac{3g_1^2}{2} - \frac{9g_2^2}{2} \right) + 12\lambda_1^2 + 4\lambda_3^2 + 4\lambda_3\lambda_4 + 2\lambda_4^2 + 2\lambda_5^2 \right. \\
&\quad \left. + \frac{3g_1^4}{2} + \frac{9g_2^4}{2} + 3g_1^2g_2^2 - 24y_B^4 - 24y_T^4 - 24y_B^2y_M^2 - 24y_T^2y_M^2 \right], \\
\frac{d\lambda_2}{d\ln\mu^2} &= \frac{1}{16\pi^2} \left[4\lambda_2 \left(3y_i^2 + 6y_X^2 + 6y_T^2 - \frac{3g_1^2}{2} - \frac{9g_2^2}{2} \right) + 12\lambda_2^2 + 4\lambda_3^2 + 4\lambda_3\lambda_4 + 2\lambda_4^2 + 2\lambda_5^2 \right. \\
&\quad \left. + \frac{3g_1^4}{2} + \frac{9g_2^4}{2} + 3g_1^2g_2^2 - 12y_i^4 - 24y_X^4 - 24y_T^4 - 24y_i^2y_T^2 - 24y_X^2y_M^2 - 24y_T^2y_M^2 \right], \\
\frac{d\lambda_3}{d\ln\mu^2} &= \frac{1}{16\pi^2} \left[2\lambda_3(3y_i^2 + 6y_T^2 + 6y_X^2 + 6y_B^2 + 6y_M^2 - 3g_1^2 - 9g_2^2) + 4\lambda_3^2 + 2\lambda_4^2 + 2\lambda_5^2 + (\lambda_1 + \lambda_2)(6\lambda_3 + 2\lambda_4) \right. \\
&\quad \left. + \frac{3g_1^4}{2} + \frac{9g_2^4}{2} - 3g_1^2g_2^2 - 24y_X^2y_M^2 - 24y_T^2y_M^2 - 24y_B^2y_M^2 \right], \\
\frac{d\lambda_4}{d\ln\mu^2} &= \frac{1}{16\pi^2} [2\lambda_4(3y_i^2 + 6y_X^2 + 6y_T^2 + 6y_B^2 + 6y_M^2 - 3g_1^2 - 9g_2^2) + 6g_1^2g_2^2 + 4\lambda_4^2 + 8\lambda_5^2 + 8\lambda_3\lambda_4 + 2\lambda_4(\lambda_1 + \lambda_2) \\
&\quad + 24y_X^2y_M^2 + 24y_T^2y_M^2 + 24y_B^2y_M^2], \\
\frac{d\lambda_5}{d\ln\mu^2} &= \frac{1}{16\pi^2} [2\lambda_5(3y_i^2 + 6y_T^2 + 6y_X^2 + 6y_B^2 + 6y_M^2 - 3g_1^2 - 9g_2^2) + 2\lambda_5(\lambda_1 + \lambda_2 + 4\lambda_3 + 6\lambda_4)]. \tag{A31}
\end{aligned}$$

g. Triplet $\mathcal{T}_Y (T, B, Y)$, $Y = -1/3$

The relevant RGEs for the Yukawa couplings are

$$\begin{aligned}
\frac{dy_i^2}{d\ln\mu^2} &= \frac{y_i^2}{16\pi^2} \left(\frac{9y_i^2}{2} + \frac{9y_T^2}{2} + \frac{3y_B^2}{2} + \frac{y_Y^2}{2} + 3y_M^2 - \frac{17g_1^2}{12} - \frac{9g_2^2}{4} - 8g_3^2 \right), \\
\frac{dy_T^2}{d\ln\mu^2} &= \frac{y_T^2}{16\pi^2} \left(\frac{9y_i^2}{2} + \frac{9y_T^2}{2} + \frac{9y_B^2}{2} + \frac{y_Y^2}{2} + 3y_M^2 - \frac{17g_1^2}{12} - \frac{9g_2^2}{4} - 8g_3^2 \right), \\
\frac{dy_B^2}{d\ln\mu^2} &= \frac{y_B^2}{16\pi^2} \left(\frac{3y_i^2}{2} + \frac{y_T^2}{2} + \frac{9y_B^2}{2} + \frac{9y_Y^2}{2} + \frac{3y_M^2}{2} - \frac{5g_1^2}{12} - \frac{9g_2^2}{4} - 8g_3^2 \right), \\
\frac{dy_Y^2}{d\ln\mu^2} &= \frac{y_Y^2}{16\pi^2} \left(\frac{9y_Y^2}{2} + \frac{9y_B^2}{2} + \frac{3y_i^2}{2} + \frac{y_T^2}{2} + 3y_M^2 - \frac{17g_1^2}{20} - \frac{9g_2^2}{4} - 8g_3^2 \right), \\
\frac{dy_M^2}{d\ln\mu^2} &= \frac{y_M^2}{16\pi^2} \left(y_T^2 + y_B^2 + y_Y^2 + \frac{15y_M^2}{2} - \frac{17g_1^2}{20} - \frac{9g_2^2}{4} - 8g_3^2 \right). \tag{A32}
\end{aligned}$$

The Higgs sector RGEs, describing the interactions between the two bosons, are

$$\begin{aligned}
\frac{d\lambda_1}{d\ln\mu^2} &= \frac{1}{16\pi^2} \left[4\lambda_1 \left(6y_B^2 + 6y_Y^2 - \frac{3g_1^2}{2} - \frac{9g_2^2}{2} \right) + 12\lambda_1^2 + 4\lambda_3^2 + 4\lambda_3\lambda_4 + 2\lambda_4^2 + 2\lambda_5^2 \right. \\
&\quad \left. + \frac{3g_1^4}{2} + \frac{9g_2^4}{2} + 3g_1^2g_2^2 - 24y_B^4 - 24y_Y^4 - 24y_B^2y_M^2 - 24y_Y^2y_M^2 \right], \\
\frac{d\lambda_2}{d\ln\mu^2} &= \frac{1}{16\pi^2} \left[4\lambda_2 \left(3y_i^2 + 6y_T^2 + 6y_B^2 - \frac{3g_1^2}{2} - \frac{9g_2^2}{2} \right) + 12\lambda_2^2 + 4\lambda_3^2 + 4\lambda_3\lambda_4 + 2\lambda_4^2 + 2\lambda_5^2 \right. \\
&\quad \left. + \frac{3g_1^4}{2} + \frac{9g_2^4}{2} + 3g_1^2g_2^2 - 12y_i^4 - 24y_T^4 - 24y_B^4 - 24y_i^2y_T^2 - 24y_T^2y_M^2 - 24y_B^2y_M^2 \right],
\end{aligned}$$

$$\begin{aligned}
\frac{d\lambda_3}{d\ln\mu^2} &= \frac{1}{16\pi^2} \left[2\lambda_3(3y_T^2 + 6y_T^2 + 6y_B^2 + 6y_Y^2 + 6y_M^2 - 3g_1^2 - 9g_2^2) + 4\lambda_3^2 + 2\lambda_4^2 + 2\lambda_5^2 + (\lambda_1 + \lambda_2)(6\lambda_3 + 2\lambda_4) \right. \\
&\quad \left. + \frac{3g_1^4}{2} + \frac{9g_2^2}{2} - 3g_1^2g_2^2 - 24y_T^2y_M^2 - 24y_B^2y_M^2 - 24y_Y^2y_M^2 \right], \\
\frac{d\lambda_4}{d\ln\mu^2} &= \frac{1}{16\pi^2} [2\lambda_4(3y_T^2 + 6y_T^2 + 6y_B^2 + 6y_Y^2 + 6y_M^2 - 3g_1^2 - 9g_2^2) + 6g_1^2g_2^2 + 4\lambda_4^2 + 8\lambda_5^2 + 8\lambda_3\lambda_4 + 2\lambda_4(\lambda_1 + \lambda_2) \\
&\quad + 24y_T^2y_M^2 + 24y_B^2y_M^2 + 24y_Y^2y_M^2], \\
\frac{d\lambda_5}{d\ln\mu^2} &= \frac{1}{16\pi^2} [2\lambda_5(3y_T^2 + 6y_T^2 + 6y_B^2 + 6y_Y^2 + 6y_M^2 - 3g_1^2 - 9g_2^2) + 2\lambda_5(\lambda_1 + \lambda_2 + 4\lambda_3 + 6\lambda_4)]. \tag{A33}
\end{aligned}$$

The coupling constants gain additional terms due to the new fermions in both triplet models as follows:

$$\frac{dg_1^2}{d\ln\mu^2} = \frac{g_1^4}{16\pi^2} \left(7 + \frac{4}{5} \right), \quad \frac{dg_2^2}{d\ln\mu^2} = \frac{g_2^4}{16\pi^2} (-3 + 4), \quad \frac{dg_3^2}{d\ln\mu^2} = \frac{g_3^4}{16\pi^2} (-7 + 2). \tag{A34}$$

3. Approximate contributions of VLQs to the \mathbb{S} and \mathbb{T} parameters in VLQ models

We give the leading order terms for right-handed and left-handed contributions to the VLQ oblique parameters in singlet, doublet and triplet representations.

a. Singlet $\mathcal{U}_1(T)$, $Y = 2/3$

$$\begin{aligned}
\Delta\mathbb{T} &\simeq \frac{m_T^2 N_c (s_L^t)^2}{16\pi c_W^2 s_W^2 M_Z^2} \left[(x_T^t (s_L^t)^2 - (c_L^t)^2 - 1 + 4(c_L^t)^2 \frac{m_T^2}{m_T^2 - m_t^2} \ln(x_T)) \right], \\
\Delta\mathbb{S} &\simeq \frac{N_c (s_L^t)^2}{18\pi} \left(\frac{(c_L^t)^2}{(x_T - 1)^3} [2\ln(x_T)(3 - 9x_T^2 - 9x_T^4 + 3x_T^6) + 5 - 27x_T^2 - 27x_T^4 - 5x_T^6] - 2\ln(x_T) \right). \tag{A35}
\end{aligned}$$

b. Singlet $\mathcal{D}_1(B)$, $Y = -1/3$

$$\begin{aligned}
\Delta\mathbb{T} &\simeq \frac{m_t^2 N_c x_B}{16\pi c_W^2 s_W^2 M_Z^2 (x_B - 1)} [(s_L^b)^4 (x_B - 1) - 2(s_L^b)^2 \ln(x_B)], \\
\Delta\mathbb{S} &\simeq \frac{N_c (s_L^b)^2}{18\pi} \left[2\ln\left(\frac{m_b}{m_B}\right) (3(s_L^b)^2 - 4) - 5(c_L^b)^2 \right]. \tag{A36}
\end{aligned}$$

c. Doublet $\mathcal{D}_2(T, B)$, $Y = 1/6$

$$\begin{aligned}
\Delta\mathbb{T} &\simeq \frac{m_t^2 N_c (s_R^t)^2}{8\pi c_W^2 s_W^2 M_Z^2} [2\ln(x_T) - 2], \\
\Delta\mathbb{S} &\simeq \frac{N_c}{18\pi} [8s_R^t \ln(x_T) - 7s_R^t - 2\ln(x_b) - 3]. \tag{A37}
\end{aligned}$$

d. Doublet $\mathcal{D}_X(X, T)$, $Y = 7/6$

$$\begin{aligned}
\Delta\mathbb{T} &\simeq \frac{m_t^2 N_c (s_R^t)^2}{16\pi c_W^2 s_W^2 M_Z^2} \left[-8\ln(x_T) + 6 + \frac{4}{3} s_R^t x_T^2 - s_R^t \right], \\
\Delta\mathbb{S} &\simeq \frac{N_c}{18\pi} [-8s_R^t \ln(x_T) + 15s_R^t - 2\ln(x_b) - 3]. \tag{A38}
\end{aligned}$$

e. Doublet $\mathcal{D}_Y(B, Y)$, $Y = -5/6$

$$\begin{aligned}
\Delta\mathbb{T} &\simeq \frac{m_t^2 N_c x_B}{128\pi c_W^2 s_W^2 M_Z^2} [-16c_R^b (-3 + c_R^{2b} \cot_R^b \ln(c_R^b)) \\
&\quad + s_R^b (-13 - 20c_R^{2b} + 4c_R^b)], \\
\Delta\mathbb{S} &\simeq \frac{N_c}{18\pi} \left[-4s_R^b \ln\left(\frac{m_B}{m_b}\right) + 11s_R^b - 2\ln(x_b) - 3 \right]. \tag{A39}
\end{aligned}$$

f. Triplet $\mathcal{T}_X(X, T, B)$, $Y = 2/3$

$$\begin{aligned}
\Delta\mathbb{T} &\simeq \frac{m_t^2 N_c (s_L^t)^2}{16\pi c_W^2 s_W^2 M_Z^2} \left[12\ln(x_T) - 10 + \frac{19}{3} (s_L^t)^2 x_T^2 - (s_L^t)^{-2} \right], \\
\Delta\mathbb{S} &\simeq \frac{N_c}{18\pi} \left\{ (s_L^t)^2 \left[4\ln(x_T) - 16\ln\left(\frac{m_B}{m_b}\right) + 13 \right] \right. \\
&\quad \left. + 32\ln\left(\frac{m_B}{m_T}\right) - 2\ln(x_b) - 3 \right\}. \tag{A40}
\end{aligned}$$

g. Triplet \mathcal{T}_Y (T, B, Y), $Y = -1/3$

$$\Delta\mathbb{T} \simeq \frac{m_t^2 N_c (s_L^t)^2}{16\pi c_W^2 s_W^2 M_Z^2} \left[-\ln(x_T) + 6 + \frac{19}{12} (s_L^t)^2 x_T^2 - (s_L^t)^{-2} \right],$$

$$\Delta S \simeq \frac{N_c}{18\pi} \left\{ (s_L^t)^2 \left[4 \ln\left(\frac{m_B}{m_b}\right) - 4 \ln(x_T) + \frac{13}{2} \right] - 2 \ln(x_b) - 3 \right\}, \quad (\text{A41})$$

where $x_i = \frac{m_i}{m_t}$ for all representations.

4. Electroweak couplings of VLQ and the SM quarks

The couplings of the Z and W-boson to VLQ and to the SM quarks play distinctive role for each representation.

a. Singlet $\mathcal{U}_1(T)$, $Y = 2/3$

$$\Omega_{Wtb}^L = \frac{ec_L^t}{\sqrt{2}s_W}, \quad \Omega_{Ztt}^L = \frac{e}{2s_W c_W} \left(c_L^2 - \frac{4}{3} s_W^2 \right),$$

$$\Omega_{Wtb}^R = 0, \quad \Omega_{Ztt}^R = -\frac{2es_W}{3c_W},$$

$$\Omega_{WTb}^L = \frac{es_L^t}{\sqrt{2}s_W}, \quad \Omega_{ZTT}^L = \frac{e}{2s_W c_W} \left(s_L^2 - \frac{4}{3} s_W^2 \right),$$

$$\Omega_{WTb}^R = 0, \quad \Omega_{ZTT}^R = -\frac{2es_W}{3c_W},$$

$$\Omega_{Zbb}^L = \frac{e}{2s_W c_W} \left(\frac{2}{3} s_W^2 - 1 \right), \quad \Omega_{Zbb}^R = \frac{es_W}{3c_W},$$

$$\Omega_{ZtT}^L = \frac{es_L^t c_L^t}{2s_W c_W}, \quad \Omega_{ZtT}^R = 0. \quad (\text{A42})$$

b. Singlet $\mathcal{D}_1(B)$, $Y = -1/3$

$$\Omega_{Wtb}^L = \frac{ec_L^b}{\sqrt{2}s_W}, \quad \Omega_{Ztt}^L = \frac{e}{2s_W c_W} \left(1 - \frac{4}{3} s_W^2 \right),$$

$$\Omega_{Wtb}^R = 0, \quad \Omega_{Ztt}^R = -\frac{2es_W}{3c_W},$$

$$\Omega_{WtB}^L = \frac{es_L^b}{\sqrt{2}s_W}, \quad \Omega_{Zbb}^L = \frac{e}{2s_W c_W} \left(\frac{2}{3} s_W^2 - c_L^2 \right),$$

$$\Omega_{WtB}^R = 0, \quad \Omega_{Zbb}^R = \frac{es_W}{3c_W},$$

$$\Omega_{ZBB}^L = \frac{e}{2s_W c_W} \left(\frac{2}{3} s_W^2 - s_L^2 \right), \quad \Omega_{ZBB}^R = \frac{es_W}{3c_W},$$

$$\Omega_{Zbb}^L = -\frac{es_L^b c_L^b}{2s_W c_W}, \quad \Omega_{Zbb}^R = 0. \quad (\text{A43})$$

c. Doublet \mathcal{D}_2 (T, B), $Y = 1/6$

$$\Omega_{Wtb}^L = \frac{e}{\sqrt{2}s_W} (s_L^t s_L^b + c_L^t c_L^b), \quad \Omega_{Ztt}^L = \frac{e}{2s_W c_W} \left(1 - \frac{4}{3} s_W^2 \right),$$

$$\Omega_{Wtb}^R = \frac{es_R^t s_R^b}{\sqrt{2}s_W}, \quad \Omega_{Ztt}^R = \frac{e}{2s_W c_W} \left(s_R^2 - \frac{4}{3} s_W^2 \right),$$

$$\Omega_{WTb}^L = \frac{e}{\sqrt{2}s_W} (s_L^t c_L^b - s_L^b c_L^t), \quad \Omega_{Zbb}^L = \frac{e}{2s_W c_W} \left(\frac{2}{3} s_W^2 - 1 \right),$$

$$\Omega_{WTb}^R = -\frac{es_R^b c_R^t}{\sqrt{2}s_W}, \quad \Omega_{Zbb}^R = \frac{e}{2s_W c_W} \left(\frac{2}{3} s_W^2 - s_R^2 \right),$$

$$\Omega_{WtB}^L = \frac{e}{\sqrt{2}s_W} (s_L^b c_L^t - s_L^t c_L^b), \quad \Omega_{ZtT}^L = 0,$$

$$\Omega_{WtB}^R = -\frac{es_R^t c_R^b}{\sqrt{2}s_W}, \quad \Omega_{ZtT}^R = -\frac{es_R^t c_R^t}{2s_W c_W},$$

$$\Omega_{WTB}^L = \frac{e}{\sqrt{2}s_W} (s_L^t s_L^b + c_L^t c_L^b), \quad \Omega_{Zbb}^R = 0,$$

$$\Omega_{WTB}^R = \frac{ec_R^t c_R^b}{\sqrt{2}s_W}, \quad \Omega_{Zbb}^R = \frac{es_R^b c_R^b}{2s_W c_W},$$

$$\Omega_{ZTT}^L = \frac{e}{2s_W c_W} \left(1 - \frac{4}{3} s_W^2 \right), \quad \Omega_{ZTT}^R = \frac{e}{2s_W c_W} \left(c_R^2 - \frac{4}{3} s_W^2 \right),$$

$$\Omega_{ZBB}^L = \frac{e}{2s_W c_W} \left(\frac{2}{3} s_W^2 - 1 \right), \quad \Omega_{ZBB}^R = \frac{e}{2s_W c_W} \left(\frac{2}{3} s_W^2 - c_R^2 \right). \quad (\text{A44})$$

d. Doublet \mathcal{D}_X (X, T), $Y = 7/6$

$$\Omega_{Wtb}^L = \frac{ec_L^t}{\sqrt{2}s_W}, \quad \Omega_{Ztt}^L = \frac{e}{2s_W c_W} \left(1 - \frac{4}{3} s_W^2 - 2s_L^2 \right),$$

$$\Omega_{Wtb}^R = 0, \quad \Omega_{Ztt}^R = -\frac{e}{2s_W c_W} \left(\frac{4}{3} s_W^2 + s_R^2 \right),$$

$$\Omega_{WTb}^L = \frac{es_L^t}{\sqrt{2}s_W}, \quad \Omega_{Zbb}^L = \frac{e}{2s_W c_W} \left(\frac{2}{3} s_W^2 - 1 \right),$$

$$\Omega_{WTb}^R = 0, \quad \Omega_{Zbb}^R = \frac{es_W}{3c_W},$$

$$\Omega_{WtX}^L = -\frac{es_L^t}{\sqrt{2}s_W}, \quad \Omega_{ZtT}^L = \frac{es_L^t c_L^t}{s_W c_W},$$

$$\Omega_{WtX}^R = -\frac{es_R^t}{\sqrt{2}s_W}, \quad \Omega_{ZtT}^R = \frac{es_R^t c_R^t}{2s_W c_W},$$

$$\Omega_{WTX}^L = \frac{ec_L^t}{\sqrt{2}s_W}, \quad \Omega_{ZTT}^L = \frac{e}{2s_W c_W} \left(1 - \frac{4}{3} s_W^2 - c_L^2 \right),$$

$$\Omega_{WTX}^R = \frac{ec_R^t}{\sqrt{2}s_W}, \quad \Omega_{ZTT}^R = -\frac{e}{2s_W c_W} \left(c_R^2 + \frac{4}{3} s_W^2 \right),$$

$$\Omega_{ZXX}^L = \frac{e}{2s_W c_W} \left(1 - \frac{10}{3} s_W^2 \right), \quad \Omega_{ZXX}^R = \frac{e}{2s_W c_W} \left(1 - \frac{10}{3} s_W^2 \right). \quad (\text{A45})$$

e. Doublet $\mathcal{D}_Y (B, Y)$, $Y = -5/6$

$$\begin{aligned}
\Omega_{Wtb}^L &= \frac{ec_L^b}{\sqrt{2}s_W}, & \Omega_{Ztt}^L &= \frac{e}{2s_Wc_W} \left(1 - \frac{4}{3}s_W^2\right), \\
\Omega_{Wtb}^R &= 0, & \Omega_{Ztt}^R &= -\frac{2es_W}{3c_W}, \\
\Omega_{WBt}^L &= \frac{es_L^b}{\sqrt{2}s_W}, & \Omega_{Zbb}^L &= \frac{e}{2s_Wc_W} \left(\frac{2}{3}s_W^2 + 2s_L^{b2} - 1\right), \\
\Omega_{WBt}^R &= 0, & \Omega_{Zbb}^R &= \frac{e}{2s_Wc_W} \left(s_R^{b2} + \frac{2}{3}s_W^2\right), \\
\Omega_{WbY}^L &= -\frac{es_L^b}{\sqrt{2}s_W}, & \Omega_{ZbB}^L &= -\frac{es_L^b c_L^b}{s_Wc_W}, \\
\Omega_{WbY}^R &= -\frac{es_R^b}{\sqrt{2}s_W}, & \Omega_{ZbB}^R &= -\frac{es_R^b c_R^b}{2s_Wc_W}, \\
\Omega_{WBY}^L &= \frac{ec_L^b}{\sqrt{2}s_W}, & \Omega_{ZBB}^L &= \frac{e}{2s_Wc_W} \left(\frac{2}{3}s_W^2 + 2c_L^{b2} - 1\right), \\
\Omega_{WBY}^R &= \frac{ec_R^b}{\sqrt{2}s_W}, & \Omega_{ZBB}^R &= \frac{e}{2s_Wc_W} \left(c_R^{b2} + \frac{2}{3}s_W^2\right), \\
\Omega_{ZYY}^L &= -\frac{e}{2s_Wc_W} \left(1 - \frac{8}{3}s_W^2\right), \\
\Omega_{ZYY}^R &= -\frac{e}{2s_Wc_W} \left(1 - \frac{8}{3}s_W^2\right). \tag{A46}
\end{aligned}$$

f. Triplet $\mathcal{T}_X (X, T, B)$, $Y = 2/3$

$$\begin{aligned}
\Omega_{Wtb}^L &= \frac{e}{\sqrt{2}s_W} (\sqrt{2}s_L^t s_L^b + c_L^t c_L^b), \\
\Omega_{Ztt}^L &= \frac{e}{2s_Wc_W} \left(c_L^{t2} - \frac{4}{3}s_W^2\right), \\
\Omega_{Wtb}^R &= \frac{es_R^t s_R^b}{s_W}, & \Omega_{Ztt}^R &= -\frac{2es_W}{3c_W}, \\
\Omega_{Wtb}^L &= \frac{e}{\sqrt{2}s_W} (s_L^t c_L^b - \sqrt{2}s_L^b c_L^t), \\
\Omega_{Zbb}^L &= \frac{e}{2s_Wc_W} \left(\frac{2}{3}s_W^2 - s_L^{b2} - 1\right), \\
\Omega_{Wtb}^R &= -\frac{es_R^b c_R^t}{s_W}, & \Omega_{Zbb}^R &= \frac{e}{2s_Wc_W} \left(\frac{2}{3}s_W^2 - 2s_R^{b2}\right), \\
\Omega_{WtB}^L &= \frac{e}{\sqrt{2}s_W} (s_L^b c_L^t - \sqrt{2}s_L^t c_L^b), & \Omega_{ZtT}^L &= \frac{es_L^t c_L^t}{2s_Wc_W}, \\
\Omega_{WtB}^R &= -\frac{es_R^t c_R^b}{s_W}, & \Omega_{ZtT}^R &= 0, \\
\Omega_{WtX}^L &= -\frac{es_L^t}{s_W}, & \Omega_{ZbB}^L &= \frac{es_L^b c_L^b}{2s_Wc_W}, \\
\Omega_{WtX}^R &= -\frac{es_R^t}{s_W}, & \Omega_{ZbB}^R &= \frac{es_R^b c_R^b}{s_Wc_W},
\end{aligned}$$

$$\begin{aligned}
\Omega_{Wtb}^L &= \frac{e}{\sqrt{2}s_W} (s_L^t s_L^b + \sqrt{2}c_L^t c_L^b), \\
\Omega_{ZTT}^L &= \frac{e}{2s_Wc_W} \left(s_L^{t2} - \frac{4}{3}s_W^2\right), \\
\Omega_{Wtb}^R &= \frac{ec_R^t c_R^b}{s_W}, & \Omega_{ZTT}^R &= -\frac{2es_W}{3c_W}, \\
\Omega_{WtX}^L &= \frac{ec_L^t}{s_W}, & \Omega_{ZBB}^L &= \frac{e}{2s_Wc_W} \left(\frac{2}{3}s_W^2 - c_L^{b2} - 1\right), \\
\Omega_{WtX}^R &= \frac{ec_R^t}{s_W}, & \Omega_{ZBB}^R &= \frac{e}{2s_Wc_W} \left(\frac{2}{3}s_W^2 - 2c_R^{b2}\right), \\
\Omega_{ZXX}^L &= \frac{e}{2s_Wc_W} \left(2 - \frac{10}{3}s_W^2\right), \\
\Omega_{ZXX}^R &= \frac{e}{2s_Wc_W} \left(2 - \frac{10}{3}s_W^2\right). \tag{A47}
\end{aligned}$$

g. Triplet $\mathcal{T}_Y (T, B, Y)$, $Y = -1/3$

$$\begin{aligned}
\Omega_{Wtb}^L &= \frac{e}{\sqrt{2}s_W} (\sqrt{2}s_L^t s_L^b + c_L^t c_L^b), \\
\Omega_{Ztt}^L &= \frac{e}{2s_Wc_W} \left(-\frac{4}{3}s_W^2 + s_L^{t2} + 1\right), \\
\Omega_{Wtb}^R &= \frac{es_R^t s_R^b}{s_W}, & \Omega_{Ztt}^R &= \frac{e}{2s_Wc_W} \left(2s_R^{t2} - \frac{4}{3}s_W^2\right), \\
\Omega_{Wtb}^L &= \frac{e}{\sqrt{2}s_W} (s_L^t c_L^b - \sqrt{2}s_L^b c_L^t), \\
\Omega_{Zbb}^L &= \frac{e}{2s_Wc_W} \left(\frac{2}{3}s_W^2 - c_L^{b2}\right), \\
\Omega_{Wtb}^R &= -\frac{es_R^b c_R^t}{s_W}, & \Omega_{Zbb}^R &= \frac{es_W}{3c_W}, \\
\Omega_{WtB}^L &= \frac{e}{\sqrt{2}s_W} (s_L^b c_L^t - \sqrt{2}s_L^t c_L^b), & \Omega_{ZtT}^L &= -\frac{es_L^t c_L^t}{2s_Wc_W}, \\
\Omega_{WtB}^R &= -\frac{es_R^t c_R^b}{s_W}, & \Omega_{ZtT}^R &= -\frac{es_R^t c_R^t}{s_Wc_W}, \\
\Omega_{WbY}^L &= -\frac{es_L^b}{s_W}, & \Omega_{ZbB}^L &= -\frac{es_L^b c_L^b}{2s_Wc_W}, \\
\Omega_{WbY}^R &= -\frac{es_R^b}{s_W}, & \Omega_{ZbB}^R &= 0, \\
\Omega_{WtB}^L &= \frac{e}{\sqrt{2}s_W} (s_L^t s_L^b + \sqrt{2}c_L^t c_L^b), \\
\Omega_{ZTT}^L &= \frac{e}{2s_Wc_W} \left(-\frac{4}{3}s_W^2 + c_L^{t2} + 1\right), \\
\Omega_{WtB}^R &= \frac{ec_R^t c_R^b}{s_W}, & \Omega_{ZTT}^R &= \frac{e}{2s_Wc_W} \left(2c_R^{t2} - \frac{4}{3}s_W^2\right),
\end{aligned}$$

$$\begin{aligned}
\Omega_{WBY}^L &= \frac{ec_L^b}{s_W}, & \Omega_{ZBB}^L &= \frac{e}{2s_W c_W} \left(\frac{2}{3} s_W^2 - s_L^{b^2} \right), \\
\Omega_{WBY}^R &= \frac{ec_R^b}{s_W}, & \Omega_{ZBB}^R &= \frac{es_W}{3c_W}, \\
\Omega_{ZYY}^L &= -\frac{e}{2s_W c_W} \left(2 - \frac{8}{3} s_W^2 \right), \\
\Omega_{ZYY}^R &= -\frac{e}{2s_W c_W} \left(2 - \frac{8}{3} s_W^2 \right).
\end{aligned} \tag{A48}$$

5. Passarino-Veltman integrals

Although a more detailed discussion about Passarino-Veltman reduction appears elsewhere [134], we give a generic one-loop tensor integral as the following:

$$T_\rho^{\nu_i} = \frac{(2\pi\mu)^{4-D}}{i\pi^2} \int d^D p \frac{p^{\nu_i} \cdots p^{\nu_n}}{\mathbb{D}_1 \cdots \mathbb{D}_\rho}, \tag{A49}$$

where the propagators are described by

$$\begin{aligned}
\mathbb{D}_1 &= p^2 - m_1^2 + i\epsilon, \\
\mathbb{D}_2 &= (p + q_1)^2 - m_2^2 + i\epsilon, \\
\mathbb{D}_3 &= (p + q_1 + q_2)^2 - m_3^2 + i\epsilon.
\end{aligned} \tag{A50}$$

After factoring out the $i/(16\pi^2)$, scalar, vector, and tensor functions are defined from the generic one-loop tensor integral Eq. (A49):

$$\begin{aligned}
A(m_1) &= \mu^{4-D} \int \frac{d^D p}{(2\pi)^D \mathbb{D}_1}, \\
[B_0, B^\mu, B^{\mu\nu}](q_1^2, m_1^2, m_2^2) &= \mu^{4-D} \int \frac{d^D p}{(2\pi)^D} \frac{[1, p^\mu, p^\mu p^\nu]}{\mathbb{D}_1 \mathbb{D}_2}, \\
[C_0, C^\mu, C^{\mu\nu}](q_1^2, q_2^2, (q_1 + q_2)^2, m_1^2, m_2^2, m_3^2) \\
&= \mu^{4-D} \int \frac{d^D p}{(2\pi)^D} \frac{[1, p^\mu, p^\mu p^\nu]}{\mathbb{D}_1 \mathbb{D}_2 \mathbb{D}_3}.
\end{aligned} \tag{A51}$$

Scalar and tensor integrals are not independent. In fact, tensor forms can be decomposed in terms of scalar functions:

$$\begin{aligned}
B^\mu &= q_1^\mu B_1, & C^\mu &= q_1^\mu C_1 + q_2^\mu C_2, \\
B^{\mu\nu} &= q_1^\mu q_1^\nu B_{11} + g^{\mu\nu} B_{00}, & C^{\mu\nu} &= \sum_{i=1}^2 q_i^\mu q_j^\nu C_{ij} + g^{\mu\nu} C_{00}, \\
C^{\mu\nu\delta} &= \sum_{i,j,k=1}^2 q_i^\mu q_j^\nu q_k^\delta C_{ijk} + \sum_{i=1}^2 (q_i^\mu g^{\nu\delta} + q_i^\nu g^{\delta\mu} + q_i^\delta g^{\mu\nu}) C_{00i}.
\end{aligned} \tag{A52}$$

Scalar integrals or vacuum integrals play a main role for all intents and purposes throughout this work. Furthermore, there are only four types of independent scalar (vacuum) integrals. The rest of the vacuum integrals carried out throughout this work are combinations of the following definitions:

$$\begin{aligned}
A_0(m_1^2) &= \frac{(2\pi\mu)^\epsilon}{i\pi^2} \int d^D p \frac{1}{p^2 - m_1^2}, \\
B_0(q_1^2, m_1^2, m_2^2) &= \frac{(2\pi\mu)^\epsilon}{i\pi^2} \int d^D p \frac{1}{[p^2 - m_1^2] [(p + q_1)^2 - m_2^2]}, \\
C_0(q_1^2, q_2^2, q_{12}^2, m_1^2, m_2^2, m_3^2) &= \frac{(2\pi\mu)^\epsilon}{i\pi^2} \int d^D p \frac{1}{[p^2 - m_1^2] [(p + q_1)^2 - m_2^2] [(p + q_{12})^2 - m_3^2]}, \\
D_0(q_1^2, q_2^2, q_3^2, q_{12}^2, q_{23}^2, m_1^2, m_2^2, m_3^2, m_4^2) &= \frac{(2\pi\mu)^\epsilon}{i\pi^2} \int d^D p \frac{1}{[p^2 - m_1^2] [(p + q_1)^2 - m_2^2] [(p + q_{12})^2 - m_3^2]} \\
&\quad \times \frac{1}{[(p + q_{123})^2 - m_4^2]},
\end{aligned} \tag{A53}$$

where $\epsilon = 4 - D$. Explicit analytical expressions of widely used PV functions are defined as

$$A_0(m^2) = m^2 \left(\Delta_\epsilon + 1 - \ln \frac{m^2}{\mu^2} \right), \tag{A54}$$

$$B_0(0, m_1^2, m_2^2) = \frac{A_0(m_1^2) - A_0(m_2^2)}{m_1^2 - m_2^2}, \tag{A55}$$

$$B_0(0, m_1^2, m_1^2) = \frac{A_0(m_1^2)}{m_1^2} - 1, \tag{A56}$$

$$B_0(m_1^2, 0, m_1^2) = \frac{A_0(m_1^2)}{m_1^2} + 1, \quad (\text{A57})$$

$$B_1(0, m_1^2, m_2^2) = \frac{2y_2 \ln y_2 - 4y_2 \ln y_2 - y_2^2 + 4y_2 - 3}{4(y_2 - 1)^2} + \frac{1}{2} \ln \frac{m_1^2}{\mu^2} - \frac{\Delta_\epsilon}{2}, \quad (\text{A58})$$

$$B_{00}(m_1^2, m_2^2, m_3^2) = \frac{(m_1 - m_2 - m_3)(m_1 + m_2 - m_3)(m_1 - m_2 + m_3)(m_1 + m_2 + m_3)B_0(m_1^2, m_2^2, m_3^2)}{4(1 - D)m_1^2} \\ + \frac{A_0(m_2^2)(m_1^2 + m_2^2 - m_3^2)}{4(1 - D)m_1^2} - \frac{A_0(m_3^2)(m_1^2 - m_2^2 + m_3^2)}{4(1 - D)m_1^2}, \quad (\text{A59})$$

$$B_{00}(0, m_2^2, m_3^2) = -\frac{A_0(m_3^2)}{2(1 - D)} - \frac{m_2^2 B_0(0, m_2^2, m_3^2)}{1 - D} - \frac{(m_2^2 - m_3^2)B_1(0, m_2^2, m_3^2)}{2(1 - D)}, \quad (\text{A60})$$

$$B_{00}(0, m^2, m^2) = -\frac{A_0(m^2)}{2(1 - D)} - \frac{m^2 B_0(0, m^2, m^2)}{1 - D}, \quad (\text{A61})$$

$$B_{00}(m_1^2, m_2^2, m_2^2) = \frac{(m_1^2 - 4m_2^2)B_0(m_1^2, m_2^2, m_2^2)}{4(1 - D)} - \frac{A_0(m_2^2)}{2(1 - D)}, \quad (\text{A62})$$

$$C_0(m_1^2, m_2^2, m_3^2) = \frac{1}{m_1^2} \frac{y_2 \ln y_2 - y_3 \ln y_3 - y_2 y_3 \ln y_2 + y_2 y_3 \ln y_3}{(y_2 - 1)(y_3 - 1)(y_2 - y_3)}, \quad (\text{A63})$$

$$C_0(m_1^2, m_2^2, m_2^2) = \frac{1}{m_1^2} \frac{\ln y_2 - y_2 + 1}{(y_2 - 1)^2}, \quad (\text{A64})$$

$$C_0(m^2, m^2, m^2) = -\frac{1}{2m^2}, \quad (\text{A65})$$

where the divergent part in the minimal subtraction (MS) scheme is given by

$$\Delta_\epsilon = \frac{1}{\epsilon} - \gamma_E + \ln 4\pi + \ln \mu^2 \quad (\text{A66})$$

and the mass ratio parameter

$$y_i = \frac{m_i^2}{m_1^2}.$$

Finally, the complementary relations to the definitions above can be summarized with the following four scalar functions:

$$B_2(p^2, m_1^2, m_2^2) = B_{21}(p^2, m_1^2, m_2^2), \quad (\text{A67})$$

$$B_3(p^2, m_1^2, m_2^2) = -B_1(p^2, m_1^2, m_2^2) - B_{21}(p^2, m_1^2, m_2^2), \quad (\text{A68})$$

$$B_4(p^2, m_1^2, m_2^2) = -m_1^2 B_1(p^2, m_2^2, m_1^2) - m_2^2 B_1(p^2, m_1^2, m_2^2), \quad (\text{A69})$$

$$B_5(p^2, m_1^2, m_2^2) = A_0(m_1^2) + A_0(m_2^2) - 4B_{22}(p^2, m_1^2, m_2^2). \quad (\text{A70})$$

- [1] G. Aad *et al.*, *Phys. Lett. B* **716**, 1 (2012).
- [2] S. Chatrchyan *et al.*, *Phys. Lett. B* **716**, 30 (2012).
- [3] G. Degrandi, S. Di Vita, J. Elias-Miró, J. R. Espinosa, G. F. Giudice, G. Isidori, and A. Strumia, *J. High Energy Phys.* **08** (2012) 098.
- [4] D. Buttazzo, G. Degrandi, P. P. Giardino, G. F. Giudice, F. Sala, A. Salvio, and A. Strumia, *J. High Energy Phys.* **12** (2013) 089.
- [5] G. Aad *et al.*, *Phys. Lett. B* **843**, 137745 (2023).
- [6] A. Tumasyan *et al.*, *Nature (London)* **607**, 60 (2022).
- [7] M. Cepeda *et al.*, CERN Yellow Rep. Monogr. **7**, 221 (2019).
- [8] J. Alison *et al.*, *Rev. Phys.* **5**, 100045 (2020).
- [9] K. Agashe, R. Contino, and A. Pomarol, *Nucl. Phys.* **B719**, 165 (2005).
- [10] G. Ferretti and D. Karateev, *J. High Energy Phys.* **03** (2014) 077.
- [11] D. B. Kaplan, *Nucl. Phys.* **B365**, 259 (1991).
- [12] G. Ferretti, *J. High Energy Phys.* **06** (2014) 142.
- [13] S. Chang, J. Hisano, H. Nakano, N. Okada, and M. Yamaguchi, *Phys. Rev. D* **62**, 084025 (2000).
- [14] T. Gherghetta and A. Pomarol, *Nucl. Phys.* **B586**, 141 (2000).
- [15] R. Contino, Y. Nomura, and A. Pomarol, *Nucl. Phys.* **B671**, 148 (2003).
- [16] S. Gopalakrishna, T. Mandal, S. Mitra, and R. Tibrewala, *Phys. Rev. D* **84**, 055001 (2011).
- [17] S. Gopalakrishna, T. Mandal, S. Mitra, and G. Moreau, *J. High Energy Phys.* **08** (2014) 079.
- [18] G. Couture, M. Frank, C. Hamzaoui, and M. Toharia, *Phys. Rev. D* **95**, 095038 (2017).
- [19] N. Arkani-Hamed, A. G. Cohen, E. Katz, A. E. Nelson, T. Gregoire, and J. G. Wacker, *J. High Energy Phys.* **08** (2002) 021.
- [20] M. Perelstein, M. E. Peskin, and A. Pierce, *Phys. Rev. D* **69**, 075002 (2004).
- [21] M. Schmaltz, *Nucl. Phys. B, Proc. Suppl.* **117**, 40 (2003).
- [22] S. P. Martin, *Phys. Rev. D* **82**, 055019 (2010).
- [23] S. P. Martin, *Phys. Rev. D* **81**, 035004 (2010).
- [24] K. S. Babu, I. Gogoladze, M. U. Rehman, and Q. Shafi, *Phys. Rev. D* **78**, 055017 (2008).
- [25] J. Kang, P. Langacker, and B. D. Nelson, *Phys. Rev. D* **77**, 035003 (2008).
- [26] S. Aoki *et al.*, *Eur. Phys. J. C* **80**, 113 (2020).
- [27] D. Bryman, V. Cirigliano, A. Crivellin, and G. Inguglia, *Annu. Rev. Nucl. Part. Sci.* **72**, 69 (2022).
- [28] G. C. Branco, J. T. Penedo, P. M. F. Pereira, M. N. Rebelo, and J. I. Silva-Marcos, *J. High Energy Phys.* **07** (2021) 099.
- [29] M. Kirk, *PoS(FPCP)2023*, 059 (2023).
- [30] F. Albergaria and G. C. Branco, [arXiv:2307.13073](https://arxiv.org/abs/2307.13073).
- [31] A. E. Cárcamo Hernández, S. F. King, and H. Lee, *Phys. Rev. D* **105**, 015021 (2022).
- [32] G. Altarelli and G. Isidori, *Phys. Lett. B* **337**, 141 (1994).
- [33] P. Ghorbani, *Nucl. Phys.* **B971**, 115533 (2021).
- [34] A. Arsenault, K. Y. Cingiloglu, and M. Frank, *Phys. Rev. D* **107**, 036018 (2023).
- [35] G. C. Branco, P. M. Ferreira, L. Lavoura, M. N. Rebelo, M. Sher, J. P. Silva, *Phys. Rep.* **516**, 1 (2012).
- [36] J. F. Gunion and H. E. Haber, *Phys. Rev. D* **67**, 075019 (2003).
- [37] B. Coleppa, F. Kling, and S. Su, *J. High Energy Phys.* **01** (2014) 161.
- [38] W. Altmannshofer, S. Gori, and G. D. Kribs, *Phys. Rev. D* **86**, 115009 (2012).
- [39] I. P. Ivanov, *Phys. Rev. D* **75**, 035001 (2007); **76**, 039902(E) (2007).
- [40] I. F. Ginzburg and I. P. Ivanov, *Phys. Rev. D* **72**, 115010 (2005).
- [41] P. Basler, P. M. Ferreira, M. Mühlleitner, and R. Santos, *Phys. Rev. D* **97**, 095024 (2018).
- [42] E. Accomando, C. Byers, D. Englert, J. Hays, and S. Moretti, *Phys. Rev. D* **105**, 115004 (2022).
- [43] H. Song, W. Su, and M. Zhang, *J. High Energy Phys.* **10** (2022) 048.
- [44] A. Cherchiglia, D. Stöckinger, and H. Stöckinger-Kim, *Phys. Rev. D* **98**, 035001 (2018).
- [45] H. E. Haber and O. Stål, *Eur. Phys. J. C* **75**, 491 (2015); **76**, 312(E) (2016).
- [46] P. S. Bhupal Dev and A. Pilaftsis, *J. High Energy Phys.* **12** (2014) 024; **11** (2015) 147(E).
- [47] J. Baglio, O. Eberhardt, U. Nierste, and M. Wiebusch, *Phys. Rev. D* **90**, 015008 (2014).
- [48] O. Eberhardt, U. Nierste, and M. Wiebusch, *J. High Energy Phys.* **07** (2013) 118.
- [49] A. Barroso, P. M. Ferreira, I. P. Ivanov, and R. Santos, *J. High Energy Phys.* **06** (2013) 045.
- [50] D. Eriksson, J. Rathsman, and O. Stal, *Comput. Phys. Commun.* **181**, 189 (2010).
- [51] A. Wahab El Kaffas, P. Osland, and O. M. Ogreid, *Phys. Rev. D* **76**, 095001 (2007).
- [52] M. Maniatis, A. von Manteuffel, O. Nachtmann, and F. Nagel, *Eur. Phys. J. C* **48**, 805 (2006).
- [53] S. Davidson and H. E. Haber, *Phys. Rev. D* **72**, 035004 (2005); **72**, 099902(E) (2005).
- [54] J. E. Kim, *Phys. Rep.* **150**, 1 (1987).
- [55] R. D. Peccei and H. R. Quinn, *Phys. Rev. Lett.* **38**, 1440 (1977).
- [56] M. Trodden, [arXiv:hep-ph/9805252](https://arxiv.org/abs/hep-ph/9805252).
- [57] P. Ferreira, R. Santos, and A. Barroso, *Phys. Lett. B* **603**, 219 (2004).
- [58] A. Barroso, P. Ferreira, and R. Santos, *Phys. Lett. B* **652**, 181 (2007).
- [59] P. M. Ferreira and B. Swieżewska, *J. High Energy Phys.* **04** (2016) 099.
- [60] P. Ferreira, L. Morrison, and S. Profumo, *J. High Energy Phys.* **04** (2020) 125.
- [61] I. P. Ivanov, *Phys. Rev. D* **77**, 015017 (2008).
- [62] P. M. Ferreira, H. E. Haber, and E. Santos, *Phys. Rev. D* **92**, 033003 (2015).
- [63] H. Bahl, M. Carena, N. M. Coyle, A. Ireland, and C. E. M. Wagner, *J. High Energy Phys.* **03** (2023) 165.
- [64] S. Kanemura, T. Kubota, and E. Takasugi, *Phys. Lett. B* **313**, 155 (1993).
- [65] J. Horejsi and M. Kladiva, *Eur. Phys. J. C* **46**, 81 (2006).
- [66] S. Kanemura, T. Kasai, and Y. Okada, *Phys. Lett. B* **471**, 182 (1999).
- [67] A. Sirlin and R. Zucchini, *Nucl. Phys.* **B266**, 389 (1986).
- [68] S. Kanemura, M. Kikuchi, and K. Yagyu, *Phys. Lett. B* **731**, 27 (2014).

- [69] R. Hempfling and B. A. Kniehl, *Phys. Rev. D* **51**, 1386 (1995).
- [70] R. Dermšček, E. Lunghi, and S. Shin, *J. High Energy Phys.* **04** (2019) 019; **10** (2020) 58(E).
- [71] R. Dermisek, E. Lunghi, and S. Shin, *J. High Energy Phys.* **03** (2020) 029.
- [72] R. Dermisek, E. Lunghi, N. McGinnis, and S. Shin, *J. High Energy Phys.* **07** (2020) 241.
- [73] R. Dermisek, E. Lunghi, N. McGinnis, and S. Shin, *J. High Energy Phys.* **08** (2021) 159.
- [74] R. Dermisek, J. Kawamura, E. Lunghi, N. McGinnis, and S. Shin, *arXiv:2203.03852*.
- [75] J. A. Aguilar-Saavedra, R. Benbrik, S. Heinemeyer, and M. Pérez-Victoria, *Phys. Rev. D* **88**, 094010 (2013).
- [76] J. A. Aguilar-Saavedra, *EPJ Web Conf.* **60**, 16012 (2013).
- [77] S. A. R. Ellis, R. M. Godbole, S. Gopalakrishna, and J. D. Wells, *J. High Energy Phys.* **09** (2014) 130.
- [78] D. Carmi, A. Falkowski, E. Kuflik, and T. Volansky, *J. High Energy Phys.* **07** (2012) 136.
- [79] S. Fajfer, A. Greljo, J. F. Kamenik, and I. Mustac, *J. High Energy Phys.* **07** (2013) 155.
- [80] J. M. Alves *et al.*, *Phys. Rept.* **1057**, 1 (2024).
- [81] G. Aad *et al.*, *J. High Energy Phys.* **02** (2016) 110.
- [82] G. Aad *et al.*, *Eur. Phys. J. C* **76**, 442 (2016).
- [83] G. Aad *et al.*, *J. High Energy Phys.* **08** (2015) 105.
- [84] G. Aad *et al.*, *Phys. Rev. D* **91**, 112011 (2015).
- [85] The ATLAS Collaboration, Reports No. ATLAS-CONF-2017-015, No. ATLAS-CONF-2017-015, 2017.
- [86] A. M. Sirunyan *et al.*, *J. High Energy Phys.* **11** (2017) 085.
- [87] A. M. Sirunyan *et al.*, *J. High Energy Phys.* **05** (2017) 029.
- [88] V. Khachatryan *et al.*, *Phys. Rev. D* **93**, 112009 (2016).
- [89] V. Khachatryan *et al.*, *J. High Energy Phys.* **06** (2015) 080.
- [90] S. Chatrchyan *et al.*, *Phys. Rev. Lett.* **112**, 171801 (2014).
- [91] S. Chatrchyan *et al.*, *Phys. Lett. B* **729**, 149 (2014).
- [92] G. Aad *et al.*, *arXiv:2307.07584*.
- [93] G. Aad *et al.*, *Phys. Lett. B* **843**, 138019 (2023).
- [94] M. Aaboud *et al.*, *J. High Energy Phys.* **08** (2017) 052.
- [95] M. Aaboud *et al.*, *J. High Energy Phys.* **07** (2018) 089.
- [96] G. Aad *et al.*, *J. High Energy Phys.* **08** (2023) 153.
- [97] T. Aaltonen *et al.*, *Science* **376**, 170 (2022).
- [98] D. López-Val and T. Robens, *Phys. Rev. D* **90**, 114018 (2014).
- [99] M.-L. Xiao and J.-H. Yu, *Phys. Rev. D* **90**, 014007 (2014); **90**, 019901(A) (2014).
- [100] S. Bahrami and M. Frank, *Phys. Rev. D* **90**, 035017 (2014).
- [101] Y. Shimizu and S. Takeshita, *Nucl. Phys.* **B994**, 116290 (2023).
- [102] J. A. Aguilar-Saavedra, *J. High Energy Phys.* **12** (2006) 033.
- [103] S. Dawson and E. Furlan, *Phys. Rev. D* **86**, 015021 (2012).
- [104] R. Benbrik, C.-H. Chen, and T. Nomura, *Phys. Rev. D* **93**, 055034 (2016).
- [105] A. Arhrib, R. Benbrik, S. J. D. King, B. Manaut, S. Moretti, and C. S. Un, *Phys. Rev. D* **97**, 095015 (2018).
- [106] R. Benbrik, M. Boukidi, and S. Moretti, *arXiv:2211.07259*.
- [107] E. Accomando, D. Englert, C. Byers, J. Hays, and S. Moretti, *arXiv:1905.07313*.
- [108] B. Grinstein, C. W. Murphy, and P. Uttayarat, *J. High Energy Phys.* (2016).
- [109] Y. Tang, *Mod. Phys. Lett. A* **28**, 1330002 (2013).
- [110] G. Hiller, T. Höhne, D. F. Litim, and T. Steudtner, *Phys. Rev. D* **106**, 115004 (2022).
- [111] S. Gopalakrishna and A. Velusamy, *Phys. Rev. D* **99**, 115020 (2019).
- [112] Belle Collaboration, *arXiv:1608.02344*.
- [113] S. Kanemura, M. Kikuchi, K. Mawatari, K. Sakurai, and K. Yagyu, *Nucl. Phys.* **B949**, 114791 (2019).
- [114] M. Misiak and M. Steinhauser, *Eur. Phys. J. C* **77**, 201 (2017).
- [115] G. Abbiendi *et al.*, *Eur. Phys. J. C* **73**, 2463 (2013).
- [116] S. K. Kang, J. Kim, S. Lee, and J. Song, *Phys. Rev. D* **107**, 015025 (2023).
- [117] S. Lee, K. Cheung, J. Kim, C.-T. Lu, and J. Song, *Phys. Rev. D* **106**, 075013 (2022).
- [118] G. Aad *et al.*, *Phys. Rev. D* **105**, 092012 (2022).
- [119] G. Hiller, T. Höhne, D. F. Litim, and T. Steudtner, *arXiv:2305.18520*.
- [120] Y. Heo, D.-W. Jung, and J. S. Lee, *Phys. Lett. B* **833**, 137274 (2022).
- [121] M. E. Machacek and M. T. Vaughn, *Nucl. Phys.* **B222**, 83 (1983).
- [122] M. E. Machacek and M. T. Vaughn, *Nucl. Phys.* **B236**, 221 (1984).
- [123] M. E. Machacek and M. T. Vaughn, *Nucl. Phys.* **B249**, 70 (1985).
- [124] M. E. Peskin and T. Takeuchi, *Phys. Rev. D* **46**, 381 (1992).
- [125] P. A. Zyla *et al.*, *Prog. Theor. Exp. Phys.* **2020**, 083C01 (2020).
- [126] T. Hahn, *Acta Phys. Pol. B* **30**, 3469 (1999).
- [127] V. Shtabovenko, R. Mertig, and F. Orellana, *Comput. Phys. Commun.* **256**, 107478 (2020).
- [128] G. Aad *et al.*, Report No. CERN-EP-2022-228, 2023.
- [129] S. Kanemura, M. Kikuchi, and K. Yagyu, *Nucl. Phys.* **B896**, 80 (2015).
- [130] S.-P. He, *Chin. Phys. C* **47**, 043102 (2023).
- [131] L. Lavoura and J. P. Silva, *Phys. Rev. D* **47**, 2046 (1993).
- [132] C.-Y. Chen, S. Dawson, and E. Furlan, *Phys. Rev. D* **96**, 015006 (2017).
- [133] J. Cao, L. Meng, L. Shang, S. Wang, and B. Yang, *Phys. Rev. D* **106**, 055042 (2022).
- [134] K. Hagiwara, S. Matsumoto, D. Haidt, and C. S. Kim, *Z. Phys. C* **64**, 559 (1994); **68**, 352(E) (1995).